# Polymer-clay nanocomposites prepared by RAFT-supported grafting

by
Helen Chirowodza

Dissertation presented for the degree of *Doctor of Philosophy (PhD) in Polymer Science in the Faculty of Science at Stellenbosch University*
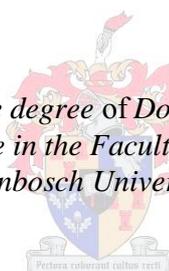
Promotor: Prof. Harald Pasch
Co-promotor: Dr. Patrice C. Hartmann

December 2012

Declaration

I, the undersigned, hereby declare that the work contained in this thesis is my own work and that I have not previously in its entirety or in part submitted it at any university for a degree.

Helen Chirowodza   December 2012

Dedications

To my parents, siblings, nephews, nieces, relatives and my beloved husband Rueben

Abstract

In materials chemistry, surface-initiated reversible deactivation radical polymerisation (SI-RDRP) has emerged as one of the most versatile routes to synthesising inorganic/organic hybrid materials consisting of well-defined polymers. The resultant materials often exhibit a remarkable improvement in bulk material properties even after the addition of very small amounts of inorganic modifiers like clay.

A novel cationic reversible addition–fragmentation chain transfer (RAFT) agent with the dual purpose of modifying the surface of Laponite clay and controlling the polymerisation of monomer therefrom, was designed and synthesised. Its efficiency to control the polymerisation of styrene was evaluated and confirmed through investigating the molar mass evolution and chain-end functionality.

The surface of Laponite clay was modified with the cationic chain transfer agent (CTA) via ion exchange and polymerisation performed in the presence of a free non-functionalised CTA. The addition of the non-functionalised CTA gave an evenly distributed CTA concentration and allowed the simultaneous growth of surface-attached and free polystyrene (PS). Further analysis of the free and grafted PS using analytical techniques developed and published during the course of this study, indicated that the free and grafted PS chains were undergoing different polymerisation mechanisms. For the second monomer system investigated n-butyl acrylate, it was apparent that the molar mass targeted and the monomer conversions attained had a significant influence on the simultaneous growth of the free and grafted polymer chains. Additional analysis of the grafted polymer chains indicated that secondary reactions dominated in the polymerisation of the surface-attached polymer chains.

A new approach to separating the inorganic/organic hybrid materials into their various components using asymmetrical flow field-flow fractionation (AF^4) was described. The results obtained not only gave an indication of the success of the *in situ* polymerisation reaction, but also provided information on the morphology of the material.

Thermogravimetric analysis (TGA) was carried out on the polymer-clay nanocomposite samples. The results showed that by adding as little as 3 wt-% of clay to the polymer matrix, there was a remarkable improvement in the thermal stability.

Opsomming

Oppervlakgeïnisieerde omkeerbare deaktiveringsradikaalpolimerisasie (SI-RDRP) is een van die veelsydigste roetes om anorganiese/organiese hibriedmateriale (wat bestaan uit goed-gedefinieerde polimere) te sintetiseer. Die produk toon dikwels 'n merkwaardige verbetering in die makroskopiese eienskappe – selfs na die toevoeging van klein hoeveelhede anorganiese modifiseerders soos klei.

'n Nuwe kationiese omkeerbare addisie-fragmentasie kettingoordrag (RAFT) middel met die tweeledige doel om die modifisering van die oppervlak van Laponite klei en die beheer van die polimerisasie van die monomeer daarvan, is ontwerp en gesintetiseer. Die klei se doeltreffendheid om die polimerisasie van stireen te beheer is geëvalueer en bevestig deur die molêre massa en die funksionele groepe aan die einde van die ketting te ondersoek.

Die oppervlak van Laponite klei is gemodifiseer met die kationiese kettingoordragmiddel (CTA) deur middel van ioonuitruiling en polimerisasie wat uitgevoer word in die teenwoordigheid van 'n vrye nie-gefunksionaliseerde CTA. Die toevoeging van die nie-gefunksionaliseerde CTA het 'n eweredig-verspreide konsentrasie CTA teweeggebring en die gelyktydige groei van oppervlak-gebonde en vry polistireen (PS) toegelaat. Verdere ontleding van die vrye- en geënte PS met behulp van analitiese tegnieke wat ontwikkel en gepubliseer is gedurende die verloop van hierdie studie, het aangedui dat die vry- en geënte PS-kettings verskillende polimerisasiemeganismes ondergaan. *n*-Butielakrilaat is in die tweede monomeer-stelsel ondersoek en dit was duidelik dat die molêre massa wat geteiken is en die monomeer omskakeling wat bereik is 'n beduidende invloed op die gelyktydige groei van die vrye- en geënte polimeerkettings gehad het. Addisionele analise van die geënte polimeerkettings het gewys dat sekondêre reaksies oorheers het in die polimerisasie van die geënte polimeerkettings.

'n Nuwe benadering tot die skeiding van die anorganiese/organiese hibriedmateriale in hulle onderskeie komponente met behulp van asimmetriese vloeiveld-vloei fraksionering (AF^4) is beskryf. Die resultate wat verkry is, het nie net 'n aanduiding gegee van die sukses van die *in-situ* polimerisasiereaksie nie, maar het ook inligting verskaf oor die morfologie van die materiaal.

Opsomming

Termogravimetriese analise (TGA) is uitgevoer op die polimeer-klei nanosaamgestelde monsters. Die resultate het getoon dat daar 'n merkwaardige verbetering in die termiese stabiliteit was na die toevoeging van so min as 3 wt% klei by die polimeermatriks.

Opsomming

Acknowledgements

Firstly I would like to thank the Lord God Almighty for carrying me throughout this study. Without him I would not be where I am today.

My immense gratitude goes to Prof. Harald Pasch for his guidance, financial and academic support.

I would also like to thank the following people and organisations for their contributions to this project:

All the staff at the Department of Chemistry and Polymer Science, Dr Margie Hurndall, Mrs Erinda Cooper, Mrs Aneli Fourie, Mr Deon Koen, Mr Jim Motshweni and Mr Calvin Maart. Mrs Elsa Malherbe for her patience and assistance with the NMR analysis. Karsten Rode (Deutsches Kunststoff-Institut, Germany) for the help with the MALDI-TOF MS experiments, Gareth Harding for the help with FT-IR microscopy.

All the members of Pasch's group past and present: Dr. Wolfgang Weber for the discussions on RAFT agent synthesis, Monika, Khumo, Werner, Imran, Pritish, Eddson, Wisdom, Trevor, Nyasha, Nadine, Ashwell, Nhlanhla, Sadiq, Rafael and Dr. Alpheus Mautjana.

Friends and family for the encouragement and motivation.

Mpact SA and the University of Stellenbosch for funding.

Rueben, my love and pillar of strength, for standing by me throughout my studies.

May God bless you all.

Table of Contents

Table of Contents

Table of Figures

Table of Schemes

List of Symbols

δ_g	Grafting density
C	Corrected carbon content
cm^{-1}	Wavenumber
Đ	Molar mass dispersity
F	Functionality
m/z	Mass-to-charge ratio
m_c	Mass of carbon in sample
M_c	Mass of carbon per mole of RAFT agent
M_n	*Number-average* molar mass
M_p	Peak molar mass
M_{st}	Molecular mass of styrene
M_w	*Weight-average* molar mass
N_A	Avogadro's number
S	Surface area
S_{spec}	Specific surface area

List of Abbreviations

AIBN	2,2′ Azobis(isobutyronitrile)
ATRP	Atom transfer radical polymerisation
CEC	Cation-exchange capacity
CTA	Chain transfer agent
DCC	1,3-Dicyclohexylcarbodiimide
DCM	Dichloromethane
DEPN	N-tert-butyl-N-[1-diethylphosphono-(2,2-dimethylpropyl)]
DMAP	Dimethyl aminopyridine
DTG	Derivative of thermogravimetric analysis curve
FFF	Field-flow fractionation
FT-IR	Fourier transform infrared spectroscopy
Lap-g-PS	Laponite clay grafted with polystyrene
MALDI-TOF MS	Matrix-assisted laser desorption/ionisation time-of-fight mass spectrometry
MALDI-TOF-CID	MALDI-TOF MS with collision induced dissociation
MMT	Montmorillonite
NMP	Nitroxide-mediated polymerisation
NMR	Nuclear magnetic resonance spectroscopy
P(n-BA)	Poly(n-butyl acrylate)
PCN	Polymer-clay nanocomposite
PS	Polystyrene
RAFT	Reversible addition-fragmentation chain transfer polymerisation
RDRP	Reversible deactivation radical polymerisation
RI	Refractive index
SEC	Size exclusion chromatography
SI-RDRP	Surface-initiated reversible deactivation radical polymerisation
TEMPO	2,2,6,6-tetramethylpiperidinyloxyl
Tert-A RAFT	Tertiary amine functionalised RAFT agent
TGA	Thermogravimetric analysis
UV	Ultraviolet
wt.-%	Weight percent

Chapter 1

Introduction and Objectives

1.1   Introduction

The process of mixing clay with polymers to prepare polymer-clay nanocomposite (PCN) materials was pioneered by the Toyota Company in 1985. By mixing a few wt-% of clay with neat polymer, a material with remarkably improved thermal stability, mechanical properties and barrier properties was synthesised. Over the years, the application of this material has extended from the automobile industry to food packaging and medical industries, and a variety of approaches to its synthesis have been investigated. In the synthesis of PCN one of the main aims is to get an even distribution of the clay in the polymer matrix. The result of the close interaction between the inorganic and organic components is a remarkable improvement in the bulk material properties. Of the widely reported methods of PCN synthesis, surface-initiated *in situ* polymerisation is the most desirable. The approach not only affords clay particles dispersed within a polymer matrix, but also clay particles decorated with polymer brushes. This has inevitably led polymer scientists to develop synthetic methods that result in PCNs consisting of well-defined polymers i.e. controlled molar mass, chain end functionality and macromolecular architecture.

Surface-initiated reversible deactivation radical polymerisation (SI-RDRP) focusing on reversible addition-fragmentation chain transfer (RAFT) polymerisation was employed in this study. The main objectives were to design a suitable cationic chain transfer agent with the dual function of (1) modifying the inorganic clay surface, thus making the clay organophilic and compatible with the monomer matrix, and (2) controlling the polymerisation of monomer from the clay surface. A non-functionalised chain transfer agent was also synthesised, and added to the polymerisation mixture in order to investigate the simultaneous growth of free and surface-confined polymer. Through investigating the molar mass and chain-end functionality of the free and grafted polymer chains, essential information on the similarities or differences in the polymerisation rate and mechanism of the free and surface-confined polymer chains can be acquired. An investigation of these parameters leads to a clearer understanding of the structure-property relationships, and limitations of the materials particularly when making PCNs consisting of block copolymers.

Because of practical limitations such as low concentrations of recovered grafted material, it has been challenging to conclusively and adequately explain SI-RDRP. The purpose of this study was thus to provide (1) novel analytical approaches to investigating the polymerisation mechanisms and (2) to provide information explaining the SI-RDRP from flat Laponite clay surfaces.

1.2   Objectives

The main objectives of this study were to:

   i)   Prepare specific polymer clay nanocomposites. Here the aims were to:

   - Design and synthesise suitable chain transfer agents (CTA) for the synthesis of PCN using the "grafting from" approach.

   - Evaluate the efficiency of the synthesised CTA to control the polymerisation of styrene in the absence of clay.

   - Modify clay using the synthesised CTA in order to improve the miscibility of clay with the organic phase, and subsequently synthesise polymer-clay hybrid material.

   ii) Analyse the macromolecular structure of the free and grafted polymer chains. The information acquired here would provide useful information on the polymerisation process.

   - Comparison of the molar masses of the free and grafted polymer chains would provide important information on the similarities or differences in the polymerisation rate of the surface-tethered and free polymer chains.

   - Comparison of the chain-end functionality would provide crucial information on the similarities and differences in the polymerisation mechanisms of the surface-tethered and free polymer chains.

   iii) Evaluate the efficiency of the synthetic method through determining the free and grafted polymer content.

   iv) Investigate the thermal stability of the synthesised material in order to determine the extent of improvement in thermal stability that arises by incorporating Laponite clay into a polymer matrix.

   v)   Use asymmetrical flow field-flow fractionation to separate the crude product into its various components. The objective of this was to acquire compositional information

regarding the complex material. This is important in understanding the structure-property relationships.

1.3   Layout of thesis

In chapter 1, a brief introduction to the topic of study and the objectives of this work are given.

An overview of the chemistry and synthesis of polymer-clay nanocomposites is given in chapter 2. The literature review focuses mainly on surface-initiated *in situ* reversible deactivation radical polymerisation or living radical polymerisation (RDRP or LRP), as a synthetic route towards PCNs containing well-defined polymer. A brief outline of the analytical techniques employed in this study is also given, in addition to the experimental design and approach.

Chapter 3 covers three aspects of the study. The first aspect is the design and synthesis of the chain transfer agents that were employed. The second part covers the RAFT mediated polymerisation of styrene in the absence of clay, with the focus being on the analysis of the macromolecular structure of the synthesised polymer. The modification of clay using the cationic chain transfer agents synthesised is described in the final part.

In chapter 4, the surface-initiated RAFT-mediated polymerisation of styrene from Laponite clay is described. Due to practical challenges brought about by low recovery of surface-tethered polymer chains, new analytical techniques for investigating the simultaneous growth of free and attached polymer chains are introduced. The thermal stability of the polystyrene-clay nanocomposite material is also investigated.

In chapter 5 the synthetic and analytical approaches developed in chapter 4, were extended to a monomer system that polymerises differently to styrene, n-butyl acrylate. The polymerisation of the free and surface-tethered polymer chains was investigated. A study of the thermal stability of poly(n-butyl acrylate)-clay nanocomposite material is also described.

A new analytical approach to fractionating the polystyrene-clay nanocomposite material into its various components using asymmetrical flow field-flow fractionation (AF[4]) is described in Chapter 6. The off-line coupling of this technique to FT-IR provided essential information on the synthetic method and the morphology of the material.

3

Chapter 2

Historical and Theoretical Background

2.1   Polymer-clay nanocomposites

Polymer-clay nanocomposites (PCN) are organic/inorganic hybrid materials comprising clay embedded within a polymer matrix. They have attracted a lot of interest in academia and industry owing to an improvement in thermal stability, flame retardancy, barrier and mechanical properties arising after adding just a few wt.-% of clay to the pure polymer.[1,2] Their application is also extensive as they form a crucial part in enhancing features of automobile components, construction materials, packaging materials, protective films etc. The property enhancement stems from the contact between the clay surface and the polymer matrix. However, clay is naturally hydrophilic and often found stacked into agglomerates via electrostatic interactions. As a result, there is need to modify the clay surfaces using suitable organic compounds to disrupt the electrostatic interactions and increase the compatibility of the clay with the polymer.

Based on the ordering and distribution of the clay particles within the polymer matrix, two distinct morphologies can be achieved: (1) Intercalated, where the polymer chains exist in the clay layers and the stacked clay structure remains intact and (2) exfoliated, where the individual platelets are dispersed in the polymer matrix (both are shown in Figure 2.1). In most cases, the PCN consists of a mixture of both.
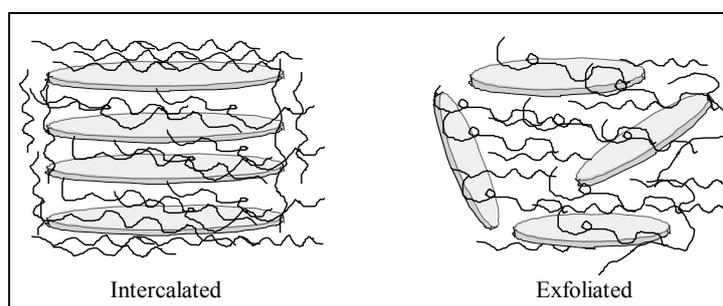
Figure 2.1 Intercalated and exfoliated morphologies of nanocomposites of polymer and clay (not drawn to scale)

2.1.1   Clay mineral structure

Clay minerals are naturally occurring as layered phyllosilicates. They comprise tetrahedral silica (SiO_4) which is bonded to octahedral alumina (AlO_6). The alumina and silica sheets may be present in the ratios of 1:1 or 2:1, hence clays are often classified as such. The most commonly used clays are the 2:1 type also referred to as smectite clays. One central octahedral sheet is sandwiched between two parallel tetrahedral sheets as illustrated in Figure 2.2. The aluminium in aluminosilicates (aluminium bearing clay) may be replaced by other metals e.g. magnesium to give magnesiosilicates. Isomorphous substitution of Mg and Al with cations of a lower oxidation state creates a negative charge on the clay surface which is balanced by hydrated ions of Na^+, K^+, Ca^{2+}, Li^+ or Mg^{2+}. Clay minerals are thus hydrophilic and can also be classified according to their cation exchange capacity (CEC).
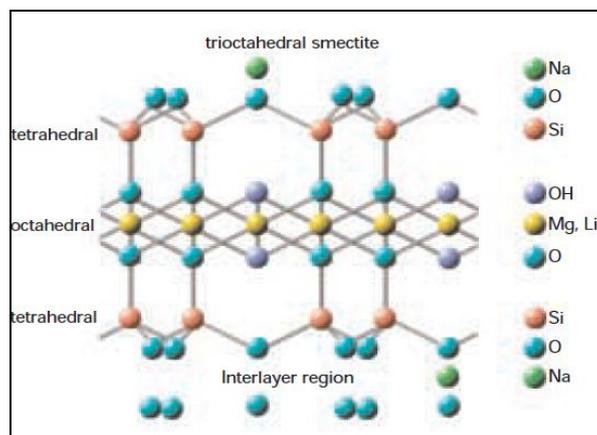
Figure 2.2 Structure of 2:1 layered silicate, hectorite[3]

Examples of clays in the smectite group are montmorillonite, saponite and hectorite. Naturally occurring clays e.g. montmorillonite are cheaper and easily accessible but, they face the limitations of variable purity. Laponite clay, a synthetic hectorite was chosen in this work not only because of its high purity but also because of its relatively uniform particle size of 25 nm diameter. It has an empirical formula of $Na^{0.7+}[(Si_8Mg_{5.5}Li_{0.3})O_{20}(OH)_4]^{-0.7}$ and a CEC of 50–55 mmol/100g as stated by the manufacturer.[3]

2.1.2   Clay modification

Clay minerals are typically hydrophilic and disperse well in water. For the preparation of PCNs there is a need to modify the clay to make it organophilic and more compatible with the

polymer matrix. Many methods have been used to accomplish this and these include adsorption, condensation/coupling and ion exchange.

Adsorption methods involve the use of nonionic or anionic organic compounds. The main adsorption modes involve ion–dipole interactions via the coordination of exchangeable cations with organic compounds, or hydrogen bond interactions between OH groups of the clay with secondary or tertiary amines.[4] The main disadvantage of this approach is that the interactions between the clay and the modifier are very weak.

Covalent attachment forms stronger interactions between the modifier and the clay. Covalent attachment is accomplished by reacting the clay hydroxyl groups e.g. the edge silanol groups with silane coupling agents.[5-11] The drawback to this approach is the relatively low concentration of accessible hydroxyl groups.[12-14]

Smectites are known as swelling clays; the metal ions within the clay galleries can be exchanged for larger organic molecules with a cationic charge. The extent of organic modification is dependent upon the CEC hence ion exchange is the most commonly used approach.[15-20]

2.1.3   Synthesis of PCN

After surface modification various approaches may be taken to synthesise PCNs and these include exfoliation/adsorption,[21,22] melt intercalation/processing[23-25] and *in situ* polymerisation.[26-30] Out of the aforementioned methods, *in situ* polymerisation is the most desirable as polymerisation occurs within the clay galleries resulting in exfoliation and improved dispersion of clay in the polymer matrix. *In situ* polymerisation can be accomplished by two approaches: (1) surface-initiated polymerisation also referred to as "grafting from" and (2) by polymerising a monomer in the presence of clay modified by mono- or bi-functional surfactants.[31,32]

Free radical polymerisation (FRP) is the most desirable route to synthesising polymers. The main factors contributing to its success are (1) it is compatible with most monomer systems, (2) it is tolerant to most functional groups and small amounts of impurities and (3) it has been successfully implemented under different reaction conditions i.e. bulk, solution, emulsion, suspension and miniemulsion. However, the main drawbacks of the technique are poor

control over macromolecular structure i.e. molar mass distribution, chemical composition and architecture.

The advent of new techniques for implementing reversible deactivation radical polymerisation (RDRP) or living radical polymerisation (LRP) has provided access to macromolecular structure control. In RDRP end capping agents (X in Scheme 2.1) are used to impart "living" characteristics[33] on a polymerisation by suppressing reactions that irreversibly terminate polymer growth.
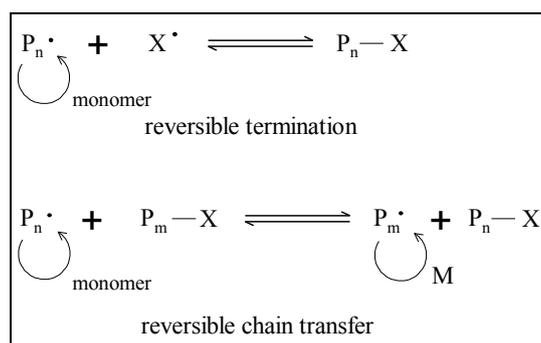
Scheme 2.1 Mechanisms governing reversible deactivation radical polymerisation

RDRP involves superimposing chain transfer reactions or reversible termination reactions (Scheme 2.1) onto a radical polymerisation process. The key step is the reaction of the propagating radical (P_n•) with end capping agents (X) so that the majority of the polymer chains remain dormant (P_n–X). Rapid equilibration between active propagating species and dormant polymer chains ensures that polymer chains grow simultaneously.

The most reported processes are atom transfer radical polymerisation (ATRP)[34-38] and nitroxide-mediated polymerisation (NMP)[39-43] which are governed by reversible termination, and reversible addition-fragmentation chain transfer (RAFT) polymerisation [44-47] and iodine-mediated polymerisation (IMP)[48-50] which are governed by degenerative chain transfer. The first three processes have been employed in the synthesis of PCN comprising well defined polymers. Some researchers have subsequently proceeded to successfully make inorganic/organic hybrid materials comprising block copolymers.[51,52]

2.2   Synthesis of PCN by SI-reversible deactivation radical polymerisation

"Grafting from" is accomplished by *in situ* polymerisation of monomer in the presence of initiator-modified clay.[16,17,30] As the tethered polymer chains grow, they force the stacked clay

platelets apart leading to their dispersion in the polymer matrix.[53,54] Surface-initiated reversible deactivation radical polymerisation (SI-RDRP) where a RAFT agent, ATRP or NMP initiator are attached to the clay surface has become a prime method of interest. It not only provides access to PCNs but also affords well-defined polymer brushes grafted to an inorganic surface.[55] These materials are interesting and have potential application in electronics, engineering and optics. Barbey *et al.* wrote an interesting review on the use of RDRP techniques to synthesise polymer brushes from a variety of inorganic and organic substrates.[55]

2.2.1   Surface-initiated nitroxide-mediated polymerisation (SI-NMP)

Credit is given to Weimer *et al.* [56] for demonstrating for the first time that polymer chains can be grown from clay surfaces via NMP. NMP involves the use of a stable radical (nitroxide) to reversibly terminate polymer growth. The most important features of the stable radical are that it does not initiate polymerisation or take part in any side reactions. There are two basic structures of nitroxides that have been reported. The first class bears two quaternary carbons in α-position to the N–O moiety e.g. 2,2,6,6-tetramethylpiperidinyloxyl (TEMPO) **(1)** and derivatives; and the second bearing a methine in α-position to the N–O, e.g. phosphonate derivatives, N-tert-butyl-N-[1-diethylphosphono-(2,2-dimethylpropyl)] (DEPN) **(2)** and arene derivatives **(3)**.
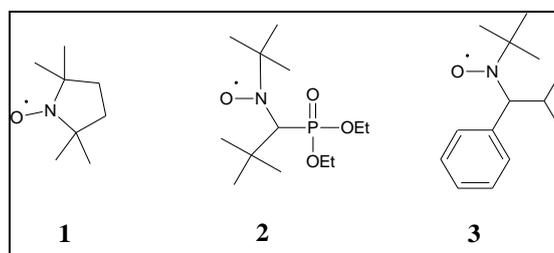
Figure 2.3 Examples of nitroxides used in NMP

The success of an SI-RDRP experiment is often measured by (1) the grafting density and (2) narrow molar mass distribution of the surface-tethered chains. Weimer *et al.* intercalated a quaternary ammonium alkoxyamine **4** (Table 2.1) within montmorillonite (MMT) clay galleries and polymerised styrene. The mediating nitroxide was TEMPO and they prepared PCNs comprising polymers with narrow molar mass dispersities (Đ<1.5). Similarly Shen *et al.*[57] polymerised styrene in the presence of TEMPO. Their approach differed to Weimer's in that the alkoxyamine initiator was synthesised *in situ*. Although TEMPO is a commercially

available nitroxide, its use has been limited owing to (1) the need for elevated polymerisation temperatures, (2) long reaction times and (3) incompatibility with a range of monomers. Konn *et al.*[58] attached a DEPN bearing initiator **5** to the surface of Laponite clay and successfully grafted polystyrene (PS) therefrom. Using high polymerisation temperatures of 110ºC increased the propensity of styrene to autoinitiate; hence they added free NMP initiator to the polymerisation mixture to control the polymerisation of free (unattached) polymer. They proceeded to compare the molar masses of the free and grafted polymer and the results were in good agreement. However, there is uncertainty surrounding the grafting densities owing to the procedure they used to remove the free polymer.

Table 2.1 Cationic NMP initiators used for grafting polystyrene from clay

NMP initiator	Polymer	Reference
4	Polystyrene	56
5	Polystyrene	58
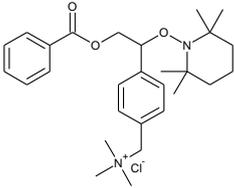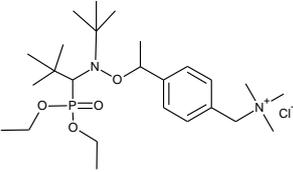
Another measure for the "livingness" of an RDRP system is its ability to chain extend and form block copolymers. In the work reported by Sogah on SI-NMP, they showed the "livingness" of the system by chain extending with polystyrene. The same group also reported on the synthesis of poly(styrene-b-caprolactone)/silicate nanocomposites. However, they used a different synthetic approach. They used a trifunctional NMP initiator attached to the clay surface to simultaneously polymerise styrene and carry out ring opening polymerisation of ε-caprolactone.[59]

2.2.2   Surface-initiated atom transfer radical polymerisation (SI-ATRP)

ATRP is the most extensively studied process in SI-RDRP from clay surfaces. It is compatible with a wider range of monomers compared to NMP. The key step in the process is atom (halide) transfer between a propagating radical and a transition metal complex.[35]

SI-ATRP is accomplished by *in situ* polymerisation of monomer in the presence of a clay that is modified with the ATRP initiator. Two avenues have been explored for the attachment of the ATRP initiators to the clay surface (1) ion exchange[32,51,52,60,61] and (2) covalent attachment.[14,62,63] Examples of the initiators used and polymer systems studied are given in Table 2.2.

Although a number of researchers have reported the synthesis of PCN consisting of polymer with narrow molar mass dispersities[51,60,61] others have reported the contrary. Mathias and coworkers[64] obtained PCN comprising poly(methyl methacrylate) (PMMA) with molar mass dispersities between 2 and 2.5. They attributed this to the excess amount of copper catalyst in the sample. Zhao and coworkers[60] also observed a similar trend in molar mass dispersity when the polymerisation was performed for long periods of time. SI-polymerisation differs from typical bulk polymerisation in that the propagating radical in the former is confined to the surface. Cochran *et al.*[65] have investigated the effects that the grafting density has on the kinetics of SI-ATRP of styrene.

Attempts to synthesise block copolymers via SI-ATRP have been successful with block copolymers of styrene with n-butyl acrylate[51,52] and caprolactone[59] being synthesised. Other researchers[66] have combined SI-ATRP with ring opening polymerisation techniques following modification of the halogenated chain ends to make block copolymers.

Table 2.2 ATRP initiators used for SI-ATRP from clay

ATRP initiator	Polymer	Reference
6	PS, PS-b-P(n-BA), PMMA, PLA	32,51,52,60,61
7	PMMA, P(n-BA)	62
8	PGMA	14
		63
9	PEA	
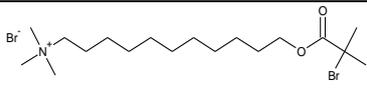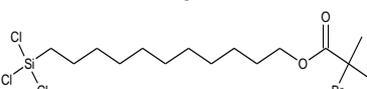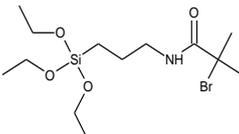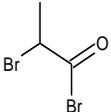
2.2.3 Surface-initiated reversible addition-fragmentation chain transfer polymerisation (SI-RAFT)

The RAFT process has become a primary choice for RDRP because of its capability to control a wide range of monomers without the use of a metal catalyst and at low temperatures. It is tolerant to various reaction conditions, hence it has been successfully implemented in heterogeneous (aqueous) media. Polymerisation by the RAFT process is controlled through a degenerative chain transfer mechanism using thiocarbonyl thio chain transfer agents, (Z(C=S)–SR), which have two characteristic moieties: the R group or leaving and reinitiating group, and the Z group which stabilises the intermediate radical formed during polymerisation.

The main step in the RAFT process (see Scheme 2.2) is the equilibrium between propagating radicals $P_n\bullet$ and $P_m\bullet$ with dormant polymeric RAFT agents, structures **10** and **12** via the intermediate radical, **11**.
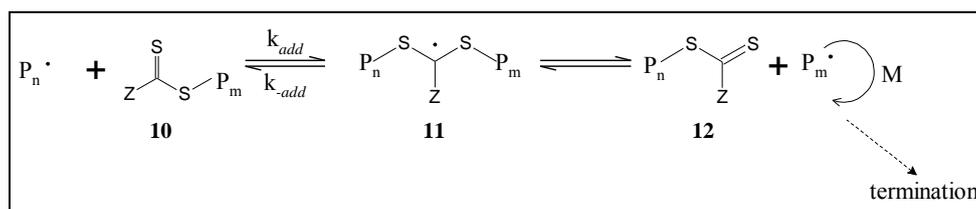
Scheme 2.2 Main equilibrium step in the RAFT process

This leads to the incorporation of the RAFT agent in the final polymeric product and is visually seen as a tint ranging from pale yellow to red depending on the structure of the RAFT agent used. The presence of colour and sulphurous odours has motivated scientists to develop post-polymerisation techniques to remove the thiocarbonyl thio moiety. Examples of these methods are aminolysis,[67,68] thermolysis,[69,70] and radically induced reduction.[71-73]

To achieve good control over a RAFT mediated polymerisation, a careful choice of RAFT agent must be made. There are four classes of RAFT agents differing by the substituent groups adjacent to the C=S moiety, these are xanthates, dithiocarbamates, dithioesters and trithiocarbonates, [44,74] their structures are illustrated in Figure 2.4.
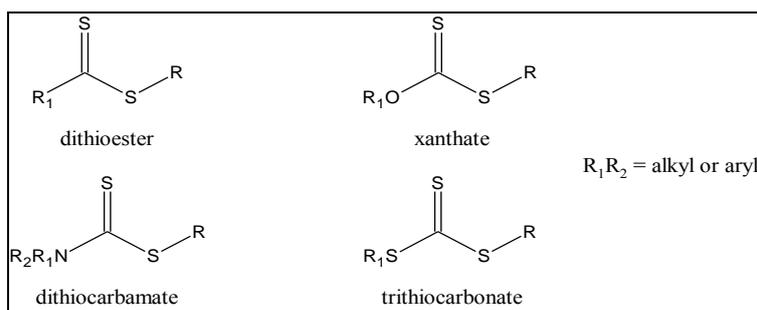
Figure 2.4 Main classes of thiocarbonyl thio based RAFT agents

The class of RAFT agents chosen depends on the structure of the monomer to be polymerised.[47] The nature of the Z-group plays a key role in the activation of the C=S bond and the stabilisation of the intermediate radical whilst the R-group must be a good leaving and reinitiating group.

RAFT agents can be functionalised at either the R-group or the Z-group during their synthesis. This leads to the terms 'R-group approach' and 'Z-group approach' for SI-RAFT polymerisation. Both approaches have their advantages and disadvantages as will be explained shortly.
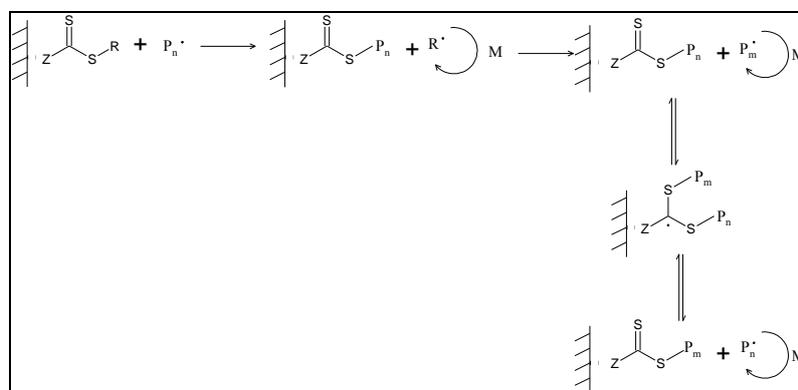
Scheme 2.3 Simplified representation of SI-RAFT via the Z-group approach

The Z-group approach is illustrated in Scheme 2.3. The RAFT agent is anchored to the surface via the thiocarbonyl thio bearing group and remains attached to the surface, whilst the propagating radicals grow in the bulk solution. The propagating radicals have to diffuse back to the surface to ensure that reversible deactivation occurs and not termination. Though this approach yields a well-defined polymer that is attached to the surface, the molar masses are limited and the grafting densities very low. [75,76]

In the R-group approach (illustrated in Scheme 2.4), the thiocarbonyl thio moiety migrates between the surface and solution whilst propagation occurs at the surface. Although this approach leads to higher grafting densities and higher molar masses of the grafted polymer compared to the former, the molar mass dispersity is broader and there is loss of the desired chain end functionality as a result of bimolecular termination reactions.[77]
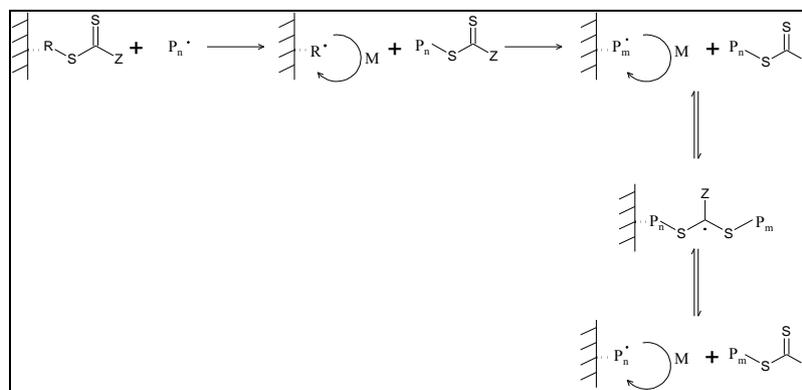
Scheme 2.4 Simplified representation of SI-RAFT via the R-group approach

Mechanistically the RAFT process is superimposed onto a conventional free radical polymerisation process so there is need to generate initiating radicals. The formation of free polymer is thus inevitable and the polymer often has ill-defined end groups and broad molar mass distributions. These shortcomings in SI-RAFT are a result of the reduced accessibility of the surface immobilised RAFT agent to the radicals initiated in solution. A number of researchers have circumvented this by adding free RAFT agent in solution to ensure that polymer chains initiated in solution do not terminate prior to taking part in RDRP. This approach has been used on silica particles[75,76,78-83] and has not been reported for clay nanoparticles.

A few reports have been published in literature on the use of cationically functionalised RAFT agents to graft polymer from clay particles. Zhang *et al.*[84] synthesised a cationically functionalised dithiocarbonate (structure **13** in Table 2.3) which they used to control the polymerisation of styrene from MMT. They had good control over the molar masses of the free polymer and the molar mass dispersities were narrow i.e. < 1.3. Around the same time, Sogah and Di[85] used the cationically functionalised dithiocarbamate **14** to modify MMT and polymerise styrene (S), methyl methacrylate (MMA), and tert-butyl acrylate (t-BA). Although the experimental molar masses were significantly higher than the calculated ones and they obtained broad molar mass dispersity values, block copolymerisation was successful.

Samakande *et al.*[86] attached a cationic dithiocarbonate **15** and a trithiocarbonate **16** onto clay and polymerised styrene. They also reported broad molar mass dispersities of >1.5 for polystyrene. In all the work described above, R-functionalised RAFT agents were used. There was no comparison of the molar mass of the grafted polymer chains and free polymer that was made, but the materials showed an improvement in thermal stability.

Table 2.3 Cationic RAFT agents used for SI-RAFT from clay

Functionalised RAFT agent	Polymer	Reference
13	PS	87
14	PS, PMMA, P(t-BA), PS-b-PMMA, PMMA-b-PS	85
15	PS	86
16	PS	86
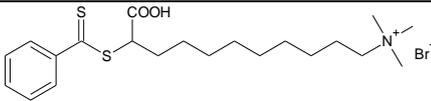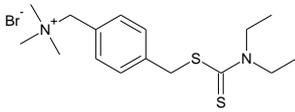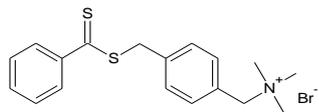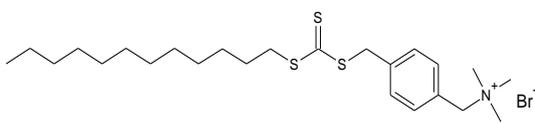
The need to use an outside source to generate initiating radicals for RAFT polymerisation offers a second approach by which SI-RAFT can be accomplished. The surface of the clay can be modified by a thermal or a photo-initiator followed by polymerisation in the presence of free RAFT agent. This approach has been reported by Samakande *et al.*[88] and has yielded free polymer with narrow molar mass distributions.

The simultaneous growth of polymer from solid surfaces and solution via RDRP has been used to evaluate the grafting density. The assumption made is that free polymer and tethered polymer grow at the same rate. Experimentally this has produced mixed results. In some cases the molar mass of the grafted polymer was similar to the free polymer,[89] while in other cases the grafted polymer had lower molar masses and broader molar mass dispersities.[90] Turgman-

Cohen and Genzer[91] recently investigated simultaneous bulk and surface-initiated RDRP using Monte-Carlo computer simulations. The model they used had initiator bound to a flat surface (like clay) as well as free initiator in solution. Their results showed that the outcome of the polymerisation was dependent upon the grafting density as well as the concentration of surface-immobilised initiator. Making an assumption that the polymerisation rates were similar was inaccurate, because the surface-confined and free propagating radicals were growing under different environments.

Differences in polymerisation rates will affect the following properties of the macromolecular structure: (1) molar mass, (2) molar mass distribution and (3) chain end functionality. In all the work that has been reported on SI-RDRP from clay, not much data are available on the differences in molar mass of the surface-confined polymer and that growing in solution. In addition, no study has been done to understand the reactions of the surface-confined radical through examining the chain end functionality of the free and grafted polymer.

In order to model and engineer a PCN with the desired properties, there is need to understand the structure-property relationships. Knowledge of the structure and composition, shape and size, clay surface chemistry and heterogeneity of the polymer matrix is of paramount importance. There is thus need to develop new analytical techniques for investigating the heterogeneity of the material.

2.3   Characterisation of polymer-clay nanocomposites

PCNs have attracted significant attention in industry as well as academia and their characterisation helps to enlighten on the mechanisms involved in their preparation, their properties as well as applications. SI-polymerisation from clay surfaces involves the following main steps: (1) modification of clay by initiator or chain transfer agent, (2) dispersion of surface modified clay into monomer followed by (3) polymerisation. Various analytical techniques have been reported in literature for the characterisation of the organo-modified clay and the resultant nanocomposite. A description of some of the analytical techniques reported will be given.

2.3.1   Characterisation of initiator or chain transfer agent modified clay

The standard technique used for proving clay surface modification qualitatively is Fourier transform-infrared spectroscopy (FT-IR). The FT-IR spectrum of the modified clay is a superimposition of the individual spectra for the pure organic modifier and the clay.[11,17,92]

Mathias and coworkers.[6,64,93] and Isoda *et al.*[5] used solid state ^{13}C and ^{29}Si NMR to qualitatively and quantitatively determine the extent of clay modification. Other spectroscopic techniques that have been used are x-ray photoelectron spectroscopy (XPS),[12,17,57] ultraviolet (UV) spectroscopy[58] and elemental analysis (EA).[31,63] To date the most convenient method for quantitation is thermogravimetric analysis (TGA). Here the organic weight loss after heating at elevated temperatures is correlated to the amount of organic modifier in the sample.

2.3.2   Characterisation of the polymer-clay nanocomposite

Different techniques have been used for the characterisation of the final nanocomposite material. These techniques provide mostly information on the bulk and compositional properties of the material which are beneficial for application. Regarding the structure of the nanocomposite i.e. whether it is intercalated or exfoliated; x-ray diffraction (XRD) is often used concurrently with transmission electron microscopy (TEM).[94] Cole and coworkers have also reported on the use of FT-IR.[95,96]

TGA and differential scanning calorimetry (DSC) provide information on the thermal stability, glass transition temperature (T_g) and crystalline melting temperature (T_m) of the material. TGA also provides a direct means of determining the amount of clay in a nanocomposite termed the clay loading. The mechanical properties of PCNs have been studied by dynamic mechanical analysis (DMA)[64] and the processibility by rheology.[97]

PCN are complex multicomponent materials. When synthesised via SI-FRP they consist of the following: free and grafted polymer as well as grafted and ungrafted clay. For better understanding of the PCN, various methods and experimental approaches have been undertaken to characterise them. The approaches taken in this work are summarised in the following sections.

2.3.2.1 Thermogravimetric analysis (TGA)

Non-isothermal thermogravimetric analysis provides three important types of information regarding a material, (1) organic constitution, (2) thermal stability and (3) thermal degradation behaviour. TGA is a reliable method for quantitatively determining the organic content in organic/inorganic hybrid materials based on the weight loss of the material. The fraction of non-volatile residue (char) remaining after heating above 600°C has been correlated to the amount of clay in the sample.[98,99] The thermal stability of a material is defined as the

temperature at which it starts to degrade. This parameter is of paramount importance for the processibility of the material. It is important that the bulk of the material does not start to decompose close to the processing temperature as this will lead to contamination of the final product with thermal decomposition products. It has been widely reported that the incorporation of the clay layers into the polymer matrix results in an improvement of the thermal stability of the polymer. [100-103] How this happens is not really clear, but it has been reported that clay layers enhance the formation of char, which reduces the diffusion of volatiles from the bulk polymer consequently reducing the rate of weight loss.[104] The general notion is that the enhancement of thermal stability in nanocomposites is brought about by (1) the manner in which the silicate layers are dispersed, (2) the strength of the interactions between the clay and the polymer, (3) the type of polymer considered and (4) the synthetic method.

The thermal degradation behaviour considers different temperatures at which the material decomposes. Considering the different weight loss steps in the thermogram can provide essential structural information on the material e.g. the presence of small molecules or functional groups that could trigger thermal decomposition during processing. [105-107] TGA coupled to a spectroscopic techniques such as FT-IR has been used to investigate mechanistic aspects of the thermal degradation of nanocomposites.[108]

2.3.2.2 Differential scanning calorimetry (DSC)

Polymers in the solid state can be classified as follows: (1) crystalline, (2) glassy and (3) network. A crystalline polymer is one in which the molecules (monomer units) are in an ordered manner forming crystals, whilst there is no long range order of the molecules in a glassy (amorphous) polymer. Some polymers comprise both the amorphous and crystalline regions and are thus termed semi-crystalline.

The glass transition temperature, T_g is the temperature at which the polymer chains in an amorphous polymer transform from being in a rigid glassy state to a rubbery state. The T_g of a polymer is the most important characteristic when choosing a polymer for a particular application. The T_g should be higher than the temperature at which the material shall be used as a solid; and below the temperature at which the material shall be used as a liquid. The T_g is dependent upon the method of nanocomposite synthesis.[109] As such DSC has been used to investigate various processes occurring whilst heating or cooling a polymer-clay

nanocomposite i.e. (1) crystalline melting, (2) crystallisation, (3) curing and (4) glass transition. [64,93]

DSC has also been used to qualitatively and quantitatively determine modifications of clay by azo-initiators.[30,110] Fan *et al.*[110] compared the ΔH after heating a pure azoinitiator and the initiator modified clay. To do this, they made the basic assumption that the attachment of the initiator to the clay did not affect the thermal decomposition of the azo group.

2.3.3   Characterisation of free and grafted polymer

Polymers are disperse with regards to (1) molar mass, (2) topology, (3) chemical composition (for copolymers) (4) chain end functionality and (5) stereoregularity as summarised in Figure 2.5.
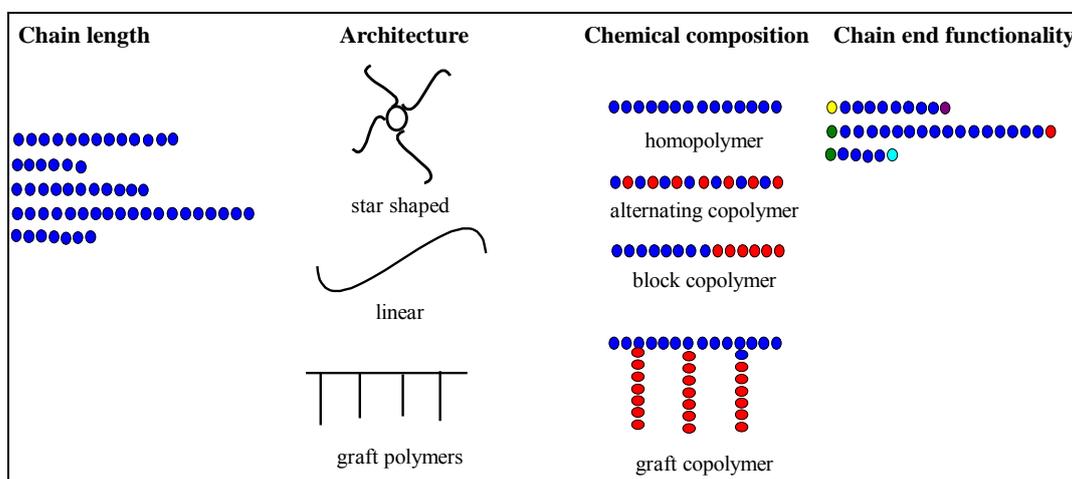
Figure 2.5 Schematic representation of polymer heterogeneity

Various techniques have been used to provide information on each of these parameters. The techniques that have been used for free and grafted polymer are summarised in the following sections.

2.3.3.1 Chromatography

Size exclusion chromatography (SEC)

The free polymer recovered by washing the PCN is often subjected directly to size exclusion chromatography (SEC). SEC is a chromatographic technique that separates macromolecules according to their hydrodynamic volume i.e. macromolecular size in solution. SEC is a relative method based on the physical behaviour of the polymer in solution, hence there is need to calibrate the method with samples of similar structure and known molar mass. Molar mass values from SEC are reported as the *number-average* molar mass (M_n) and *weight-*

average molar mass (M_w). The breadth of the distribution termed molar mass dispersity is then given by the ratio of M_w/M_n.

The grafted polymer must be detached from the clay prior to SEC analysis. Polymer molecules attached via covalent attachment are cleaved by acid catalysed hydrolysis;[64,111] whilst polymer molecules attached via electrostatic interactions are cleaved by ion exchange using Li^+.[32,58] However, this approach is often complicated by the very low concentrations of recovered polymer. In some cases the small concentration of recovered polymer is thwarted by recovered unpolymerised initiator making it challenging to get useful information on the molar mass and molar mass distribution.[91] Often people inaccurately quote the molar mass of the free polymer and make the assumption that it is the same for the grafted polymer. As such there is need to develop alternative analytical techniques to acquire information on the molar mass of the grafted polymer.

2.3.3.2 Spectroscopic techniques

Nuclear magnetic resonance spectroscopy (NMR)

Solution NMR is a useful technique for determining the chemical structure of molecules. In polymer analysis it has been used for the determination of monomer sequences,[112-114] reactivity ratios, [115-117] stereoregularity, [118-120] and end group composition.[67,121,122] It is also a useful technique for determining molar masses of polymers.[123] It falls under the group of equivalent methods for molar mass determination as it is based on comparing the area intensity of end group proton signals to those of the polymer backbone. Though it has been used effectively for low molar mass polymers[122-124] its application to higher molar mass polymers is often challenging due to the reduced intensity of the signals of the end group protons relative to the signals from back bone protons. In addition, the exact structure and number of end groups must be known.
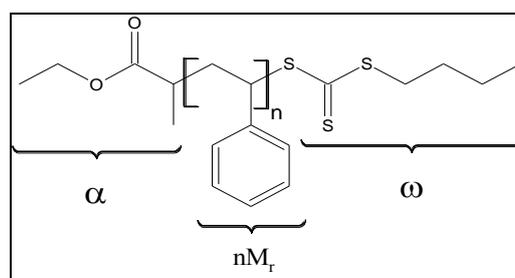
Figure 2.6 Ideal structure of RAFT polymerised polystyrene

For a given polymer (Figure 2.6) with known end groups, the number average molar mass is given by equation 2.1.

$$M_n = M_{\text{end group}}(\alpha) + n*M_{\text{monomer}} + M_{\text{end group}}(\omega) \qquad (2.1)$$

where $M_{\text{end group}}$ (α) and $M_{\text{end group}}$ (ω) are the molar masses (in g/mol) of the initiating and terminating groups; n is the number of repeat units estimated by comparing the signals of any of the end group protons to backbone protons and M_r is the molecular mass of the repeat unit. With reference to PCN characterisation, ^{1}H NMR has been used to investigate the stereoregularity of PMMA.[125]

Matrix-assisted laser desorption/ionisation time-of-flight mass spectrometry (MALDI-TOF MS)

Mass spectrometry using soft ionisation techniques such as electrospray and matrix-assisted laser desorption/ionisation (ESI-MS and MALDI-MS) has attracted significant attention in polymer analysis. This is because macromolecules can be analysed with little or no fragmentation. As a result, important information on the molar mass and molar mass distribution,[126-129] chemical composition,[130] chain end functionality [131,132] and polymer architecture[133,134] can be obtained. In addition, ESI-MS and MALDI-MS have been used to probe reaction and polymerisation mechanisms[134-139] and investigate polymer degradation.[140] MALDI-MS is often preferred over ESI-MS as only singly charged species are observed. Thus it offers a less tedious way of determining the absolute molar mass of polymer as well as the chemical structure of individual polymer chains.

There are three basic steps in the MALDI-MS process and these are shown schematically below:

Ionisation $\longrightarrow$ Separation of ionised molecules $\longrightarrow$ Detection
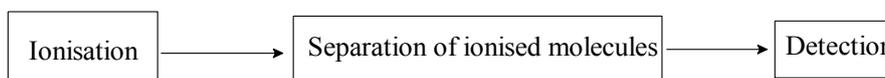
The polymer sample is embedded in an organic matrix to enable desorption and ionisation of the polymer upon irradiation with a pulsed UV laser. For polymers that do not ionise readily on their own, cationising salts are often added containing e.g. Ag^+, Na^+, Li^+ or Cu^+. The charged polymer species in the gas phase are then separated according to their mass-to-charge ratio (m/z) in the mass analyser prior to being detected. The advantage of MALDI-MS is that

only singly charged species are detected hence the m/z value of a particular peak can be used to calculate the molar mass of the end groups as shown in equation 2.2.

$$m/z = M_{\text{end group}}(\alpha) + n*M_{\text{monomer}} + M_{\text{end group}}(\omega) + M_{\text{counterion}} \quad (2.2)$$

where $M_{\text{end group}}$ (α) and $M_{\text{end group}}$ (ω) are the molar masses of the groups at the initiating and terminating ends of the polymer, n is the number of repeat units, M_{monomer} is the molecular mass of the monomer repeat unit, $M_{\text{counterion}}$ is the molecular mass of the cationising salt.

The main limitation of the MALDI-MS process comes when analysing samples with broad molar mass distributions.[129,141,142] Challenges have also been met when analysing polymers with labile end groups (prepared by RDRP).[132] Halogen, thiocarbonylthio and nitroxide end groups are known to fragment during MALDI-MS analysis yielding unsaturated end groups.[48,49,132,143] Favier *et al*[144] reported on the formation of a thioester end group following the oxidation of the dithioester.[145]

Analysing polymers that are heterogeneous with respect to chain end functionality is also challenging.[146] Polymers with different end groups have different ionisation efficiencies. This together with molar mass discrimination effects makes the use of MALDI MS as a quantitative tool challenging.

MALDI-MS was used by Choi *et al*[147] to determine the molar mass of PMMA from a nanocomposite they synthesised via emulsion polymerisation. The oligomers they recovered by ion exchange had low molar masses of <500 g/mol (from MALDI-MS). In the present work, we took a new approach to this analysis. Polymer grafted from Laponite clay was analysed directly by MALDI-MS without the need to detach it. This approach was possible because the polymer was attached to the clay via electrostatic interactions between the negative charges of the clay surface and the positive charge of the reinitiating group. Zagorevskii *et al.*[148] reported also on the direct analysis of oligonucleotides (RNA and DNA) from montmorillonite clay. Their synthetic approach was different as the nucleotides were not attached to the clay i.e. the clay was used as a catalyst for the synthesis of these oligonucleotides.

2.3.4   Separation of the PCN into its components

Liquid chromatography (LC) techniques have been efficient for separating and characterising complex polymer mixtures for decades. For separating polymer mixtures according to their size in solution, SEC has been the most effective. However, column based techniques are limiting when it comes to the analysis of high molecular weight polymers and nanoparticles. Analyte species tend to adsorb to the stationary phase and shearing forces tend to degrade them. These challenges with column based techniques have been circumvented by using open channels in an external field called field-flow fractionation (FFF).

Field-flow fractionation (FFF)

FFF differs from other chromatographic techniques in that there is no stationary phase used and separation occurs in one phase in empty open channels. Problems associated with sample loss due to adsorption and shear degradation are thus eliminated. As a result, analyte species ranging from a few nanometres to tens of micrometres can be effectively characterised.[149] To retain the analyte species and thus separate them according to size, an external force field is applied perpendicular to the axial or channel flow. Examples of fields that can be applied include sedimentation, thermal, cross-flow, magnetic, dielectric and acoustic.[149,150]

Flow field flow fractionation (FlFFF) is the most versatile sub-technique of FFF. The retention of the analyte is accomplished by applying a secondary mobile phase as the cross-flow. FlFFF can be divided into two types (1) asymmetrical FlFFF (AF^4) and (2) symmetrical FlFFF (F^4). The difference between the two lies in the generation of the crossflow. In the former, the channel consists of an upper solid impermeable wall and a lower wall with porous frits as illustrated in Figure 2.7. The lower wall, also called the accumulation wall is covered by a membrane with pores large enough to allow solvent to pass through but sufficiently small to minimise sample loss. The cross-flow is thus generated as follows: two input flows referred to as the tip/axial flow and the focus flow enter the channel close to the upper wall. The focus flow enters close to the centre of the channel and splits into two sub streams. The first part meets the tip flow close to the entry of the channel and the two leave the channel as the cross flow. The other part forms a parabolic flow profile and leaves the channel as the detector flow.
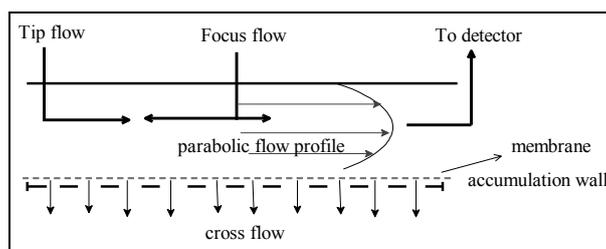
Figure 2.7 Schematic representation of AF^4 instrument setup

In the symmetrical FlFFF setup both channel walls are permeable thus the cross-flow is generated by pumping the carrier fluid through the porous frits of the upper wall.

Unlike in liquid chromatography where retention results from interaction between analyte and stationary phase, in FFF retention occurs when analyte particles exist in regions where the velocity is lower than that of carrier fluid. After sample injection, the generated cross-flow pushes the analyte species towards the accumulation wall (where the carrier fluid velocity is near zero). The resulting concentration build-up causes the analyte species to diffuse back to the centre of the channel and occupy regions of varying flow velocities according to their diffusion coefficients. Smaller molecules diffuse faster and occupy regions of higher velocity and are thus eluted first. For the theoretical aspects of FFF, the reader is referred to the following publications.[149-151]

There are three main mechanisms that govern analyte separation namely normal mode, steric mode and hyperlayer mode, illustrated in Figure 2.8. The normal mode predominates for analyte species with a diameter of < 1µm, and occurs as described above. In the steric mode the smaller particles occupy spaces closest to the accumulation wall compared to the larger ones. Consequently larger particles get caught up in regions of higher flow velocity and elute earlier than the smaller species.
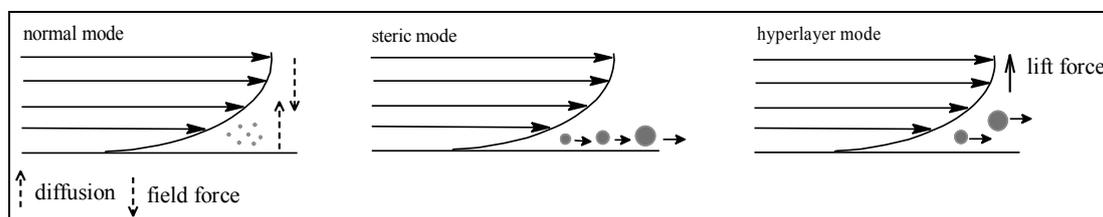
Figure 2.8 Schematic representation of the modes of separation in FFF

In the hyperlayer mode, lift forces cause analyte species to diffuse to regions of high flow velocities as illustrated in the diagram. Similar to the steric mode, larger species elute earlier than smaller ones.

FlFFF has been used in the analysis of a range of complex materials from dissolved polymers to organic and inorganic nanoparticles.[152] It has been very useful for determining the component distributions in a complex sample. When connected to suitable detectors e.g. multi-angle light scattering (MALS), additional information on the molar mass, size (radius of gyration) and conformation of the analyte species can be acquired.[153]

2.4   Our approach

The process of mixing clay with polymers to make PCN was pioneered by the Toyota Company in 1985. They found that mixing a few wt.-% of clay with nylon resulted in a material with remarkably improved thermal stability, mechanical and barrier properties compared to the pure polymer.[1,2] Since then, this technology has developed; with new approaches to their synthesis being designed and its depth of application extending to the food packaging and electric industries. What makes nanocomposites superior to the conventional composites is the proper dispersion of silicate layers within the polymer matrix. The improved mixing of the two components leads to an improvement in material properties and in some cases the appearance of new properties. [154]

The aim of this work was to synthesise specific PCNs. The first approach taken was to use Laponite clay which has disk-shaped particles with a uniform size of 25 nm in diameter. This is in contrast to the widely used montmorillonite which has a particle size ranging from 30–300 nm. It was envisaged that uniformly sized silicate layers would be better dispersed in the polymer matrix, leading to a greater improvement in the nanocomposite properties. In addition, Laponite clay is synthetic meaning it is free from inorganic impurities present in naturally occurring clay. Uniform size and lack of inorganic impurities make it an interesting candidate in both industry and academia.

The second point considered was the method of nanocomposite synthesis. Surface-initiated *in situ* polymerisation ("grafting from") was opted for as it leads to the dispersion of silicate layers during polymerisation. Having clay coated with polymer is ideal, as this improves miscibility of the clay with the host polymer. Free radical polymerisation was chosen over ionic and ring opening polymerisation because of its versatility and simplicity. The drawbacks of conventional radical polymerisation include poor control over molar mass and molar mass distribution, chain end functionality and architecture hence RDRP processes were opted for. Molar mass control is of paramount importance in the synthesis of nanocomposites as it has a

huge effect on the processibility of the resultant material. Of the three most used techniques in PCN synthesis i.e. ATRP, NMP and RAFT, [63,155] the RAFT process was chosen.

The class of RAFT agents employed in this work was determined mainly by the monomer systems that were investigated. Trithiocarbonates have been known to effectively control the polymerisation of styrene and meth(acrylates).[44,78,156-158] In order to functionalise the clay particles via SI-RAFT polymerisation, we synthesised novel RAFT agents bearing a quaternary ammonium functional group for attaching to the clay surface. Free RAFT agent was added to the polymerisation mixture to create an overall concentration of RAFT agent, to ensure simultaneous growth of the surface-immobilised polymer and the polymer growing in solution.

An assumption often made by others is that the surface-immobilised and the free polymers grow at the same rate. This is highly unlikely because the surface-immobilised polymer is confined within its space and depends on the diffusion of monomer from solution to ensure propagation and not termination. This was confirmed by the recent findings of Turgman-Cohen and Genzer.[91] To answer some of these questions, we compared the molar masses of the free and the grafted polymers.

The key feature of the RAFT process is that the RAFT agent be incorporated in the final polymeric product. This would not only mean that the polymer chains were growing simultaneously, but also enable grafting of polymer chains with controlled architectures. In line with this, we went a step further into investigating the nature of the end groups formed in solution and at the surface. This would provide useful information on the side reactions of the confined propagating radical. This approach is new to the characterisation of polymer-clay nanocomposites and will open ways of understanding their synthesis via RDRP and will lead to a better understanding of the processibility.

PCNs are complex mixtures. To get a better understanding of these materials, there is a need to separate them into the various components and look at them individually. New analytical methods for the separation and characterisation of the PCN via asymmetrical FlFFF will be developed. Separation of the clay into the various components will give an idea on the efficiency of the synthesis method employed. This type of analysis is new to polymer-clay nanocomposites.

Bulk properties of these materials particularly the thermal stability was investigated.

References

(1)   Kojima, Y.; Usuki, A.; Kawasumi, M.; Okada, A.; Fukushima, Y.; Kurauchi, T.; Kamigaito, O. *J. Mater. Res.* **1993**, *8*, 1185–1189.

(2)   Okada, A.; Usuki, A. *Macromol. Mater. Eng.* **2006**, *291*, 1449–1476.

(3)   Tasdelen, M. A.; Kahveci, M. U.; Yagci, Y. *Prog. Polym. Sci.* **2011**, *36*, 455–567.

(4)   Yoon, K.-b.; Sung, H.-d.; Hwang, Y.-y.; Kyun Noh, S.; Lee, D.-h. *Appl Clay Sci.* **2007**, *38*, 1–8.

(5)   Isoda, K.; Kuroda, K.; Ogawa, M. *Chem. Mater.* **2000**, *12*, 1702–1707.

(6)   Wheeler, P. A.; Wang, J.; Baker, J.; Mathias, L. J. *Chem. Mater.* **2005**, *17*, 3012–3018.

(7)   Gültek, A.; Seçkin, T.; Őnal, Y.; Içduygu, M. G. *Turk J Chem* **2002**, *26*, 925–937.

(8)   Karthikeyan, C. S.; Nunes, S. P.; Prado, L. A. S. A.; Ponce, M. L.; Silva, H.; Ruffmann, B.; Schulte, K. *J. Membr. Sci.* **2005**, *254*, 139–146.

(9)   Sedláková, Z.; Pleštil, J.; Baldrian, J.; Šlouf, M.; Holub, P. *Polym. Bull.* **2009**, *63*, 365–384.

(10)   Negrete; Letoffe, J.-M.; Putaux, J.-L.; David, L.; Bourgeat-Lami, E. *Langmuir* **2004**, *20*, 1564–1571.

(11)   Park, M.; Shim, I.-K.; Jung, E.-Y.; Choy, J.-H. *J. Phys. Chem. Solids* **2004**, *65*, 499–501.

(12)   Daniel, L.; Frost, R.; Zhu, H. *J. Colloid Interface Sci.* **2008**, *321*, 302–309.

(13)   Nia, H.; Aaserud, D. J.; Jr, W. J. S.; Soucek, M. D. *Polymer* **2000**, *41*, 57–71.

(14)   Djouani, F.; Herbst, F.; Chehimi, M. M.; Benzarti, K. *Surf. Interface Anal.* **2010**, *42*, 1019–1024.

(15)   Oral, A.; Tasdelen, M. A.; Demirel, A. L.; Yagci, Y. *Polymer* **2009**, *50*, 3905–3910.

(16)   Meier, L. P.; Shelden, R. A.; Caseri, W. R.; Suter, U. W. *Macromolecules* **1994**, *27*, 1637–1642.

(17)   Fan, X.; Xia, C.; Advincula, R. *Langmuir* **2003**, *19*, 4381–4389.

(18)   Zeng, C.; Lee, L. J. *Macromolecules* **2001**, *34*, 4098–4103.

(19)   Klapyta, Z.; Fujita, T.; Iyi, N. *Appl. Clay Sci.* **2001**, *19*, 5–10.

(20)   Lee, S. Y.; Cho, W. J.; Hahn, P. S.; Minhee Lee; Lee, Y. B.; Kim, K. J. *Appl Clay Sci.* **2005**, *30*, 174–180.

(21)   Ludueña, L. N.; Alvarez, V. A.; Vazquez, A. *Mater. Sci. Eng., A* **2007**, *460–461*, 121–129.

(22)   Ahmadi, S. J.; Huang, Y. D.; Li, W. *J. Mater. Sci* **2004**, *39*, 1919–1925.

(23)   Lerari, D.; Peeterbroeck, S.; Benali, S.; Benaboura, A.; Dubois, P. *J. Appl. Polym. Sci.* **2011**, *121*, 1355–1364.

(24)   Fornes, T. D.; Hunter, D. L.; Paul, D. R. *Macromolecules* **2004**, *37*, 1793–1798.

(25)   Tiwari, R. R.; Khilar, K. C.; Natarajan, U. *J. Appl. Polym. Sci.* **2008**, *108*, 1818–1828.

(26)   Wang, D.; Zhu, J.; Yao, Q.; Wilkie, C. A. *Chem. Mater.* **2002**, *14*, 3837–3843.

(27)   Tasdelen, M. A.; Camp, W. V.; Goethals, E.; Dubois, P.; Prez, F. D.; Yagci, Y. *Macromolecules* **2008**, *41*, 6035–6040.

(28)   Anthoulis, G. I.; Kontou, E.; Fainleib, A.; Bei, I.; Gomza, Y. *J. Polym. Sci., Part B: Polym. Phys.,* **2008**, *46*, 1036–1049.

(29)   Chang, K.-C.; Chen, S.-T.; Lin, H.-F.; Lin, C.-Y.; Huang, H.-H.; Yeh, J.-M.; Yu, Y.-H. *Eur. Polym. J.* **2008**, *44*, 13–23.

(30)   Uthirakumar, P.; Kim, C.-J.; Nahm, K. S.; Hahn, Y. B.; Lee, Y.-S. *Colloids Surf., A* **2004**, *247*, 69–75.

(31)   Moet, A. S.; Akelah, A. *Mater. Lett.* **1993**, *18*, 97–102.

(32)   Salem, N.; Shipp, D. A. *Polymer* **2005**, *46*, 8573–8581.

(33)   Mayadunne, R. T. A.; Jeffery, J.; Moad, G.; Rizzardo, E. *Macromolecules* **2003**, *36*, 1505–1513.

(34)   Min, K.; Gao, H.; Matyjaszewski, K. *J. Am. Chem. Soc* **2005**, *127*, 3825–3830.

(35)   Coessens, V.; Matyjaszewski, K. *Macromol. Rapid Commun.* **1999**, *20*, 127–134.

(36)   Kato, M.; Kamigaito, M.; Sawamoto, M.; Higashimura, T. *Macromolecules* **1995**, *28*, 1721–1723.

(37)   Matyjaszewski, K.; Tsarevsky, N. V. *Nat. Chem.* **2009**, *1*, 276–288.

(38)   Patten, T. E.; Matyjaszewski, K. *Adv. Mater.* **1998**, *10*, 901–915.

(39)   Listigovers, N. A.; Georges, M. K.; Odell, P. G.; Keoshkerian, B. *Macromolecules* **1996**, *29*, 8992–8993.

(40)   Fukuda, T.; Goto, A. *Macromol. Rapid Commun.* **1997**, *18*, 683–688.

(41)   Fukuda, T.; Terauchi, T.; Goto, A.; Ohno, K.; Tsujii, Y.; Miyamoto, T.; Kobatake, S.; Yamada, B. *Macromolecules* **1996**, *29*, 6393–6398.

(42)   Thang, S. H.; Chong, Y. K.; Ercole, F.; Moad, G.; Rizzardo, E.; Anderson, A. G. *Macromolecules* **1999**, *32*, 6895–6903.

(43)   Saban, M. D.; Georges, M. K.; Veregin, R. P. N.; Hamer, G. K.; Kazmaier, P. M. *Macromolecules* **1995**, *28*, 7032–7034.

(44)   Moad, G.; Chong, Y. K.; Postma, A.; Rizzardo, E.; Thang, S. H. *Polymer* **2005**, *46* 8458–8468.

(45)   Moad, G.; Rizzardo, E.; Thang, S. H. *Aust. J. Chem.* **2005**, *58*, 379–410.

(46)   Moad, G.; Rizzardo, E.; Thang, S. H. *Acc. Chem. Res.* **2008** *41*, 1133–1142.

(47)   Moad, G.; Rizzardo, E.; Thang, S. H. *Aust. J. Chem.* **2009**, *62*, 1402–1472.

(48)   Boyer, C.; Lacroix-Desmazes, P.; Robin, J.; Boutevin, B. *Macromolecules* **2006**, *39*, 4044–4053.

(49)   Lacroix-Desmazes, P.; Severac, R.; Boutevin, B. *Macromolecules* **2005**, *38*, 6299–6309.

(50)   David, G.; Boyer, C.; Tonnar, J.; Ameduri, B.; Lacroix-Desmazes, P.; Boutevin, B. *Chem. Rev.* **2006**, *106*, 3936–3962.

(51)   Zhao, H.; Farrel, B. P.; Shipp, D. A. *Polymer* **2004**, *45*, 4473–4481.

(52)   Zhao, H.; Shipp, D. A. *Chem. Mater.* **2003**, *15*, 2693–2695.

(53)   Zeng, C.; Lee, L. J. *Macromolecules* **2001**, *34*, 4098–4103.

(54)   Fu, X.; Qutubuddin, S. *Polymer* **2001**, *42*, 807–813.

(55)   Barbey, R.; Lavanant, L.; Paripovic, D.; Schüwer, N.; Sugnaux, C.; Tugulu, S.; Klok, H.-A. *Chem. Rev.* **2009**, *109*, 5437–5527.

(56)   Weimer, M. W.; Chen, H.; Giannelis, E. P.; Sogah, D. Y. *J. Am. Chem. Soc.* **1999**, *121*, 1615–1616.

(57)   Shen, Y.; Wang, Y.; Chen, J.; Li, H.; Li, Z.; Li, C. *J. Appl. Polym. Sci.* **2010**, *118*, 1198–1203.

(58)   Konn, C.; Morel, F.; Beyou, E.; Chaumont, P.; Bourgeat-Lami, E. *Macromolecules* **2007**, *40*, 7464–7472.

(59)   Di, J.; Sogah, D. Y. *Macromolecules* **2006**, *39*, 5052–5057.

(60)   Zhao, H.; Argoti, S. D.; Farrell, B. P.; Shipp, D. A. *J. Polym. Sci., Part A: Polym. Chem.* **2004**, *42*, 916–924.

(61)   Böttcher, H.; Hallensleben, M. L.; Nuß, S.; Wurm, H.; Bauer, J.; Behrens, P. *J. Mater. Chem.* **2002**, *12*, 1351–1354.

(62)   Karesoja, M.; Jokinen, H.; Karjalainen, E.; Pulkkinen, P.; Torkkeli, M.; Soininen, A.; Ruokolainen, J.; Tenhu, H. *J. Polym. Sci., Part A: Polym. Chem.* **2009**, *47*, 3086–3097.

(63)   Datta, H.; Bhowmick, A. K.; Singha, N. K. *J. Polym. Sci., Part A: Polym. Chem.* **2008**, *46*, 5014–5027.

(64)   Wheeler, P. A.; Wang, J.; Mathias, L. J. *Chem. Mater.* **2006**, *18*, 3937–3945.

(65)   Cochran, E. W.; Behling, R. E.; Williams, B. A.; Staade, B. L.; Wolf, L. M. *Macromolecules* **2009**, *42*, 1867–1872.

(66)   Yagci, Y.; Yenice, Z.; Tasdelen, M. A.; Oral, A.; Guler, C. *J. Polym. Sci., Part A: Polym. Chem.* **2009**, *47*, 2190–2197.

(67)   Postma, A.; Davis, T. P.; Moad, G.; O'Shea, M. S. *React. Funct. Polym.* **2006**, *66*, 137–147.

(68)   Xu, J.; He, J.; Fan, D.; Wang, X.; Yang, Y. *Macromolecules* **2006**, *39*, 8616–8624.

(69)   Moad, G.; Chong, B.; Rizzardo, E.; Skidmore, M.; Thang, S. H. *Aust. J. Chem.* **2006**, *59*, 755–762.

(70)   Postma, A.; Davis, T. P.; Moad, G.; O'Shea, M. S. *Macromolecules* **2005**, *38*, 5371–5374.

(71)   Chong, Y. K.; Moad, G.; Rizzardo, E.; Thang, S. H. *Macromolecules* **2007**, *40*, 4446–4455.

(72)   Chen, M.; Moad, G.; Rizzardo, E. *J. Polym. Sci., Part A: Polym. Chem.* **2009**, *47*, 6704–6714.

(73)   Postma, A.; Davis, T. P.; Evans, R. A.; Li, G.; Moad, G.; O'Shea, M. S. *Macromolecules* **2006**, *39*, 5293–5306.

(74)   Favier, A.; Charreyre, M.-T. *Macromol. Rapid Commun.* **2006**, *27*, 653–692.

(75)   Zhao, Y.; Perrier, S. *Macromolecules* **2006**, *39*, 8603–8608.

(76)   Zhao, Y.; Perrier, S. *Macromolecules* **2007**, *40*, 9116–9127.

(77)   Stenzel, M. H. *Macromol. Rapid Commun.* **2009**, *30*, 1603–1624.

(78)   Ranjan, R.; Brittain, W. J. *Macromol. Rapid Commun.* **2008**, *29*, 1104–1110.

(79)   Baum, M.; Brittain, W. *Macromolecules* **2002**, *35*, 610–615.

(80)   Li, C.; Benicewicz, B. *Macromolecules* **2005**, *38*, 5929–5936.

(81)   Ranjan, R.; Brittain, W. J. *Macromolecules* **2007**, *40*, 6217–6223.

(82)   Tsujii, Y.; Ejaz, M.; Sato, K.; Goto, A.; Fukuda, T. *Macromolecules* **2001**, *34*, 8872–8878.

(83)   Li, C.; Benicewicz, B. C. *Macromolecules* **2005**, *38*, 5929–5936.

(84)   Zhang, B.-Q.; Pan, C.-Y.; Hong, C.-Y.; Luan, B.; Shi, P.-J. *Macromol. Rapid Commun.* **2006**, *27*, 97–102.

(85)   Di, J.; Sogah, D. Y. *Macromolecules* **2006**, *39*, 1020–1028.

(86)   Samakande, A.; Juodaityte, J. J.; Sanderson, R. D.; Hartmann, P. C. *Macromol. Mater. Eng.* **2008**, *293*, 428–437.

(87)   Zhang, B.; Pan, C.; Hong, C.; Luan, B.; Shi, P. *Macromol. Rapid Commun.* **2006**, *27*, 97–102.

(88)   Samakande, A.; Sanderson, R. D.; Hartmann, P. C. *Eur. Polym. J.* **2009**, *45* 649–657.

(89)   Kruk, M.; Dufour, B.; Celer, E. B.; Kowalewski, T.; Jaroniec, M.; Matyjaszewski, K. *Macromolecules* **2008**, *41*, 8584–8591.

(90)   Pasetto, P.; Blas, H.; Audouin, F.; Boissière, C.; Sanchez, C.; Save, M.; Charleux, B. *Macromolecules* **2009**, *42*, 5983–5995.

(91)   Turgman-Cohen, S.; Genzer, J. *J. Am. Chem. Soc.* **2011**, *133*, 17567–17569.

(92)   Herrera, N.; Letoffe, J.-M.; Reymond, J.-P.; Pourgeat-Lami, E. *J. Mater. Chem.* **2005**, *15*.

(93)   Wang, J.; Wheeler, P. A.; Jarret, W. L.; Mathias, L. J. *J. Appl. Polym. Sci.* **2007**, *106*, 1496–1506.

(94)   Monticelli, O.; Musina, Z.; Russo, S.; Bals, S. *Mater. Lett.* **2007**, *61*, 3446–3450.

(95)   Cole, K. C. *Macromolecules* **2008**, *41*, 834–843.

(96)   Cole, K. C.; Perrin-Sarazin, F.; Dorval-Douville, G. *Macromol. Symp.* **2005**, *230*, 1–10.

(97)   Samakande, A.; Sanderson, R. D.; Hartmann, P. C. *Polymer* **2009**, *50*, 42–49.

(98)   Su, S.; Jiang, D. D.; Wilkie, C. A. *Polym. Adv. Technol.* **2004**, *15*, 225–231.

(99)   Chigwada, G.; Jiang, D. D.; Wilkie, C. A. *Thermochim. Acta* **2005**, *436*, 113–121.

(100)   Yei, D.; Fu, H.; Chang, Y.; Kuo, S.; Huang, J.; Chang, F. *J. Polym. Sci., Part B: Polym. Phys.* **2007**, *45*, 1781–1787.

(101)   Leszczyńska, A.; Njuguna, J.; Pielichowski, K.; Banerjee, J. R. *Thermochim. Acta* **2007**, *454*, 1–22.

(102)   Leszczýnska, A.; Njuguna, J.; Pielichowski, K.; Banerjee, J. R. *Thermochim. Acta* **2007**, *453*, 75–96.

(103)   Pandey, J. K.; Raghunatha Reddy, K.; Pratheep Kumar, A.; Singh, R. P. *Polym. Degrad. Stab.* **2005**, *88*, 234–250.

(104)   Leszcynska, A.; Pielichowski, K. *J. Therm. Anal. Cal* **2008**, *93*, 677–687.

(105)   Bellucci, F.; Camino, G.; Frache, A.; Saffa, A. *Polym. Degrad. Stab.* **2007**, *92*, 425–436.

(106)   Ding, P.; Zhang, M.; Gai, J.; Qu, B. *J. Mater. Chem.* **2007**, *17*, 1117–1122.

(107)   Biasci, L.; Aglietto, M.; Ruggeri, G.; Ciardelli, F. *Polymer* **1994**, *34*, 3296–3304.

(108)   Chen, K.; Susner, M. A.; Vyazovkin, S. *Macromol. Rapid Commun.* **2005**, *26*, 690–695.

(109)   Meneghetti, P.; Qutubuddin, S. *Thermochim. Acta* **2006**, *442*, 74–77.

(110)   Fan, X.; Xia, C.; Advincula, R. C. *Langmuir* **2005**, *21*, 2537–2544.

(111)   Liu, C.; Pan, C. *Polymer* **2007**, *48*, 3679–3685.

(112)   Harwood, H. J.; McNamara, K.; Johnson, J. J.; Wyzgoski, F. J. *J. Polym. Sci., Part A: Polym. Chem.* **2008**, *46*, 2347–2356.

(113)   Cais, R. E.; Bovey, F. A. *Macromolecules* **1977**, *10*, 169–177.

(114)   Eastwood, E. A.; Dadmun, M. D. *Macromolecules* **2001**, *34*, 740–747.

(115)   Bevington, J. C.; Cywar, D. A.; Huckerby, T. N.; Senogles, E.; Tirrell, D. A. *Eur. Polym. J.* **1990**, *26*, 41–46.

(116)   Soga, K.; Nakatani, H.; Monoi, T. *Macromolecules* **1990**, *23*, 953–957.

(117)   Bevington, J. C.; Cywar, D. A.; Huckerby, T. N.; Senogles, E.; Tirrell, D. A. *Eur. Polym. J.* **1988**, *24*, 699–702.

(118)   Chirowodza, H.; Zou, M.; Sanderson, R. D. *J. Appl. Polym. Sci.* **2010**, *117*, 3460–3465.

(119)   Matsuzaki, K.; Uryu, T.; Osada, K.; Kawamura, T. *Macromolecules* **1972**, *5*, 816–818.

(120)   Pasch, H.; Hiller, W.; Haner, R. *Polymer* **1998**, *39*, 1515–1523.

(121)   Postma, A.; Davis, T. P.; Donovan, A. R.; Li, G.; Moad, G.; Mulder, R.; O'Shea, M. S. *Polymer* **2006**, *47*, 1899–1911.

(122)   Bevington, J. C.; Huckerby, T. N. *Eur. Polym. J.* **2006**, *42*, 1433–1436.

(123)   Izunobi, J. U.; Higginbotham, C. L. *J. Chem. Educ* **2011**, *88*, 1098–1104.

(124)   Saito, T.; Lusenkova, M. A.; Matsuyama, S.; Shimada, K.; Itakura, M.; Kishine, K.; Sato, K.; Kinugasa, S. *Polymer* **2004**, *45*, 8355–8365.

(125)   Choi, Y. S.; Choi, M. H.; Wang, K. H.; Kim, S. O.; Kim, Y. K.; Chung, I. J. *Macromolecules* **2001**, *34*, 8978–8985.

(126)   Guttman, C. M.; Wetzel, S. J.; Blair, W. R.; Fanconi, B. M.; Girard, J. E.; Goldschmidt, R. J.; Wallace, W. E.; VanderHart, D. L. *Anal. Chem.* **2001**, *73*, 1252–1262.

(127)   Dey, M.; Castoro, J. A.; Wilkins, C. L. *Anal. Chem.* **1995**, *67*, 1575–1579.

(128)   Bahr, U.; Deppe, A.; Karas, M.; Hillenkamp, F. *Anal. Chem.* **1992**, *64*, 2866–2869.

(129)   Nielen, M. W. F.; Malucha, S. *Rapid Commun. Mass Spectrom.* **1997**, *11*, 1194–1204.

(130) Crecelius, A. C.; Becer, C.; Knop, K.; Schubert, U. S. *J. Polym. Sci., Part A: Polym. Chem.* **2010**, *48*, 4375–4384.

(131) Gruendling, T.; Hart-Smith, G.; Davis, T. P.; Stenzel, M. H.; Barner-Kowollik, C. *Macromolecules* **2008**, *41*, 1966–1971.

(132) Ladavière, C.; Lacroix-Desmazes, P.; Delolme, F. *Macromolecules* **2009**, *42*, 70–84.

(133) Venkatesh, R.; Staal, B. B. P.; Klumperman, B.; Monteiro, M. J. *Macromolecules* **2004**, *37*, 7906–7917.

(134) Kwak, Y.; Goto, A.; Komatsu, K.; Sugiura, Y.; Fukuda, T. *Macromolecules* **2004**, *37*, 4434–4440.

(135) Geelen, P.; Klumperman, B. *Macromolecules* **2007**, *40*, 3914–3920.

(136) Zhou, G.; Harruna, I. I. *Anal. Chem.* **2007**, *79*, 2722–2727.

(137) Zammit, M. D.; Davis, T. P.; Haddleton, D. M.; Suddaby, K. G. *Macromolecules* **1997**, *30*, 1915–1920.

(138) Ameduri, B.; Ladavire, C.; Delolme, F.; Boutevin, B. *Macromolecules* **2004**, *37*, 7602–7609.

(139) Pasch, H.; Gores, F. *Polymer* **1995**, *36*, 1995–2005.

(140) Carroccio, S.; Rizzarelli, P.; Puglisi, C.; Montaudo, G. *Macromolecules* **2004**, *37*, 6576–6586.

(141) Byrd, H. C. M.; McEwen, C. N. *Anal. Chem.* **2000**, *72*, 4568–4576.

(142) Thomson, B.; Suddaby, K.; Rudin, A.; Lajoie, G. *Eur. Polym. J.* **1996**, *32*, 239–256.

(143) Tonnar, J.; Lacroix-Desmazes, P.; Boutevin, B. *Macromolecules* **2007**, *40*, 186–190.

(144) Favier, A.; Ladavière, C.; Charreyre, M.-T.; Pichot, C. *Macromolecules* **2004**, *37*, 2026–2034.

(145) Ruttink, P. J. A.; Burgers, P. C.; Francis, J. T.; Terlouw, J. K. *J. Phys. Chem* **1996**, *100*, 9694–9697.

(146) Cox, F. J.; Johnston, M. V. *J. Am. Soc. Mass. Spectrom.* **2003**, *14*, 648–657.

(147) Choi, Y. S.; Choi, M. H.; Wang, K. H.; Sang Ouk Kim; Kim, Y. K.; Chung, I. J. *Macromolecules* **2001**, *34*, 8978–8985.

(148) Zagorevskii, D. V.; Aldersley, M. F.; Ferris, J. P. *J. Am. Soc. Mass. Spectrom.* **2006**, *17*, 1265–1270.

(149) Schimpf, M. E.; Caldwell, K.; Giddings, J. C. *Field-Flow Fractionation Handbook*; John Wiley and Sons: New York, 2000.

(150) Messaud, F. A.; Sanderson, R. D.; Runyon, J. R.; Otte, T.; Pasch, H.; Williams, S. K. R. *Prog. Polym. Sci.* **2009**, *34*, 351–368.

(151) Giddings, J. C.; Yang, F. J.; Myers, M. N. *Anal. Chem.* **1976**, *48*, 1126–1132.

(152) Fedotov, P. S.; Vanifatova, N. G.; Shkinev, V. M.; Spivakov, B. Y. *Anal. Bioanal. Chem.* **2011**, *400*, 1787–1804.

(153) Kammer, F. v. d.; Baborowski, M.; Friese, K. *Anal. Chim. Acta.* **2005**, *552*, 166–174.

(154) Chen, B.; Evans, J. R. G.; Greenwell, H. C.; Boulet, P.; Coveney, P. V.; Bowden, A. A.; Whiting, A. *Chem. Soc. Rev.* **2008**, *37*, 568–594.

(155) Tasdelen, M. A.; Kreutzer, J.; Yagci, Y. *Macromol. Chem. Phys.* **2010**, *211*, 279–285.

(156) Mayadunne, R. T. A.; Rizzardo, E.; Chiefari, J.; Krstina, J.; Moad, G.; Postma, A.; Thang, S. H. *Macromolecules* **2000**, *33*, 243–245.

(157) Rotzoll, R.; Nguyen, D. H.; Vana, P. *Macromol. Symp.* **2009**, *275–276*, 1–12.

(158) Moad, G.; Chong, Y. K.; Le, T. P. T.; Rizzardo, E.; Thang, S. H. *Macromolecules* **1999**, *32*, 2071–2074.

Chapter 3

RAFT agent synthesis, styrene polymerisation and clay modification

This chapter is split into three sections. The first section gives the experimental details regarding the synthesis of the RAFT agents used in this study. The second section covers the RAFT-mediated polymerisation of styrene using the synthesised chain transfer agents. Details regarding macromolecular structure i.e. molar mass, molar mass distribution and chain end functionality are also given. Surface modification using cationic RAFT agents is described in the final section. A description of the qualitative and quantitative analysis of the surface modified materials is given. For clarity, in each section a brief introduction, experimental and results are given.

3.1 RAFT agent synthesis

3.1.1 Introduction

One of the objectives of this work was to synthesise PCNs containing well-defined polymers via SI-RAFT polymerisation. For a successful RAFT mediated polymerisation, the correct choice of chain transfer agent (CTA) must be made. The suitability of a CTA is determined by the monomer type as well as the properties of the free radical leaving group, R and the stabilising group, Z. There are four main classes of RAFT agents which differ by the Z-group substituent: dithioesters (Z=alkyl or aryl), trithiocarbonates (Z=SR), dithiocarbamates (Z=NR$_2$) and xanthates (Z=O-alkyl).[1] Given a suitable R group, trithiocarbonates are most effective for the "more activated"[2] monomers such as styrene, methacrylates, acrylates and acrylamides, hence they were chosen for this work.

It is important in SI-RAFT polymerisation that the CTA is synthesised with a suitable functionality. The chosen functionality is largely influenced by the complimentary functional groups on the surface. Prior to synthesis various considerations influenced by the mode of attachment must be made. For attachment via the Z-group approach, the RAFT agent must be functionalised at the stabilising group, and for the R-group approach the RAFT agent must be functionalised at the reinitiating group. It is important that the attached functional group does not influence the reactivity of the C=S bond towards radical addition, and the reinitiation efficiency of the R-group.

The functionalised CTAs that were synthesised in this work were for attachment to a surface that bears negative charges. The cationic charge was attached to the CTAs through functionalising the R-group with a quaternary ammonium moiety, **RAFT1** and **RAFT3**. As highlighted in Section 2.2.3, there is need to add free CTA to ensure the concentration of CTA remains constant throughout the polymerisation; as a result two non-functionalised CTA, **RAFT2** and **RAFT4** were also synthesised. Primary and secondary R groups were chosen as they are efficient for reinitiating styrene and acrylate polymerisations.[3] The structures of the synthesised CTAs are given in Figure 3.1.
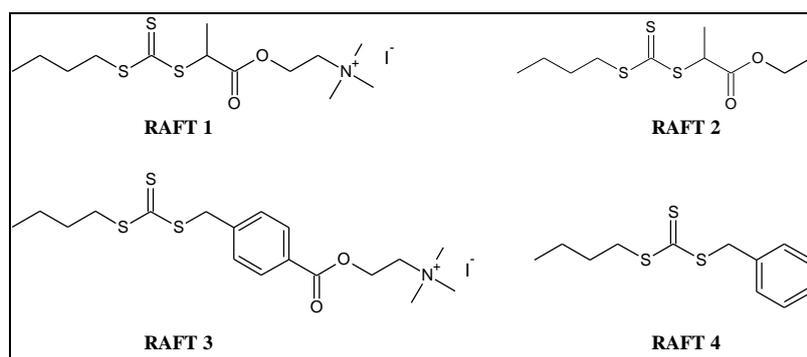
Figure 3.1 RAFT agents synthesised in this work

Carboxy-functionalised CTAs were the starting point in the synthesis of catatonically functionalised CTAs (Schemes 3.1 and 3.2). The carboxyl group offers a means of converting the CTA to other functionalities. Converting carboxy-functionalised CTAs to other functionalities has been reported by other researchers;[4,5] the approach is desirable because a number of carboxy-functionalised CTAs are commercially available.

In this study, carboxy-functionalised CTAs were synthesised, and converted to tertiary amine-functionalised CTAs through esterification with a bifunctional alcohol. This was followed by alkylation with methyl iodide to give the desired quaternary amine-functionalised CTA.

3.1.2   Experimental

Materials

Butanethiol (Fluka), potassium hydroxide (KOH, Merck), carbon disulphide (CS$_2$, Labchem), 2-bromopropionic acid (Aldrich), ethyl 2-bromopropionate (Merck), 4-(bromomethyl)benzoic acid, benzyl bromide (Sigma-Aldrich) 1,3-dicyclohexylcarbodiimide

(DCC, Sigma-Aldrich), 4-(dimethylamino)pyridine (DMAP, Fluka), 2-dimethylaminoethanol (Riedel de Haën), methyl iodide (MeI, Merck), pentane, ethyl acetate, diethyl ether, HCl (32%) were supplied by Labchem and were used as received. THF (Kimix) was distilled from sodium-benzophenone and stabilised with 0.0125% butylhydroxy toluene (BHT, Aldrich), dichloromethane (DCM, Labchem) was dried over $CaCl_2$ (Merck) and distilled over CaH_2 (Aldrich). Both THF and DCM were stored over molecular sieves.

Synthesis of RAFT agents with a secondary leaving group

Scheme 3.1 summarises the steps involved in the synthesis of the CTAs with secondary R-groups.
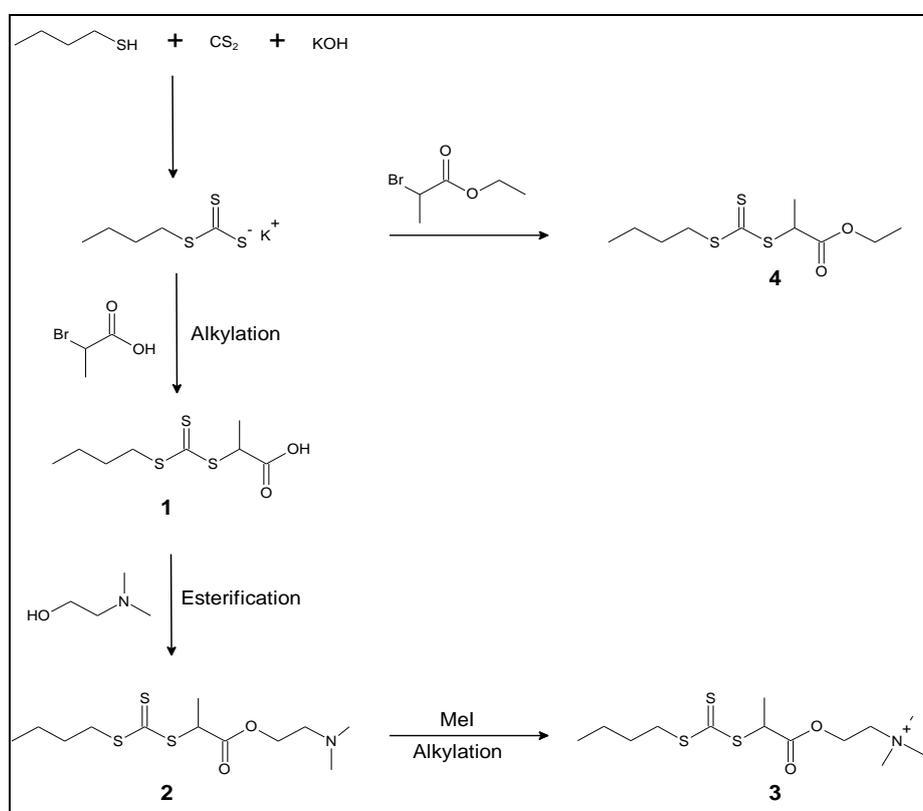
Scheme 3.1 Synthesis of 2-(2-(butylthiocarbonothioylthio)propanoyloxy)-N,N,N-trimethylethanaminium iodide and ethyl 2-(butylthiocarbonothioylthio)propanoate

Synthesis of 2-(2-(butylthiocarbonothioylthio)propanoyloxy)-N,N,N-trimethylethanaminium iodide, RAFT1

2-(Butylthiocarbonothioylthio)propanoic acid, **1**

Potassium butyl carbonotrithioate salt was prepared according to a procedure in literature[6] that was modified as follows: Potassium hydroxide (9.02 g, 16.1 mmol) was crushed and

added to 150 mL of THF in a three-neck round-bottom flask. Butanethiol (16.01 g, 17.8 mmol) in 50 mL of THF was added dropwise, and after complete addition the reaction mixture was stirred for 10 min at 0 °C. Carbon disulphide (17.04 g, 22.4 mmol) in 50 mL of THF was added dropwise and the ice bath removed after complete addition; the reaction mixture was then stirred for 2 h at room temperature. A yellow crystalline salt was obtained after removal of the solvent under vacuum. The yield was 28.0 g, 85%. This trithiocarbonate salt was used for the synthesis of the RAFT agents.

Potassium butyl carbonotrithioate (3.00 g, 14.7 mmol) was dissolved in dry THF (50 mL) and 2-bromopropionic acid (2.24 g, 14.7 mmol) was added slowly under stirring at room temperature. After 18 h the reaction mixture was filtered and the solid washed several times with THF. The solvent was removed by rotary evaporation. The crude product (yellow oil) was then dissolved in pentane and washed twice with water. After removal of solvent under vacuum, the carboxy-functionalised RAFT agent, **1** was obtained as a yellow solid. The yield was 3.04 g, 87%.

^{1}H-NMR (400 MHz, CDCl$_3$): δ (ppm) 10.95 (br, 1**H**, CO$_2$**H**), 4.81 (q, *J*=7.4 Hz, 1H, SC**H**), 3.37 (t, *J*=7.4 Hz, 2H, C**H**$_2$S), 1.68 (quint, *J*=7.4 Hz, 2H, C**H**$_2$CH$_2$S), 1.61 (d, *J*=7.4 Hz, 3H, SCHC**H**$_3$), 1.43 (sext, *J*=7.4 Hz, 2H, CH$_3$C**H**$_2$CH$_2$), 0.94 (t, *J*=7.4 Hz, 3H, C**H**$_3$CH$_2$).

^{13}C-NMR (100 MHz, CDCl$_3$): δ (ppm) 221.7 (**C**=S), 177.1 (**C**=O), 47.4 (S**C**H), 37.1 (**C**H$_2$S), 29.8 (**C**H$_2$CH$_2$S), 22.0 (**C**H$_3$CH$_2$), 16.6 (SCH**C**H$_3$), 13.5 (CH$_2$**C**H$_3$).

2-(Dimethylamino)ethyl 2-(butylthiocarbonothioylthio)propanoate, **2**
To a solution of **1** (1.05 g, 4.40 mmol) in 50 mL DCM dimethylaminoethanol (0.42 g, 4.71 mmol) was added. The mixture was cooled to 0 °C and DCC (1.05 g, 5.08 mmol) added. After stirring the reaction mixture for 5 minutes DMAP (0.066 g, 0.54 mmol) (in 2 mL DCM) was added and the mixture stirred overnight at room temperature. The product was filtered, concentrated under vacuum and purified via column chromatography on silica using pentane/ethyl acetate=4:1 with 5% triethylamine, as the eluent. Three fractions were isolated and the solvent removed by rotary evaporation. The first fraction gave a yellow oil, and the second a yellow solid; both were not characterised further. The third fraction consisted of the desired product; the tertiary amine-functionalised RAFT agent, **2**. Yield was 0.73 g, 54%.

^{1}H-NMR (400 MHz, CDCl$_3$): δ (ppm) 4.85 (q, *J*=7.4 Hz, 1H, SC**H**), 4.25 (t, *J*=5.8 Hz, 2H, C**H**$_2$CH$_2$N), 3.35 (t, *J*=7.4 Hz, 2H, C**H**$_2$S), 2.58 (m, *J*=5.8 Hz, 2H, C**H**$_2$N), 2.28 (s, 6H, N(C**H**$_3$)$_2$), 1.68 (quint, *J*=7.4 Hz, 2H, C**H**$_2$CH$_2$S), 1.60 (d, *J*=7.4 Hz, 3H, SCHC**H**$_3$), 1.41 (sext, *J*=7.4 Hz, 2H, CH$_3$C**H**$_2$CH$_2$), 0.94 (t, *J*=7.4 Hz, 3H, C**H**$_3$CH$_2$).

^{13}C-NMR (100 MHz, CDCl$_3$): δ (ppm) 221.6 (**C**=S), 170.8 (**C**=O), 63.4 (**C**H$_2$CH$_2$N), 57.1 (CH$_2$**C**H$_2$N), 47.6 (S**C**H), 36.6 (**C**H$_2$S), 29.6 (**C**H$_2$CH$_2$S), 21.7 (**C**H$_3$CH$_2$), 16.5 (SCH**C**H$_3$), 13.2 (CH$_2$**C**H$_3$)

2-(2-(Butylthiocarbonothioylthio)propanoyloxy)-N,N,N-trimethylethanaminium iodide, **3**

2 (2.5 g, 8.08 mmol) was dissolved in THF (20 mL) in a three-neck round-bottom flask equipped with a condenser. MeI (4.59 g, 32.3 mmol) was added dropwise with stirring at 40 ^{o}C. An excess of the MeI was used to ensure the reaction went to completion. After 24 h the excess MeI and solvent were evaporated. The product was then dissolved in water and the less polar components extracted in diethyl ether or pentane. The solvent was removed by rotary evaporation. The yield was 3.20 g, 88%.

^{1}H-NMR (400 MHz, CDCl$_3$): δ (ppm) 4.80 (q, *J*=7.4 Hz, 1H, SC**H**), 4.65 (m, 2H, C**H**$_2$CH$_2$N), 4.10 (m, 2H, CH$_2$C**H**$_2$N), 3.52 (s, 9H, N(C**H**$_3$)$_3$), 3.36 (m, *J*=7.4 Hz, 2H, C**H**$_2$S), 1.68 (quint, *J*=7.4 Hz, 2H, C**H**$_2$CH$_2$S), 1.64 (d, *J*=7.4 Hz, 3H, SCHC**H**$_3$), 1.43 (sext, *J*=7.4 Hz, 2H, CH$_3$C**H**$_2$CH$_2$), 0.94 (t, *J*=7.4 Hz, 3H, C**H**$_3$CH$_2$).

^{13}C-NMR (100 MHz, CDCl$_3$): δ (ppm) 222.4 (**C**=S), 170.2 (**C**=O), 65.0 (**C**H$_2$CH$_2$N), 59.3 (CH$_2$**C**H$_2$N), 54.8 (N(**C**H$_3$)$_3$), 47.3 (S**C**H), 37.3 (**C**H$_2$S), 29.8 (**C**H$_2$CH$_2$S), 22.0 (**C**H$_3$CH$_2$), 16.4 (SCH**C**H$_3$), 13.6 (CH$_2$**C**H$_3$).

The mass spectra for the above compounds are given in Appendix 1.

Synthesis of ethyl 2-(butylthiocarbonothioylthio)propanoate, RAFT2

Ethyl 2-(butylthiocarbonothioylthio)propanoate, **4**

To a solution of potassium butyl carbonotrithioate (3.00 g, 14.7 mmol) in 50 mL THF ethyl 2-bromopropionate (2.67 g, 14.7 mmol) was added under stirring at room temperature. After 18 h the reaction mixture was filtered and the solid washed several times with THF. The solvent was removed by rotary evaporation and the crude product purified via column

Chapter 3: RAFT agent synthesis, styrene polymerisation and clay modification

chromatography on silica with 100% pentane followed by a solution of pentane/ethyl acetate (20:1) giving a yellow oil. Yield 3.20 g, 81%.

^{1}H-NMR (400 MHz, CDCl$_3$): δ (ppm) 4.79 (q, *J*=7.4 Hz, 1H, SC**H**), 4.18 (q, *J*=7.0 Hz, 2H, OC**H**$_2$CH$_3$), 3.35 (t, *J*=7.4 Hz, 2H, C**H**$_2$S), 1.67 (quint, *J*=7.4 Hz, 2H, C**H**$_2$CH$_2$S), 1.58 (d, *J*=7.4 Hz, 3H, SCHC**H**$_3$), 1.42 (sext, *J*=7.4 Hz, 2H, CH$_3$C**H**$_2$CH$_2$), 1.26 (t, *J*=7.0, 3H, OCH$_2$C**H**$_3$), 0.94 (t, *J*=7.4 Hz, 3H, C**H**$_3$CH$_2$).

^{13}C-NMR (100 MHz, CDCl$_3$): δ (ppm) 222.0 (**C**=S), 171.0 (**C**=O), 61.8 (O**C**H$_2$CH$_3$), 48.0 (S**C**H), 36.9 (**C**H$_2$S), 29.9 (**C**H$_2$CH$_2$S), 22.0 (**C**H$_3$CH$_2$), 16.9 (SCH**C**H$_3$), 14.0 (OCH$_2$**C**H$_3$), 13.6 (CH$_2$**C**H$_3$).

Synthesis of RAFT agents with primary leaving group

The RAFT agents with the primary leaving group (see Scheme 3.2) were synthesised as described in the following section.
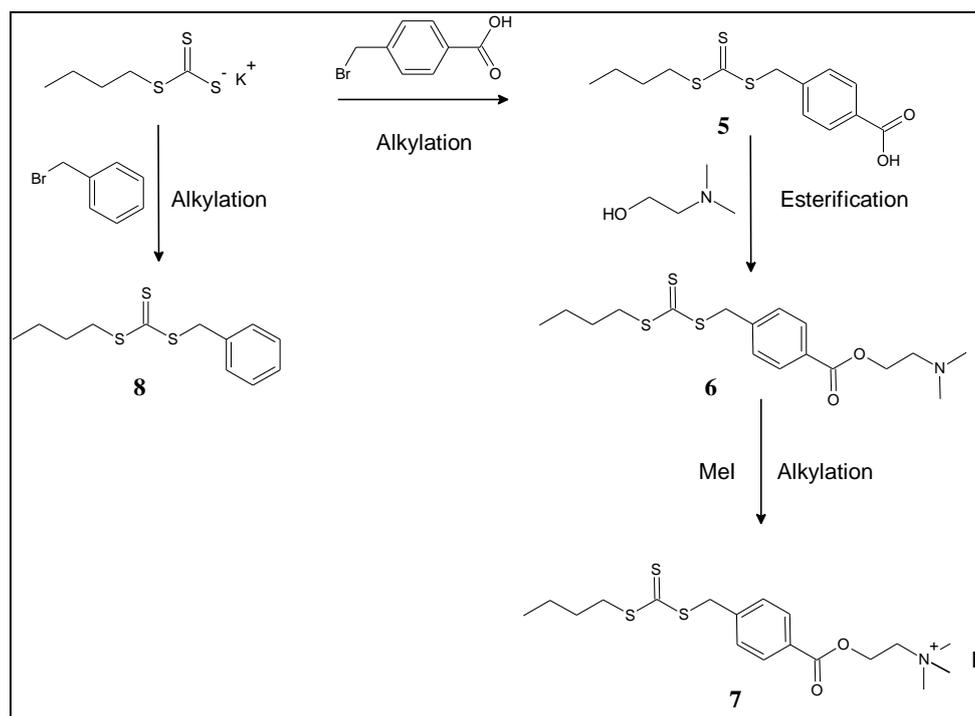
Scheme 3.2 Synthesis of 2-(4-((Butylthiocarbonothioylthio)methyl)benzoyloxy)-N,N,N-trimethylethanaminium iodide) and of benzyl butyl carbonotrithioate

Synthesis of 2-(4-((Butylthiocarbonothioylthio)methyl)benzoyloxy)-N,N,N-trimethylethanaminium iodide), RAFT3

4-((butylthiocarbonothioylthio)methyl)benzoic acid), **5**

Potassium butyl carbonotrithioate (3.00 g, 14.7 mmol) was dissolved in dry THF (50 mL), and 4-(bromomethyl)benzoic acid (3.16 g, 14.7 mmol) was added slowly under stirring at room temperature. After 18 h the reaction mixture was filtered and the solid washed several times with THF. The yellow solution was then washed 3 times with 0.1 M HCl, following which the organic portions were combined and dried with anhydrous $MgSO_4$. The $MgSO_4$ was filtered and the solvent removed under vacuum. The carboxylic acid functionalised RAFT agent **5** was obtained as a yellow crystalline solid. The yield was 3.22 g, 73%.

^{1}H-NMR (400 MHz, d_6-acetone): δ (ppm) 8.00 (d, *J*=8.2 Hz, 2**H**, Ar**H**), 7.50 (d, *J*=8.2 Hz, 2H, Ar**H**), 4.76 (s, 2H, ArC**H**$_2$), 3.42 (t, *J*=7.4 Hz, 2H, C**H**$_2$S), 1.68 (quint, *J*=7.4 Hz, 2H, C**H**$_2$CH$_2$S), 1.43 (sext, *J*=7.4 Hz, 2H, CH$_3$C**H**$_2$CH$_2$), 0.92 (t, *J*=7.4 Hz, 3H, C**H**$_3$CH$_2$).

2-(Dimethylamino)ethyl 4-((butylthiocarbonothioylthio)methyl)benzoate, **6**

To a solution of **5** (1.05 g, 3.50 mmol) in 50 mL DCM dimethylaminoethanol (0.34 g, 3.86 mmol) was added. The mixture was cooled to 0 °C and DCC (0.81 g, 3.92 mmol) added. After stirring the reaction mixture for 5 min DMAP (0.047 g, 0.38 mmol) was added and the mixture stirred overnight at room temperature. The product was filtered, concentrated under vacuum and purified via column chromatography on silica using pentane/ethyl acetate=4:1 with 5% triethylamine, as the eluent. Three fractions were isolated and the solvent removed by rotary evaporation. The third fraction consisted of the desired product; the tertiary amine functionalised RAFT agent. The yield was 0.68 g, 52%.

^{1}H-NMR (400 MHz, CDCl$_3$): δ (ppm) 7.98 (d, *J*=8.6 Hz, 2**H**, Ar**H**), 7.40 (d, *J*=8.6 Hz, 2H, Ar**H**), 4.64 (s, 2H, ArC**H**$_2$), 4.41 (t, J=5.9 Hz, 2H, C**H**$_2$O) 3.37 (t, *J*=7.4 Hz, 2H, C**H**$_2$S), 2.70 (t, J=5.9 Hz, 2H, C**H**$_2$N), 2.32 (s, 6H, N(CH$_3$)$_2$), 1.68 (quint, *J*=7.4 Hz, 2H, C**H**$_2$CH$_2$S), 1.43 (sext, *J*=7.4 Hz, 2H, CH$_3$C**H**$_2$CH$_2$), 0.93 (t, *J*=7.4 Hz, 3H, C**H**$_3$CH$_2$).

*2-(4-((Butylthiocarbonothioylthio)methyl)benzoyloxy)-N,N,N-trimethylethanaminium iodide,***7**

6 (2 g, 8.08 mmol) was dissolved in THF (20 mL) in a three-neck round-bottom flask equipped with a condenser. MeI (4.59 g, 32.3 mmol) was then added dropwise with stirring at 40 °C. An excess of MeI was used to ensure the reaction went to completion. After 24 h the excess MeI and solvent were evaporated. The product was then dissolved in water and the

less polar components extracted in diethyl ether or pentane. The solvent was removed by rotary evaporation. The yield was 3.20 g, 88%.

^{1}H-NMR (400 MHz, CDCl$_3$): δ (ppm) 4.80 (q, *J*=7.4 Hz, 1H, SC**H**), 4.65 (m, 2H, C**H**$_2$CH$_2$N), 4.10 (m, 2H, CH$_2$C**H**$_2$N), 3.52 (s, 9H, N(C**H**$_3$)$_3$), 3.36 (m, *J*=7.4 Hz, 2H, C**H**$_2$S), 1.68 (quint, *J*=7.4 Hz, 2H, C**H**$_2$CH$_2$S), 1.64 (d, *J*=7.4 Hz, 3H, SCHC**H**$_3$), 1.43 (sext, *J*=7.4 Hz, 2H, CH$_3$C**H**$_2$CH$_2$), 0.94 (t, *J*=7.4 Hz, 3H, C**H**$_3$CH$_2$).

^{13}C-NMR (100 MHz, CDCl$_3$): δ (ppm) 222.8 (**C**=S), 165.3 (**C**=O), 142.0 (O–**C**–Ar), 130.2 (Ar), 129.6 (Ar), 127.8 (Ar), 65.2 (**C**H$_2$CH$_2$N), 58.5 (CH$_2$**C**H$_2$N), 54.8 (N(**C**H$_3$)$_3$), 40.4 (Ar–**C**H$_2$), 37.0 (**C**H$_2$S), 29.9 (**C**H$_2$CH$_2$S), 22.0 (**C**H$_3$CH$_2$), 13.6 (CH$_2$**C**H$_3$)

Synthesis of benzyl butyl carbonotrithioate, RAFT4

To a solution of potassium butyl carbonotrithioate (3.00 g, 14.7 mmol) in 50 mL THF, benzyl bromide (0.57 mL g, 14.7 mmol) was added under stirring at room temperature. After 18 h the reaction mixture was concentrated under vacuum, dissolved in pentane and washed twice with water. Pentane was then removed from the organo-soluble portion by rotary evaporation and the product dried under vacuum. The product was further purified by column chromatography on silica using 100% pentane. The yield was 2.83 g, 75%.

^{1}H-NMR (300 MHz, CDCl$_3$): δ (ppm) 7.36–7.21 (m, 5**H**, Ar**H**), 4.60 (s, 2H, ArC**H**$_2$), 3.37 (t, *J*=7.4 Hz, 2H, C**H**$_2$S), 1.68 (quint, *J*=7.4 Hz, 2H, C**H**$_2$CH$_2$S), 1.43 (sext, *J*=7.4 Hz, 2H, CH$_3$C**H**$_2$CH$_2$), 0.92 (t, *J*=7.4 Hz, 3H, C**H**$_3$CH$_2$).

^{13}C-NMR (100 MHz, CDCl$_3$): δ (ppm) 223.7 (**C**=S), 135.0 (Ar), 129.2 (Ar), 128.6 (Ar), 127.6 (Ar), 41.3 (Ar–**C**H$_2$), 36.7 (**C**H$_2$S), 30.0 (**C**H$_2$CH$_2$S), 22. (**C**H$_3$CH$_2$), 13.6 (CH$_2$**C**H$_3$)

3.1.3   Discussion

The carboxy-functionalised CTAs were synthesised in high yields by reacting potassium butyl trithiocarbonate with carboxy-functionalised brominated alkylating agents. For conversion to a tertiary amine, esterification was carried out using a bifunctional alcohol, dimethylaminoethanol.

Carboxylic acids are not reactive enough, to react directly with alcohols. As a result catalysts or coupling agents are often added to the mixture, to activate the acid and drive the reaction

forward.[4] Another drawback to esterification is the generation of water which hydrolyses the product back to the starting material. In this study these drawbacks were circumvented by employing the Steglich esterification (DCC/DMAP coupling).[7] Dicyclohexylurea the by-product of the reaction was removed by column chromatography on silica. The yields after esterification were moderately high.

The complete conversion of the carboxy-functionalised CTA to a tertiary amine-functionalised CTA was confirmed by ^{1}H and ^{13}C NMR (see experimental section). For **RAFT1**, the signal attributed to the acid proton (COO**H**) present at ~10.95 ppm disappeared and new signals attributed to the new attached moiety were observed at 2.25 ppm (N(**CH**$_3$)$_2$), 2.58 ppm (**CH**$_2$N) and 4.25 ppm (**CH**$_2$CH$_2$N). The acid proton was not observed in the ^{1}H NMR spectrum for **RAFT3**. However, after esterification new signals attributed to the attached moiety were observed at 2.32 ppm (N(**CH**$_3$)$_2$), 2.70 ppm (**CH**$_2$N) and 4.41 ppm (**CH**$_2$CH$_2$N).

The final step in the synthesis of the cationic CTAs was the alkylation of the tertiary amine-functionalised CTA with methyl iodide (MeI). The reactions were conducted in the dark because alkyl iodides are light sensitive. A five-fold excess of MeI and long reaction times were employed to ensure that the reaction went to completion. The yields were very high and ^{1}H NMR showed the complete conversion of the tertiary amine-functionalised CTA to a quaternary amine-functionalised CTA, through the shifting of the signal attributed to (N(**CH**$_3$)$_2$) at 2.28 ppm to 3.52 ppm for N(**CH**$_3$)$_3$) for **RAFT1**, and 2.32 ppm to 3.52 ppm for **RAFT3**.

For the synthesis of the non-functionalised CTAs, high yields were obtained, following the alkylation of potassium butyl trithiocarbonate with brominated alkylating agents.

3.2   Polymerisation of styrene

3.2.1   Introduction

Prior to clay modification the efficiency of the synthesised CTAs to control styrene polymerisation in the absence of clay was investigated. An ideal "living" polymerisation is characterised by polymer with the following characteristics: (1) narrow molar mass distribution, (2) predictable molar mass, based on the ratio of initiator or CTA to consumed monomer (see equation 3.2) and (3) continuation of polymer growth upon sequential monomer addition.

The most fundamental aspect to the RAFT process is the incorporation of the RAFT agent in the final polymer. This together with a narrow molar mass distribution (Đ<1.5), are often an indication that degenerative chain transfer processes were in place. In light of the complex RAFT mechanism, various analytical techniques including ^{1}H NMR, and mass spectrometry (MS) using soft ionisation techniques, have been used to investigate polymer end groups. The analysis of intact polymer chains provides useful information on the molar mass and chemical composition, particularly the chain end functionality. Accurate structural identification of end groups is of paramount importance, as it provides very crucial information on the polymerisation mechanism.

This section and subsequent chapters focus mainly on **RAFT1** and **RAFT2**. All polymerisations were conducted in bulk to mimic the conditions used for the SI-polymerisations. Small amounts of initiator were added in order to generate the initiating radicals, as required by the RAFT process. The molar mass and molar mass distributions of the synthesised polymers were determined by SEC, and the chain end functionality by MALDI-TOF MS and ^{1}H NMR. Low molar masses were targeted to make it easier for end group analysis.

3.2.2   Experimental

Materials

Styrene (Sigma-Aldrich) was purified by washing successively with 0.03 M KOH and deionised water (obtained from a Millipore Milli-Q purification system), dried over anhydrous magnesium sulphate (MgSO$_4$, Saarchem), and then distilled under reduced

pressure. The monomer was then stored in the refrigerator at <4 °C. 2,2′-Azobisisobutyronitrile (AIBN, Riedel de Haën) was recrystallized from methanol and dried under vacuum.

Styrene polymerisation

Styrene was polymerised in the absence of clay as follows: A dry 100 mL Schlenk flask was charged with styrene (2.00 g, 19.2 mmol), tertiary amine functionalised CTA (0.131 g, 0.42 mmol) and AIBN (0.014 g, 0.085 mmol), and a magnetic stirrer bar added. The mixture was stirred until all the RAFT agent and initiator had dissolved. The mixture was thoroughly degassed by three successive freeze-pump-thaw cycles, backfilled with argon, sealed and placed in an oil bath set at 70 °C for a set time. Following the polymerisation, the polymer was diluted with THF and precipitated from cold methanol. The polymer was filtered and then dried under vacuum, at room temperature. The conversions were determined gravimetrically.

Conversions by gravimetry

The mass of the dried polymer (yield) was used to determine the monomer conversions at time t, as shown in equation 3.1.

$$\text{conversion (\%)} = \frac{\text{yield (g)} - \text{initiator (g)} - \text{CTA (g)}}{\text{monomer (g)}} \times 100 \qquad (3.1)$$

Analyses

Size exclusion chromatography (SEC)

SEC was carried out using a Waters system comprising a Waters 717$_{plus}$ Autosampler, Waters 2487 dual wavelength absorbance detector and Waters 2414 refractive index detector. The columns used were two PLgel 5µm Mixed-C columns and a PLgel 5µm guard column. The column injection volume was 60 µL and the column oven was kept at a temperature of 30 °C. THF (HPLC grade, BHT stabilised) was the eluent and a flow rate of 1 mL/min was used. Calibration was carried out using narrow polystyrene (PS) standards with a molecular weight range of 800–2 × 10^6 g/mol.

Matrix-assisted laser desorption/ionisation mass spectrometry (MALDI-MS)

The MALDI-MS spectra were recorded using an Axima TOF^2 spectrometer (Shimadzu Biotech, Manchester, UK) equipped with a nitrogen laser at 337 nm. The samples were prepared as follows: typically, solutions of 20 mg dithranol/mL, 2 mg polymer/mL in THF were prepared. For the cationising salts, 10 mg/mL of CuCl in THF and 10 mg/mL of AgNO$_3$ in ethanol were used. The solutions were mixed in the following ratios 15:15:1 (v/v). Approximately 0.3 μL of the sample was transferred to the target plate and air dried prior to analysis. The mass resolution of the instrument was better than 5000 and the mass accuracy was ±2 Da.

NMR spectroscopy

All NMR spectra were acquired on a Varian Unity INOVA 400 MHz instrument. CDCl$_3$ was the solvent and tetramethylsilane (TMS) the internal standard. A minimum of 128 scans were acquired per sample.

3.2.3   Results and Discussion

Cationic CTA, **RAFT1,** dissolved partially in styrene at room temperature and completely at elevated temperature; but no polymer was observed even after 24 h of heating at 70°C. As a result the tertiary amine-functionalised RAFT agent, **2** (Scheme 3.1) was used. The tertiary amine-functionalised CTA will be referred to as **_tert_A-RAFT**. Conditions used for the polymerisation reactions are given in Table 3.1.

Table 3.1 Conditions for polymerisation of styrene using _tert_A-RAFT and RAFT2

Run	Monomer (RAFT) [a]	[M]/[RAFT]/I (mols) [b]	Temp (^{o}C)	Time (h)	Conv. (%) [c]	M$_n$ (calc) [d]	M$_n$ (SEC) [e]	Đ [f]
1	St (_tert_A)	225/5/1	70	17	70	2180	2860	1.15
2	St (_tert_A)	471/5/1	70	24	66	6780	4280	1.16
3	St (2)	230/5/1	75	24	65	3380	2780	1.14

[a] _tert_A refers to **_tert_A-RAFT**, 2 refers to **RAFT2,** [b] [monomer]/[RAFT]/[initiator], [c] Conversions determined gravimetrically using equation 3.1, [d] Theoretical molar mass calculated using equation 3.2, [e] Experimental *number-average* molar mass determined by using SEC, [f] Đ is the molar mass dispersity

Molar mass determination and polymerisation kinetics

The theoretical molar mass was calculated by comparing the ratio of the initial CTA to the consumed monomer as shown in equation 3.2.

$$M_n \text{ (calc)} = \frac{[M]_0 \times M_{w,St} \times f\text{conv.}}{[RAFT]_0} + M_{w,RAFT} \qquad (3.2)$$

where $[M]_o$ and $[RAFT]_o$ are the initial monomer and RAFT agent concentrations, $M_{w,St}$ and $M_{w,RAFT}$ are the molecular masses of styrene and RAFT agent, and $f$conv. is the fractional monomer conversion.

In order to determine the "living" character of the polymerisation, samples were withdrawn from run 2 (mediated by ***tert*A-RAFT**). As shown in Figure 3.2A, ***tert*A-RAFT** controls the polymerisation of styrene, giving an increase in molar mass with monomer conversion and narrow molar mass distributions (Đ< 1.35). The experimental molar masses were smaller than the theoretical molar masses probably due to an overestimation of the conversion, emanating from residual styrene monomer. The first order kinetic plot was linear (Figure 3.2B), an indication that the concentration of active species remained constant throughout the polymerisation.[8]

Figure 3.3 shows the SEC molar mass distributions of PS at selected monomer conversions. The distributions were monomodal and a shift from low to high molar masses with an increase in monomer conversion was evident.
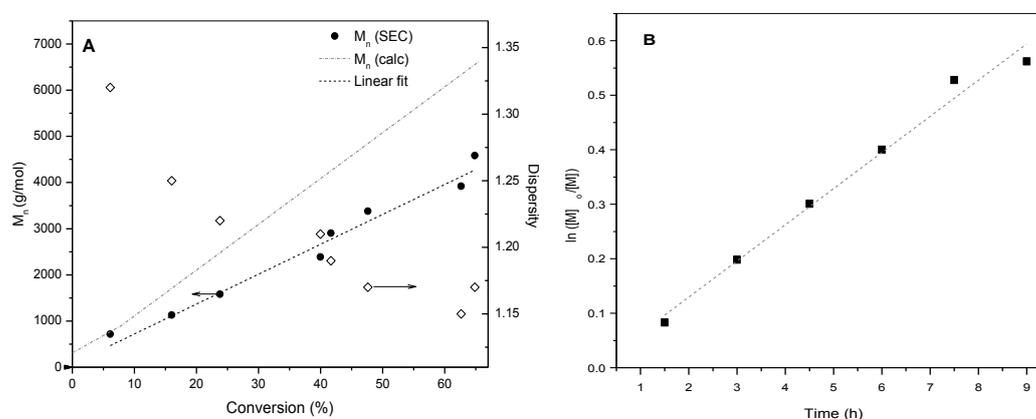
Figure 3.2 (A) Evolution of molar mass and molar mass dispersity vs. time (B) first order kinetic plot, R^2 (M_n(SEC)) = 0.96 and R^2 (first order kinetic plot) = 0.98
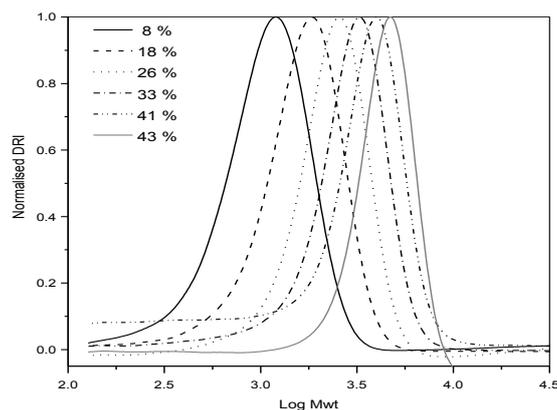
Figure 3.3 Size exclusion molar mass distributions of PS prepared with RAFT2 at selected conversions

Chain end functionality and end group analysis

A linear increase in molar mass with conversion and clear shift from low to high molar masses implied that most of the polymer chains were "living". To confirm the incorporation of the RAFT agent into the polymer, the end groups of the synthesised PS were investigated by MALDI-TOF MS and ^{1}H NMR spectroscopy.

RAFT2 derived PS

The MALDI-MS analysis of PS is very tricky because PS is non-polar, and when labile end groups are present, they can be easily lost through fragmentation. The ionisation step is a crucial step in mass spectrometry; hence for non-polar analytes like PS cationising agents e.g. Ag^+ and Cu^+ are often added. The cation attaches to PS through interactions with the π–electrons of the aromatic ring.[9] In the current study, various attempts were made to alter the analytical conditions in order to minimise fragmentation, thus increasing the chances of observing the dormant polymer chains. Low laser powers were employed and different cationising agents i.e. Cu^+ and Ag^+ were compared. In general we found that when Ag^+ was added as the cationising agent, higher laser powers were required to desorb the analyte species. This led to severe fragmentation of the polymer chains, as seen in the low molar mass region of the MALDI-MS spectrum labelled B in Figure 3.4. The two stacked spectra are for PS synthesised using **RAFT2**. Spectrum A was acquired using Cu^+ as the cationising salt, whilst Ag^+ was used for spectrum B.
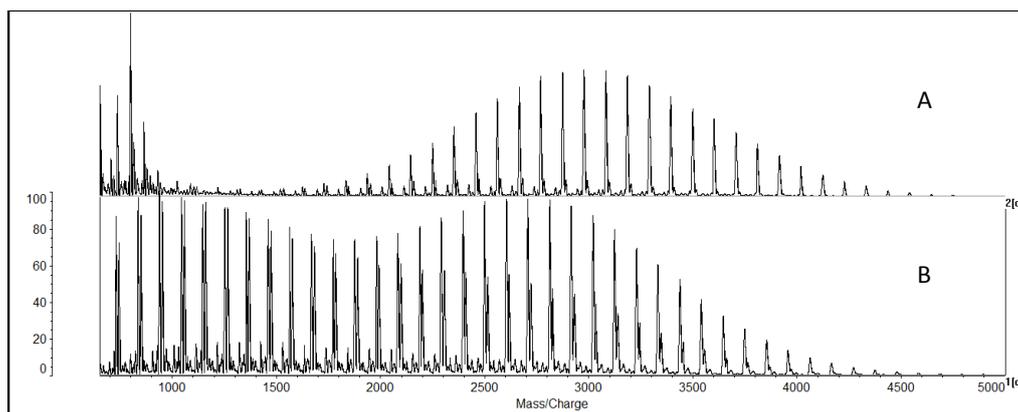
Figure 3.4 Effect of cationising salt on MALDI MS of PS, (A) Cu^+ added and (B) Ag^+ added

Focusing on the low molar mass region of spectrum B as shown in Figure 3.5, the presence of two major and 5 minor distributions can be seen. The dormant PS species were not observed, implying the observed distributions arose from fragmented species.

The collision induced dissociation (CID) of silver-cationised PS occurs via free radical chemistry.[10,11] For PS with robust end groups, fragmentation begins with random homolytic C–C bond cleavages along the polymer chain. When the end groups are labile e.g. in PS synthesised via RDRP, fragmentation begins with the weaker labile moiety prior to C–C bond homolysis.[10]
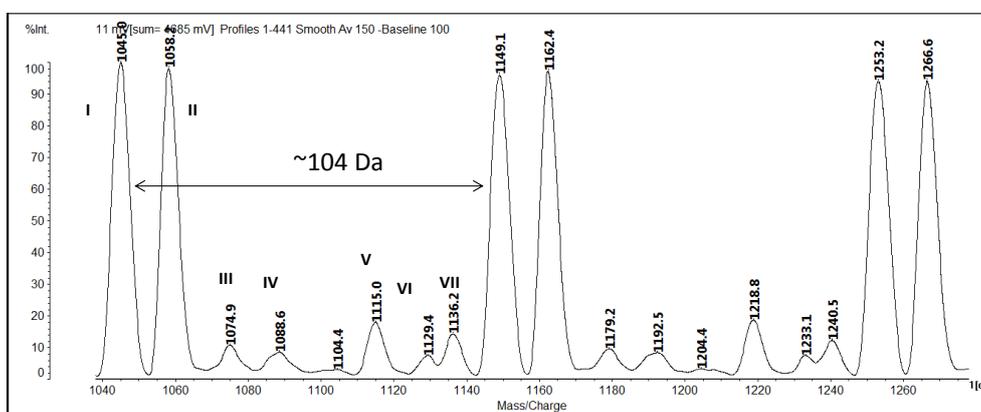
Figure 3.5 Selected part of MALDI-MS spectrum of PS cationised by Ag^+

Random C–C bond homolytic cleavage generates primary or secondary (benzylic) radical centres, with either the initiating or terminating chain ends. Scheme 3.3 shows the fragmentation pathway for PS chains with initiating and terminating groups X and Y, respectively. The symbols I_A and II_A represent the primary and secondary radicals respectively, with the initiating end, X. I_B and II_B represent the secondary and primary

radicals respectively, with the terminating end Y. Subsequent β-Ph• or β-H• loss, leads to the formation of unsaturated species I_A^1, I_A^2, I_B^1, II_A^1, II_B^1 and II_B^2.
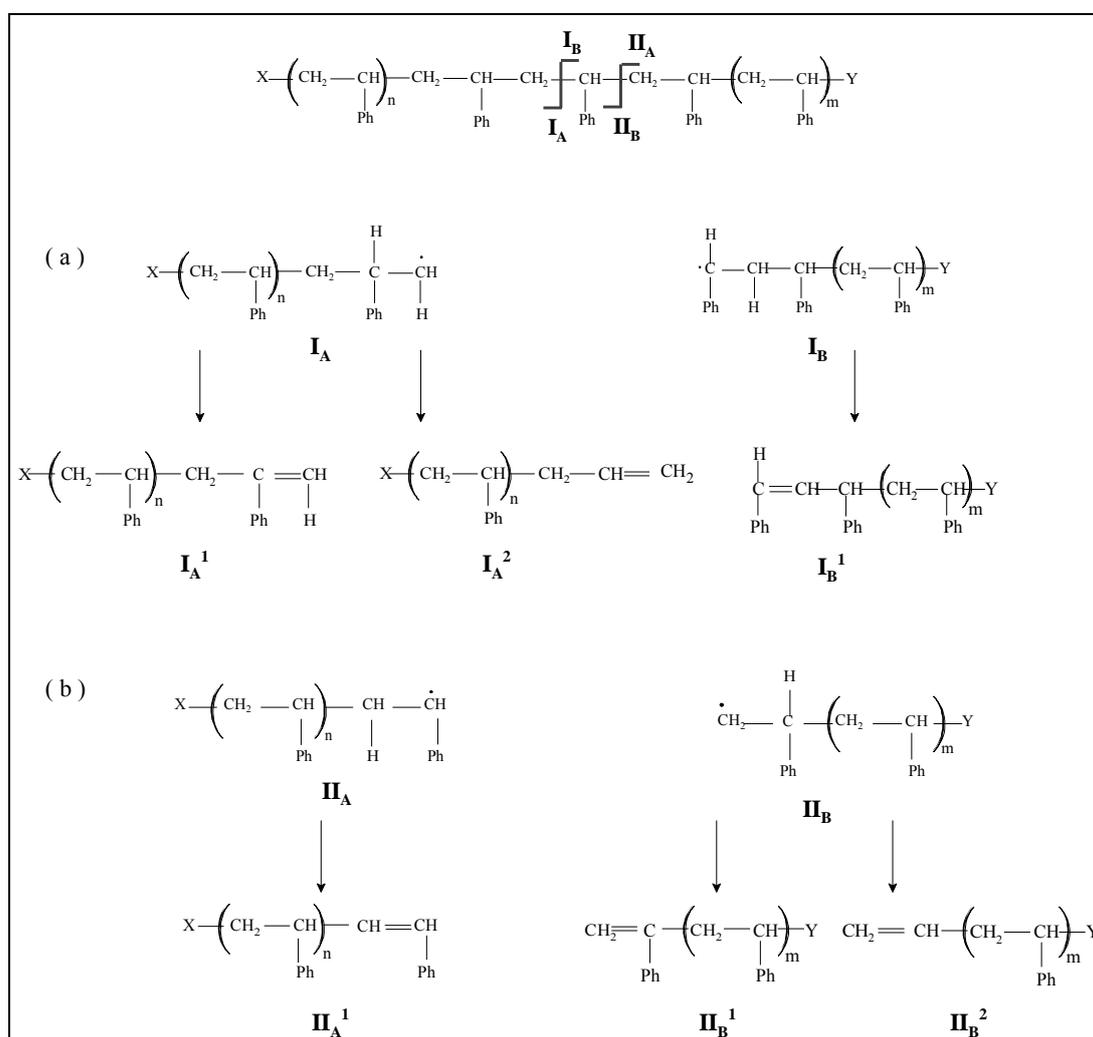
Scheme 3.3 Fragmentation pathway for PS

The structures given in Table 3.2 were identified from Scheme 3.3. The polymer chains were assigned to PS fragments cationised by Ag^+ ions, $[M+Ag^+]$. X_{term} and Y_{init} are the groups at the terminating and initiating ends of the fragmented species.

The peak masses observed matched **RAFT2** and AIBN-initiator derived fragments. It is worth mentioning that it was possible to observe the initiator-derived species because of the relatively high initiator-to-RAFT agent ratio used.[12,13] The 1,2-disubstituted alkene end group, Y emanated from the fragmentation of the RAFT moiety at the terminating end of the dormant polymer species.

When Cu^+ was used as the cationising salt, a nearly Gaussian distribution was observed, see Figure 3.4A. No fragmented species were observed in the lower molar mass region, but the peak intensity was lower compared to the Ag^+ cationised sample, as expected.

Table 3.2 Structures corresponding to various peaks in Figure 3.5

Peak	Frag-ment	X [a]	X_{term} [b]	Y_{init} [c]	Y [d]	m/z (theo) [e]	m/z (expt) [f]
I	$II_A{}^1$	$C_5H_9O_2$	CH=CH(Ph)			1042	1045
II	$I_A{}^1$	$C_5H_9O_2$	CH_2–CH(Ph)=CH_2			1056	1058
III	$II_B{}^2$			CH_2=CH	CH=CH(Ph)	1072	1075
IV		–	–	–	–	–	1089
V	$II_A{}^1$	C_4H_6N	CH=CH(Ph)			1113	1115
VI	$I_A{}^1$	C_4H_6N	CH_2–CH(Ph)=CH_2			1127	1129
VII	$I_B{}^1$			CH(Ph)=CH–CH(Ph)	CH=CH(Ph)	1134	1136

[a] X represents the group at the initiating end of the PS chains, [b] X_{term} represents the group at the terminal end of X initiated PS fragment, [c] Y_{init} represents the group at the initiating end of Y terminated PS fragment, [d] Y represents the group at the terminating end of the PS chains, [e] Calculated molar mass based on proposed peak structure, [f] Observed peak molar mass

Figure 3.6 is a magnification of a selected region of Figure 3.4A. The major distribution at peak mass m/z 2873 corresponds to the calculated molar mass of **RAFT2**-derived species with a 1,2-disubstituted alkene end group. The distribution at m/z 2889 was also attributed to **RAFT2**-derived species but in this case they had the 1,1-disubstituted alkene end group. The peak at m/z 2944 corresponds to the calculated molar mass of AIBN-initiator derived species with a 1,2-disubstituted alkene end group.
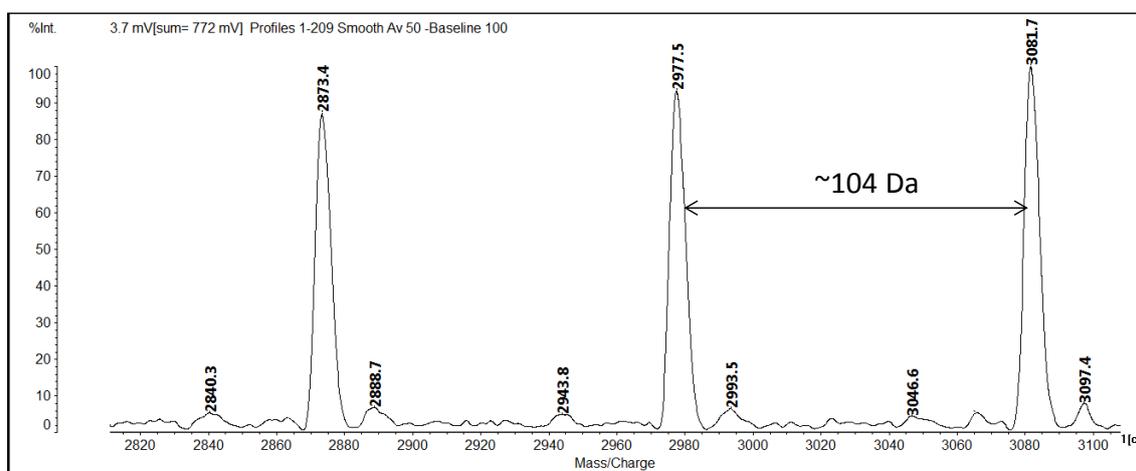
Figure 3.6 Selected region of MALDI-MS spectrum of RAFT2-polymerised PS with Cu^+ as the cationising salt.

Although the fragmentation of the thiocarbonyl thio moiety to form 1,1- and 1,2-disubstituted alkene end groups is well reported in literature,[12] we used ^{1}H NMR to confirm whether the unsaturated end groups were a result of termination via disproportionation, or fragmentation during MALDI-MS analysis. Figure 3.7 shows the ^{1}H NMR spectrum of the polymer.
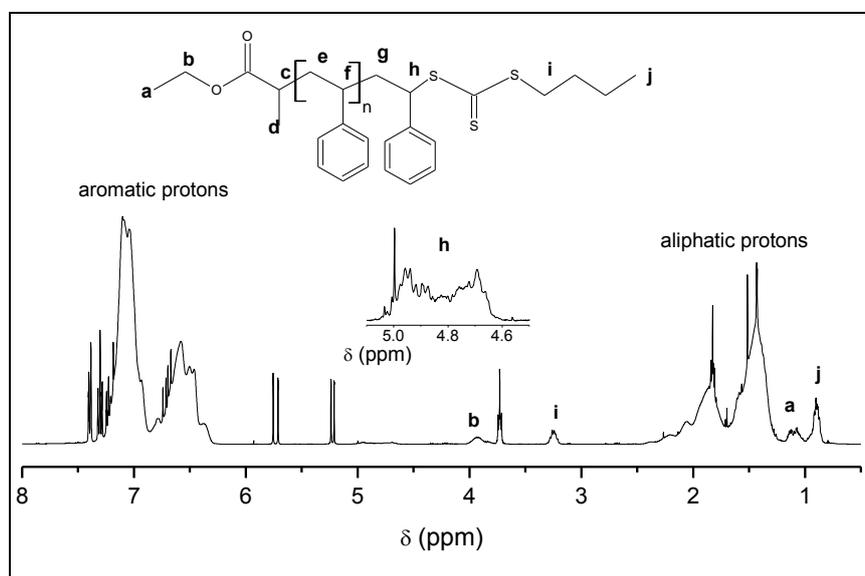
Figure 3.7 ^{1}H NMR spectrum of RAFT2 polymerised PS

The proton assignments made were based on the chemical shifts of the starting CTA. The functionality of the polymer, defined as the percentage of polymer chains with the RAFT agent incorporated was determined using equation 3.3.

$$\text{Functionality} \quad = \frac{\int h}{\int b \Big/ 2} \times 100 \qquad\qquad (3.3)$$

where $\int h$ is the area intensity of the signal attributed to the methine proton adjacent to the thiocarbonyl thio moiety, and $\int b$, is the area intensity of the signal attributed to the methylene protons of the R-group.

The value obtained was 103%. The functionality exceeds 100% probably because of the presence of the AIBN-initiator derived dormant species (as confirmed by MALDI-MS).

TertA-RAFT-derived PS

Similarly to **RAFT2**-derived PS, when copper was added as the cationising agent, a low laser power was required to desorb the analyte species from the target, see Figures 3.8 and 3.9. A

study by Cox and Johnston.[14] showed that PS chains with tertiary amine end groups can also be observed in the protonated form (M+H$^+$), in addition to Ag$^+$-cationised species.
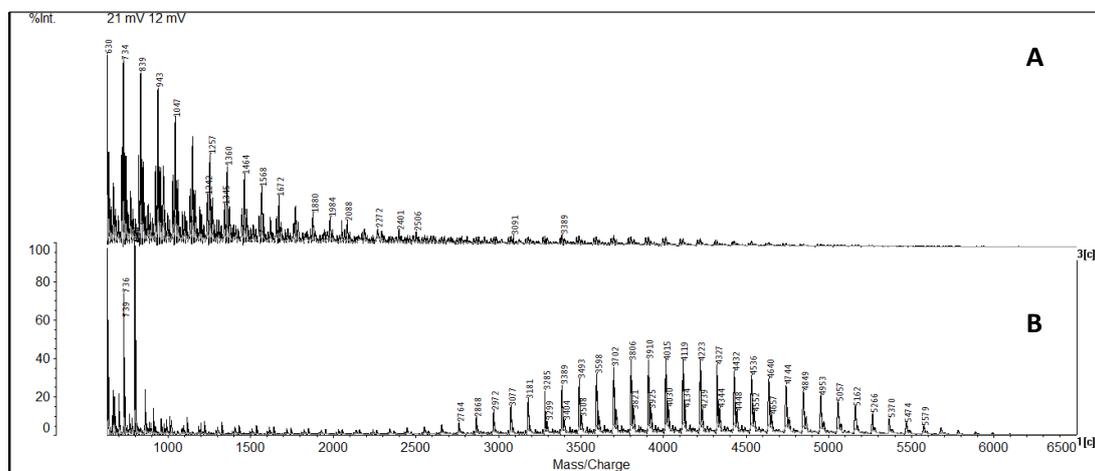
Figure 3.8 MALDI-MS spectrum of tertiary amine synthesised PS with different cationising salts, (A) Ag$^+$ and (B) Cu$^+$

The major distribution observed in the spectra at peak mass m/z 3910 was attributed to two possible structures. The first possible structure is the dormant polymer chains cationised by Cu$^+$, with a calculated molar mass of 3914 g/mol. The second possible structure was attributed to **tertA-RAFT**-derived PS, with a 1,1-disubstituted alkene end group and cationised by a proton. The calculated molar mass for this species is 3907 g/mol.
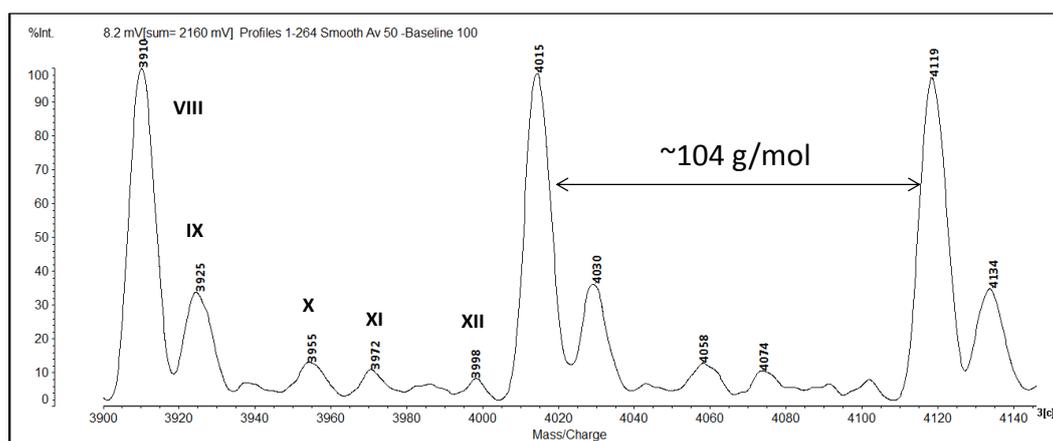
Figure 3.9 Selected region of MALDI-MS spectrum of **tertA-RAFT**-polymerised PS with Cu$^+$ as the cationising salt.

To determine functionality, the PS was examined using ^{1}H NMR spectroscopy; the spectrum is shown in Figure 3.10. Signals characteristic of the starting RAFT agent were observed and assigned as shown in the figure; at 0.94 ppm (r), 2.25 ppm (k), 3.25 ppm (q) and 4.01 ppm

(m). The ratio of the area intensity of the methine proton adjacent to the sulphur (labelled p) and the methylene protons adjacent to the oxygen (labelled m) were used to quantitatively determine the functionality. The values obtained for functionality were slightly over 100%, an indication that most of the polymer chains were indeed living.
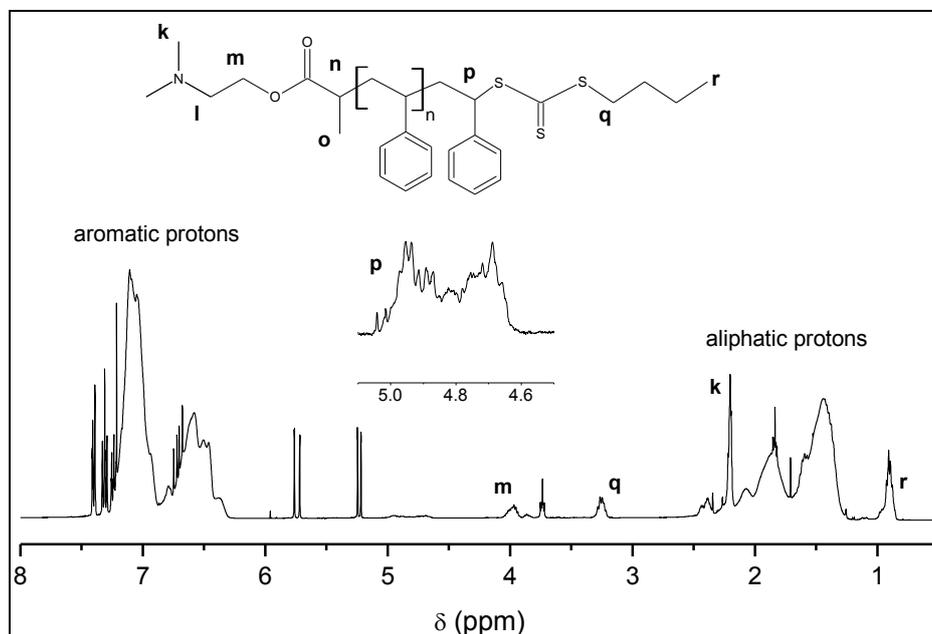
Figure 3.10 ^{1}H NMR spectrum of tertiary amine synthesised PS

3.3   Clay surface modification

3.3.1   Introduction

The need to modify clay prior to PCN synthesis was pointed out in Section 2.1.2. The best way to improve the miscibility of clay with polymer to get an even dispersion, is to coat the clay with polymer during the synthesis of the PCN i.e. SI-*in situ* polymerisation.

Laponite clay has attracted significant attention in academia and industry because of its uniform shape and size. In addition it is synthetic; therefore it does not have the impurities associated with similar naturally occurring smectite clays. Laponite clay comprises disc-shaped platelets with an average diameter of 25 nm and a thickness of 0.92 nm. It has an empirical formula of $Na^{0.7+}[(Si_8Mg_{5.5}Li_{0.3})O_{20}(OH)_4]^{-0.7}$ and a CEC of 50–55 mmol/100g.[15] At the edges of Laponite clay are readily accessible hydroxyl groups whose modification has been explored extensively in literature.[16]

In this study, Laponite clay surfaces were modified by exchanging cationic CTA, **RAFT1,** for the Na^+ ions on the clay surface.

3.3.2   Experimental

Materials

Laponite clay (RD grade) was purchased from Rockwood Additives Limited, UK. 2-(2-(Butylthio-carbonothioylthio)propanoyloxy)-N,N,N-trimethylethanaminium iodide (**RAFT1**) was synthesised as described in Section 3.1.

Intercalation of cationic RAFT agent within the clay galleries

Laponite (4 g) was suspended in an acetone/water mixture (50/50 v/v) (400 mL) and stirred for 1 h to totally exfoliate the clay tactoids. A separate solution of the cationic RAFT agent **RAFT1** (1.77 g, 3.92 mmol) was prepared in acetone/water (50/50 v/v) and added to the Laponite clay suspension. The mixture was stirred for 24 h at room temperature. Acetone was then removed using a rotary evaporator and the water by freeze drying. The physisorbed RAFT agent was removed by dispersion in DCM followed by centrifugation for 15 min at 5000 rpm. The dispersion/centrifugation process was repeated until no iodide ions could be detected in the supernatant as determined by the silver nitrate test. The RAFT modified clay was dried under vacuum at room temperature. The amount of intercalated RAFT agent that was successfully ion-exchanged was determined quantitatively by thermogravimetric analysis (TGA), according to equations 3.4 and 3.5.[17]

$$\text{Grafted amount (mol/100g)} = \frac{\left(\dfrac{W_{150-600}}{100-W_{150-600}}\right) \times 100 - W_{\text{Laponiteclay}}}{M} \qquad (3.4)$$

$$\text{Graft density} = \frac{\text{grafted amount} \times 10^6}{100 \times S_{\text{spec}}} \qquad (3.5)$$

where $W_{150-600}$ is the weight loss between 150 and 600 ^{o}C, which corresponds to the thermal decomposition of **RAFT1**; $W_{\text{Laponite clay}}$ is the observed weight loss of Laponite clay between 150 and 600 ^{o}C prior to modification; M is the molecular mass of **RAFT1** (minus the

molecular mass of the iodide ion); S_{spec} is the specific surface area of Laponite clay, i.e. 370 m^2/g.[18]

For elemental analysis, equations 3.6 and 3.7[19] were used.

$$m_c = \frac{\Delta C\,(\%)}{100 - \Delta C\,(\%)\,M/M_c} \qquad (3.6)$$

$$\delta_g = \frac{m_c \times 10^6}{M_c \times S_{spec}} \qquad (3.7)$$

where m_c is the mass of carbon in the sample; $\Delta C\,(\%)$ is the percentage weight loss; M is the molecular mass of **RAFT1** (minus the molecular mass of the iodide ion); M_c is the mass of carbon per mole of **RAFT1**; and δ_g is the grafting density in $\mu mol/m^2$.

The average number of molecules per clay particle was determined using equation 3.8

$$\text{Number of molecules} = S \times \delta_g \times N_A \times 10^{-6} \qquad (3.8)$$

where S is the surface area of a single clay particle and N_A is Avogadro's number.

Analyses

Photoacoustic Fourier transform infrared (PAS FT-IR) spectroscopy was conducted using a Perkin-Elmer Paragon 1000 PC FT-IR spectrometer equipped with a photoacoustic MTEC 300 cell. Thermogravimetric analysis (TGA) was carried out using a TA Instruments Q500 thermogravimetric analyser. The samples were heated from 25 to 700 ^{o}C at a heating rate of 15 ^{o}C/min under nitrogen atmosphere.

3.3.3   Results and Discussion

FT-IR was used to obtain qualitative information on organic modification of clay. The FT-IR spectrum of the organo-modified clay after washing with DCM is shown in Figure 3.11A. The peaks characteristic of **RAFT1** were present at 2960 and 1735 cm^{-1} (attributed to C–H and C=O, respectively), whilst the peak for the Si–O group of the clay was present at 1000 cm^{-1}. The broad peak at 3500 cm^{-1} is attributed to adsorbed moisture.
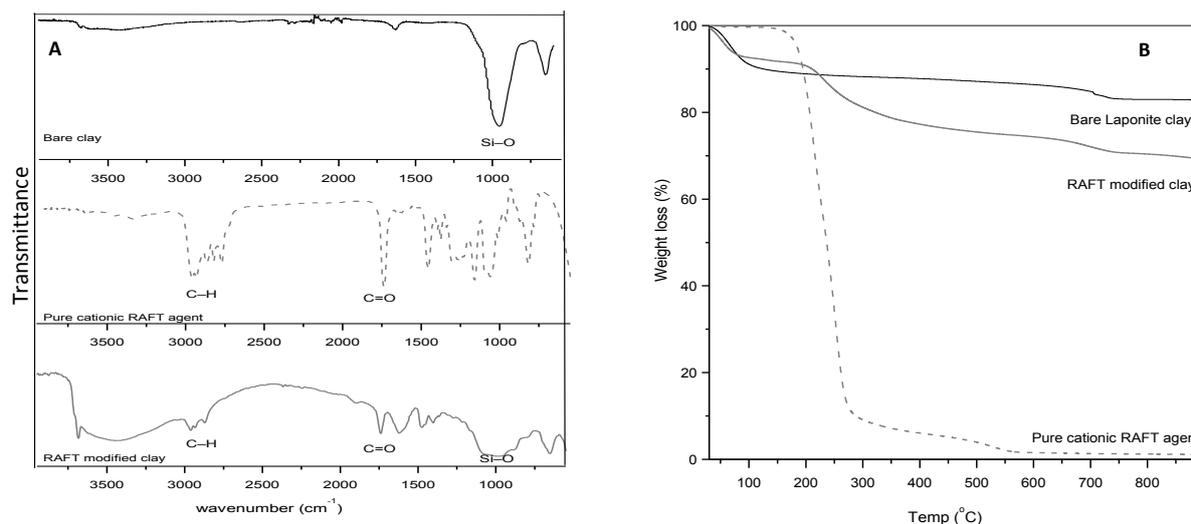
Figure 3.11 (A) FT-IR spectra of bare Laponite clay, cationic RAFT agent and RAFT modified clay, (B) TGA thermograms of bare Laponite clay, RAFT modified Laponite clay and pure cationic RAFT agent

Figure 3.11B shows the TGA curves for neat Laponite clay, RAFT agent-modified clay and the pure cationic CTA, **RAFT1**. The thermal decomposition of bare Laponite is characterised by loss of adsorbed moisture at temperatures <150 ^{o}C, removal of interlayer water between 200 and 550 ^{o}C and dehydroxylation from 550–800 ^{o}C.[20] The thermal decomposition of **RAFT1** occurs between 250 and 600 ^{o}C. The observed changes in weight loss between 150 and 600 ^{o}C, and in the onset temperature for thermal degradation for the organo-modified clay, are indicative of surface modification.

The RAFT agent grafting density, δ_g was determined using EA and TGA; results are tabulated in Table 3.3. What is obvious from the results is that the two techniques did not give similar values. For samples Lap-1_1 and Lap-1_2, similar amounts of CTA were used for the modification. Using TGA or EA data alone gave inconsistencies in δ_g. However, an average of 800 molecules per clay platelet (equivalent to 50 mmol of **RAFT1** per 100 g of clay) was determined when data from the two techniques was considered. This was within the range of the CEC for Laponite clay assuming that all the metal cations were exchanged for the cationic CTA. The amount of modifier determined for sample Lap-1_3 exceeded the CEC of Laponite clay (67 mmol of **RAFT1** per 100 g of clay). It is known that when quaternary amines are added in excess during the modification of clay, the excess modifier can adsorb to the already attached modifier or to the clay itself.[21,22]

Table 3.3 Analysis of RAFT modified clay by TGA and EA

Sample	[RAFT1]	Weight loss [a]	δ_g [b]	C [c]	δ_g [d]	No. molecules[e] (CEC)[f]
	(μmol/m^2)	(%)	(μmol/m^2)	(%)	(μmol/m^2)	
Bare Laponite	–	3.06	–	–	–	–
Lap-**1**_1	1.72	17.01	1.45	6.27	1.23	~800 (50)
Lap-**1**_2	1.70	13.74	1.05	7.39	1.51	~800 (47)
Lap-**1**_3	2.65	22.24	2.13	7.82	2.98	~1620 (67)

[a] Weight loss between 150 and 600 ^{o}C, [b] Grafting density from TGA, [c] Corrected carbon content (%), [d] Grafting density from EA, [e] Average number of molecules per clay particle estimated from TGA and EA, [f] Equivalent cation exchange capacity in mmol/100 g clay

3.4 Conclusions

The CTAs for use in this study were synthesised, characterised and tested in order to evaluate their efficiency. The results from this section show that in the absence of clay, the CTAs behave in an "ideal" manner. Side reactions leading to the termination of propagating species were not detected by NMR or MALDI-TOF MS. MALDI-MS provided little reliable information on the end group structures due to fragmentation of the labile RAFT end groups. However, ^{1}H NMR confirmed the RAFT mechanism as PS chains with the RAFT agent incorporated at the initiating and terminating ends were observed.

The surface of the hydrophilic clay was successfully made organophilic through modification with a cationic CTA. The modification was confirmed by FT-IR and the extent of modification determined using TGA and EA.

References

(1)   Moad, G.; Rizzardo, E.; Thang, S. H. *Acc. Chem. Res.* **2008** *41*, 1133–1142.

(2)   Postma, A.; Davis, T. P.; Li, G.; Moad, G.; O'Shea, M. S. *Macromolecules* **2006**, *39*, 5307–5318.

(3)   Favier, A.; Charreyre, M.-T. *Macromol. Rapid Commun.* **2006**, *27*, 653–692.

(4)   Ercole, F.; Harrisson, S.; Davis, T. P.; Evans, R. A. *Soft Matter* **2011**, *7*, 2687–2696.

(5)   Chong, Y. K.; Le, T. P. T.; Moad, G.; Rizzardo, E.; Thang, S. H. *Macromolecules* **1999**, *32*, 2071–2074.

(6)   Akeroyd, N.; Pfukwa, R.; Klumperman, B. *Macromolecules* **2009**, *42*, 3014–3018.

(7)   Neises, B.; Steglich, W. *Angew. Chem. Int. Ed* **1978**, *17*, 522–524.

(8)   Moad, G.; Rizzardo, E.; Thang, S. H. *Aust. J. Chem.* **2005**, *58*, 379–410.

(9)   Deery, M. J.; Jennings, K. R.; Jasieczek, C. B.; Haddleton, D. M.; Jackson, A. T.; Yates, H. T.; Scrivens, J. H. *Rapid Commun. Mass Spectrom.* **1997**, *11*, 57–62.

(10)   Polce, M. J.; Ocampo, M.; Quirk, R. P.; Leigh, A. M.; Wesdemiotis, C. *Anal. Chem.* **2007**, *80*, 355–362.

(11)   Polce, M. J.; Ocampo, M.; Quirk, R. P.; Wesdemiotis, C. *Anal. Chem.* **2008**, *80*, 347–354.

(12)   Ladavière, C.; Lacroix-Desmazes, P.; Delolme, F. *Macromolecules* **2009**, *42*, 70–84.

(13)   Xu, J.; He, J.; Fan, D.; Wang, X.; Yang, Y. *Macromolecules* **2006**, *39*, 8616–8624.

(14)   Cox, F. J.; Johnston, M. V. *J. Am. Soc. Mass. Spectrom.* **2003**, *14*, 648–657.

(15)   Tasdelen, M. A.; Kahveci, M. U.; Yagci, Y. *Prog. Polym. Sci.* **2011**, *36*, 455–567.

(16)   Wang, J.; Wheeler, P. A.; Jarret, W. L.; Mathias, L. J. *J. Appl. Polym. Sci.* **2007**, *106*, 1496–1506.

(17)   Bartholome, C.; Beyou, E.; Bourgeat-Lami, E.; Chaumont, P.; Zydowicz, N. *Macromolecules* **2003**, *36*, 7946–7952.

(18)   Negrete; Letoffe, J.; Putaux, J.; David, L.; Bourgeat-Lami, E. *Langmuir* **2004**, *20*, 1564–1571.

(19)   Tamayo, F. G.; Titirici, M. M.; Martin-Esteban, A.; Sellergren, B. *Anal. Chim. Acta* **2005**, *542*, 38–46.

(20)   Bellucci, F.; Camino, G.; Frache, A.; Saffa, A. *Polym. Degrad. Stab.* **2007**, *92*, 425–436.

(21)   Swartzen-Allen, S. L.; Matijević, E. *Chem. Rev.* **1974**, *74*, 385–400.

(22)   Zhang, Z.; Sparks, D. L.; Scrivner, N. C. *Environ. Sci. Technol* **1993**, *27*, 1625–1631.

Chapter 4

SI-RAFT polymerisation of styrene from Laponite clay surfaces

The SI-RAFT-mediated polymerisation of styrene from Laponite clay is described in this chapter. The macromolecular structure of the free and grafted polymer chains was systematically investigated, using new analytical techniques, to get insight into the polymerisation occurring at the surface and in solution. To measure the effectiveness of the grafting technique, the free polymer content and the grafting density were determined using thermogravimetry.

4.1   Introduction

There is an on-going hype in material science to prepare the "ideal" material. For polymer scientists, this means a material consisting of polymer with controlled molar mass and architecture. With the advent of RDRP techniques this has become achievable. NMP, ATRP and RAFT mediated polymerisation have been used in the synthesis of a variety of organic/inorganic hybrid materials, consisting of polymers with well-defined macromolecular structures.

The advantages of using Laponite clay over the widely reported montmorillonite (MMT) clay[1-5] have been highlighted before. Laponite clay is chemically pure and has regular dimensions, which lead to single layer dispersion of the clay particles within the polymer matrix. The first reports on SI-RDRP from Laponite clay were by Mathias and coworkers[6] (SI-ATRP) and Bourgeat-Lami and coworkers[7] (SI-NMP). SI-RAFT from Laponite clay has not been reported to date, which is the purpose of this study.

The best conditions for obtaining organic/inorganic hybrid materials consisting of well-defined polymers through SI-RDRP have been described. In the case of RAFT mediated polymerisation, the addition of free or "sacrificial" RAFT agent to the polymerisation mixture ensures the simultaneous growth of surface-tethered and free polymer chains. Most of the work reported on SI-RAFT polymerisation from clay only used the surface-immobilised CTA.[3] As a result the experimental molar masses deviated significantly from the

theoretical and the molar mass dispersities were broad; no data were provided on the molar mass of the grafted polymer and grafting parameters.

In all the work that has been reported on SI-RDRP from clay, the macromolecular structure of the grafted polymer chains has not been carefully studied. Investigating the molar mass of the grafted and free polymer chains provides information on the similarities or differences in their polymerisation rates, whilst end group analysis gives insight on the polymerisation mechanisms of the surface-confined and free polymers.

The standard protocol for analysing grafted polymer is to first detach the polymer using ion exchange before analysis by SEC. However, this approach often results in very low concentrations of recovered polymer. In some cases, the low concentration of recovered polymer is thwarted by recovered unpolymerised initiator or CTA, making it challenging to obtain useful information on the molar mass and molar mass distribution. There is therefore a need to develop alternative analytical techniques to acquire information on the molar mass of the grafted polymer.[8] MALDI-MS is a suitable alternative as it requires only a very small amount of sample. The technique was used by Choi *et al.*[9] to determine the molar mass of PMMA recovered by ion exchange from a nanocomposite that was synthesised via emulsion polymerisation. The oligomers they recovered had low molar mass values of <500 g/mol.

In this study, PCNs were prepared via *in situ* polymerisation of styrene in the presence of CTA-modified clay. The experiments were carried out in the absence or presence of free CTA as illustrated in Scheme 4.1.
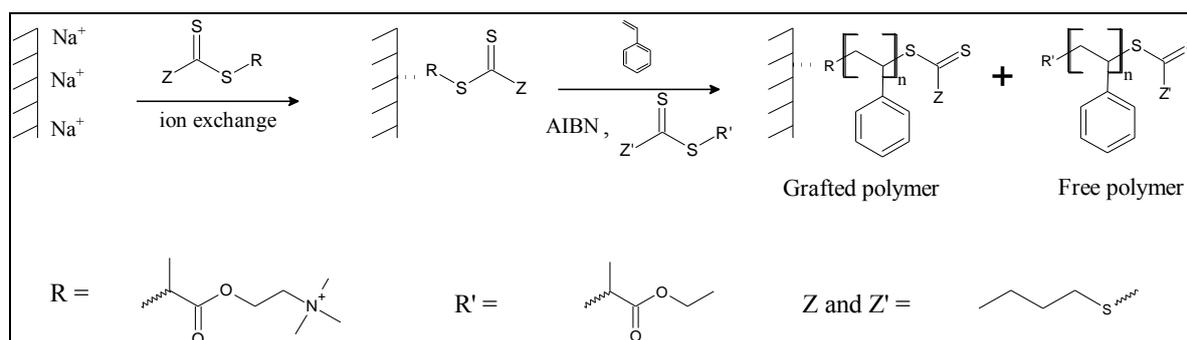
Scheme 4.1 Modification of Laponite clay followed by SI-RAFT polymerisation of styrene in the presence of free CTA

The macromolecular structure of the free and grafted PS was analysed systematically using SEC, NMR and MALDI-MS. A new analytical approach to characterise the grafted polymer

was developed in this study.[10] Polymer grafted from Laponite clay was analysed directly by MALDI-MS without the need to detach it. This approach was possible because the polymer was attached to the clay via electrostatic interactions between the negative charges of the clay surface and the positive charge of the reinitiating group. Zagorevskii *et al.*[11] have also reported on the direct analysis of oligonucleotides from MMT clay. However, their synthetic approach was different to ours as the nucleotides were not attached to the clay. To the best of our knowledge, the direct MALDI-MS analysis of polymer molecules attached to clay surfaces and the subsequent systematic characterisation of PCN has not been reported to date.

4.2   Experimental

4.2.1   Materials

Styrene and 2,2′-azobis(isobutyronitrile) (AIBN) were purified as described in Section 3.2.2. The surface of Laponite clay was modified as described in Section 3.3.2. Free RAFT agent, ethyl 2-(butylthiocarbonothioylthio)propanoate was synthesised as described in Section 3.1.2.

4.2.2   SI-RAFT polymerisation of styrene

The following procedure was typical for the surface-initiated polymerisation of styrene: RAFT-modified clay (0.266 g), styrene (10 mL, 87.0 mmol), free RAFT agent, **RAFT2** (0.039 g, 0.18 mmol), and AIBN (0.0024 g, 0.0146 mmol) were added to a 100 mL Schlenk flask. The mixture was stirred overnight in order to homogeneously disperse the clay in the solution allowing monomer, free RAFT agent and initiator to enter the clay galleries. The mixture was degassed by three successive freeze-pump-thaw cycles, backfilled with argon, sealed and placed in an oil bath set at 70 °C for 24 h. The free polymer was separated from the grafted clay by successive dispersion-centrifugation processes in toluene. The supernatant was then concentrated, and PS precipitated from cold methanol. The free PS and grafted clay were dried under vacuum at room temperature.

Recovery of bound polymer

The electrostatically bound PS was recovered from the grafted clay using the following procedure: 100 mg of grafted clay (Lap-g-PS) was dispersed in THF (10 mL) and LiBr (0.005 g, 0.058 mmol) added. The mixture was degassed for at least 15 minutes using argon, and then refluxed for 24 h. The detached polymer was separated from the clay by centrifugation.

The polymer solution was concentrated and PS precipitated from cold methanol. The recovered polymer was dried under vacuum at room temperature

4.2.3 Analyses

SEC

SEC analysis was performed as described in Section 3.2.2.

NMR

All NMR spectra were acquired on a Varian Unity INOVA 400 MHz instrument. Prior to analysis, the free polymer and grafted clay particles were dialysed against toluene using SnakeSkin® pleated dialysis tubing, with a molar mass cutoff of 3500 g/mol. The polymer samples were prepared by dissolving in $CDCl_3$, and the grafted clay was dispersed in $CDCl_3$ using ultrasonication. The unmodified clay in the grafted clay samples was allowed to settle prior to spectrum acquisition. A minimum of 128 scans were acquired per spectrum. All spectra were processed using MestRe-C 2.3a. The phase and the baseline were corrected manually prior to signal integration.

MALDI-TOF MS

Instrumentation and sample preparation was as described in Section 3.2.2. The grafted clay samples were ultrasonicated in order to disperse them in THF. The samples were prepared as follows: typically, solutions of 20 mg dithranol/mL, 2 mg grafted-clay/mL in THF were prepared. The solutions were mixed in the following ratios 15:15(v/v). Approximately 0.3 μL of the sample was transferred to the target plate and air dried prior to analysis. The mass resolution of the instrument was better than 5000 and the mass accuracy was ±2 Da.

TGA

TGA was carried out as described in Section 3.3.2.

4.3   Results and Discussion

Optimising conditions for the dispersion of CTA-modified clay in monomer

The conditions adapted for the SI polymerisation of styrene were similar to those used in Chapter 3. A small amount of AIBN initiator was added to the polymerisation mixture to generate the initiating radicals. The experiments were performed either in the presence or

absence of free CTA. The former allows for a comparison between the polymerisation mechanism of the surface-tethered and free polymer to be made. In addition, it provides information on the control of the polymerisation of free polymer, in the presence of clay particles.

Prior to *in situ* polymerisation, there is need to homogeneously disperse the CTA-modified clay in the monomer. Two different approaches were investigated. In the first approach CTA-modified clay was first dispersed in a mixture of styrene and free CTA, before AIBN was added, and the mixture subsequently polymerised. In the second approach, the CTA-modified clay was dispersed in a styrene-free CTA-AIBN mixture, which was subsequently polymerised.

The widely used test for a successful SI-RDRP is measuring the molar mass of the free polymer. In the first approach where the initiator was added after clay dispersion (runs 5 and 6, in Table 4.1), the SEC traces of the free polymer exhibited bimodality, regardless of whether free CTA was added or not. This was a result of the initiator not getting sufficient time to enter the clay galleries, and get evenly distributed throughout the mixture. When the initiator was given sufficient time to enter the clay galleries (runs 1–4 and 7), the molar mass distributions of the free polymer were monomodal, and the dispersities in the presence of free CTA were narrow i.e. <1.4. We thus proceeded to use the second approach (as described in Section 4.2.2) to disperse CTA-modified clay in monomer prior to polymerisation.

Table 4.1 Experimental conditions for SI-RAFT polymerisation of styrene and SEC data of free and grafted PS

Run	[M]/[RAFT] (mol/mol) [c]	Conv. (%)	M_n(calc) (g/mol)[d]	Free PS			Grafted PS	
				M_n [e]	M_p [f]	Đ [g]	M_n [h]	Đ
1[a),‡]	205	22	4200	4700	6270	1.27	5000	1.66
2[a),‡]	402	26	8600	8900	11 870	1.28	8300	1.36
3[a),‡]	485	56	33 100	18 800	26 630	1.29	12 000	1.50
4[a),‡]	614	15	9890	12 030	17 580	1.40	7410	2.44
5[a),†]	107	35	4200	6590	5840	1.67	10 590	1.31
					14 320			
6[b),†]	180	25	4980	13 140	15 620	1.90	16 750	2.8
					26 110			
7[b),‡]	475	33	16 620	22 760	31 660	1.86	–	–

[a] Free CTA added, [b] No free CTA added, [c] Ratio of monomer to total RAFT agent, [d] Calculated number average molar mass [e] Number average molar mass of free PS, [f] Peak molar mass of free PS, [g] molar mass dispersity [h] Number average molar mass of grafted PS, [‡] Polymerisation mixture with AIBN in, stirred for 24 h, [†]The polymerisation mixture was stirred for 3 h before adding AIBN

Molar mass of free and grafted PS by SEC

The molar mass distributions of the free PS from the runs performed in the absence of free CTA (runs 6 and 7) were broad, see Figure 4.1. This was consistent with the results reported by others.[3,12] Samples were withdrawn from run 7 at set intervals of time in order to determine the "livingness" of the polymerisation. High molar masses were obtained in the first two hours of the reaction and remained fairly constant throughout the polymerisation. This behaviour is typical of conventional radical polymerisation, where polymer chains are continuously generated and terminated. Figure 4.1B shows the SEC traces of free PS acquired at different times. The chromatograms did not show any significant shift in elution volume. The conventional polymerisation behaviour of the free PS was a result of the reduced accessibility of the surface-confined CTA to the polymer chains initiated and propagating in solution.
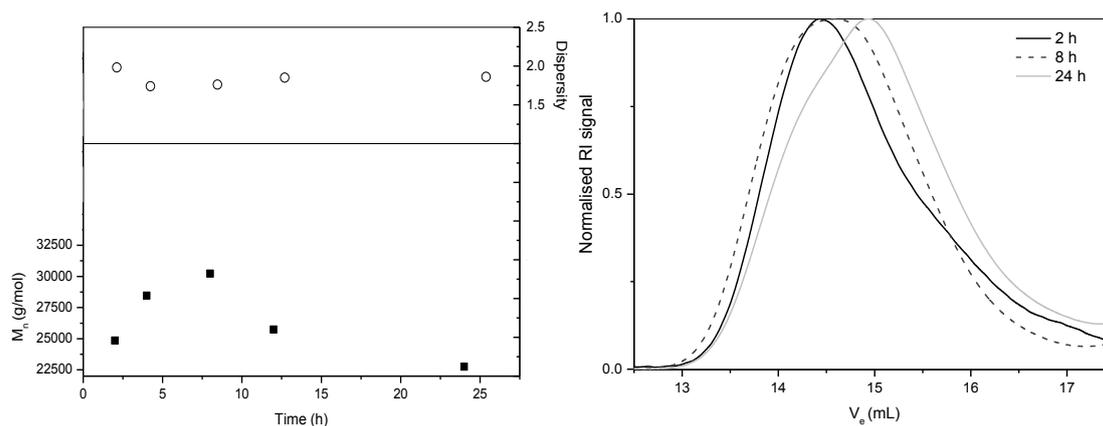
Figure 4.1 A) Evolution of molar mass and molar mass dispersity over time (B) SEC chromatograms at selected times of run 7

In the presence of free CTA, the molar mass dispersities of the free polymer were narrow, as expected for "living" radical polymerisation (runs 1–4). The molar mass of the final polymer could be altered by varying the CTA (free + intercalated) to styrene ratio, see equation 3.2.

The molar mass of the free and cleaved (grafted) PS were compared in order to get insight into the polymerisation process. The number average molar mass (M_n) values were in agreement with a scenario where the surface-bound and free CTA were taking part in the polymerisation, as the values were quite close to the calculated molar mass.

Figure 4.2 shows an overlay of the SEC traces of cleaved and free PS from runs 1–3. What is obvious in the cleaved PS molar mass distributions (see Figure 4.2D) is the presence of a low molar mass fraction at $M_n<1000$ g/mol. This region remained unchanged regardless of the targeted molar mass, whilst the higher molar mass region (narrower peak) shifted significantly with a decrease in the concentration of CTA. All this indicated that the cleaved polymer consisted of dormant and dead polymer chains.
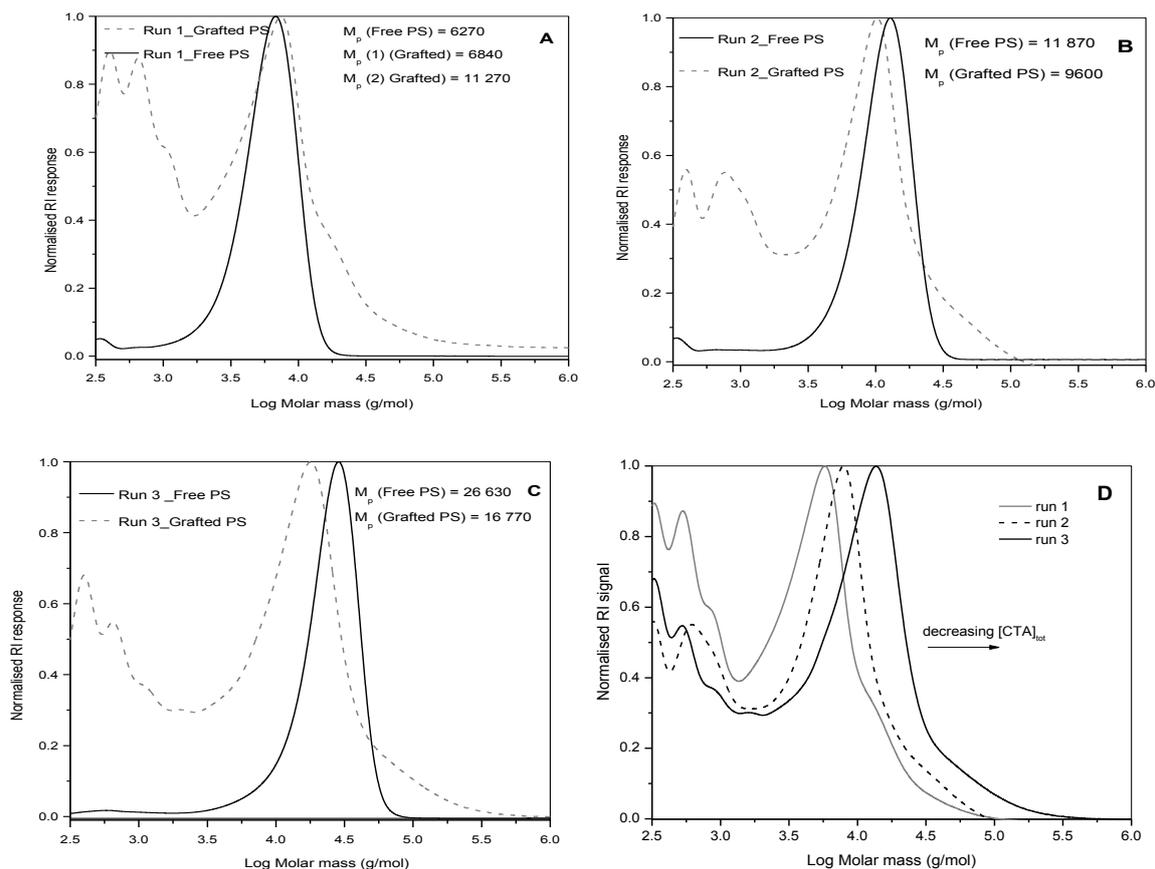
Figure 4.2 Molar mass distributions of free and grafted PS from runs 1 (A), 2 (B) 3 (C) and overlay of grafted PS (D)

The high molar mass part of the grafted PS SEC chromatograms from runs 2 and 3 showed monomodal distributions. It is worth mentioning that what appears to be bimodality in the RI responses of the chromatograms for runs 2 and 3 is not. An overlay of the RI and UV responses (using λ=254 nm for the latter) did not show the high molar mass shoulder.

For run 1 the situation was different: the grafted PS showed bimodality (RI and UV responses) as a shoulder corresponding to doubled peak mass (M_p) was observed. This was attributed to recombination reactions which are prevalent in surface-initiated RAFT polymerisation.[13] The reason why this was observed in run 1 and not in 2 and 3 is the higher clay content (wt.-%) of the aforementioned, which inevitably leads to higher viscosity of the polymerisation mixture. This minimises the diffusion of monomer to the clay surface, resulting in termination occurring by recombination of neighbouring propagating chains.

In SI-RAFT polymerisation the nature in which the CTA is attached to the solid surface plays a significant role in controlling polymerisation.[14] When the RAFT agent is attached to the solid surface via the R-group, polymer chains grow from the surface, and the thiocarbonyl thio bearing Z-group migrates between solution and the surface. If access to the propagating radicals at the surface is hindered, this leads to polymer chains growing at different rates with some undergoing termination. This inevitably leads to broadening of the molar mass distribution as shown by the molar mass dispersities of the grafted PS.
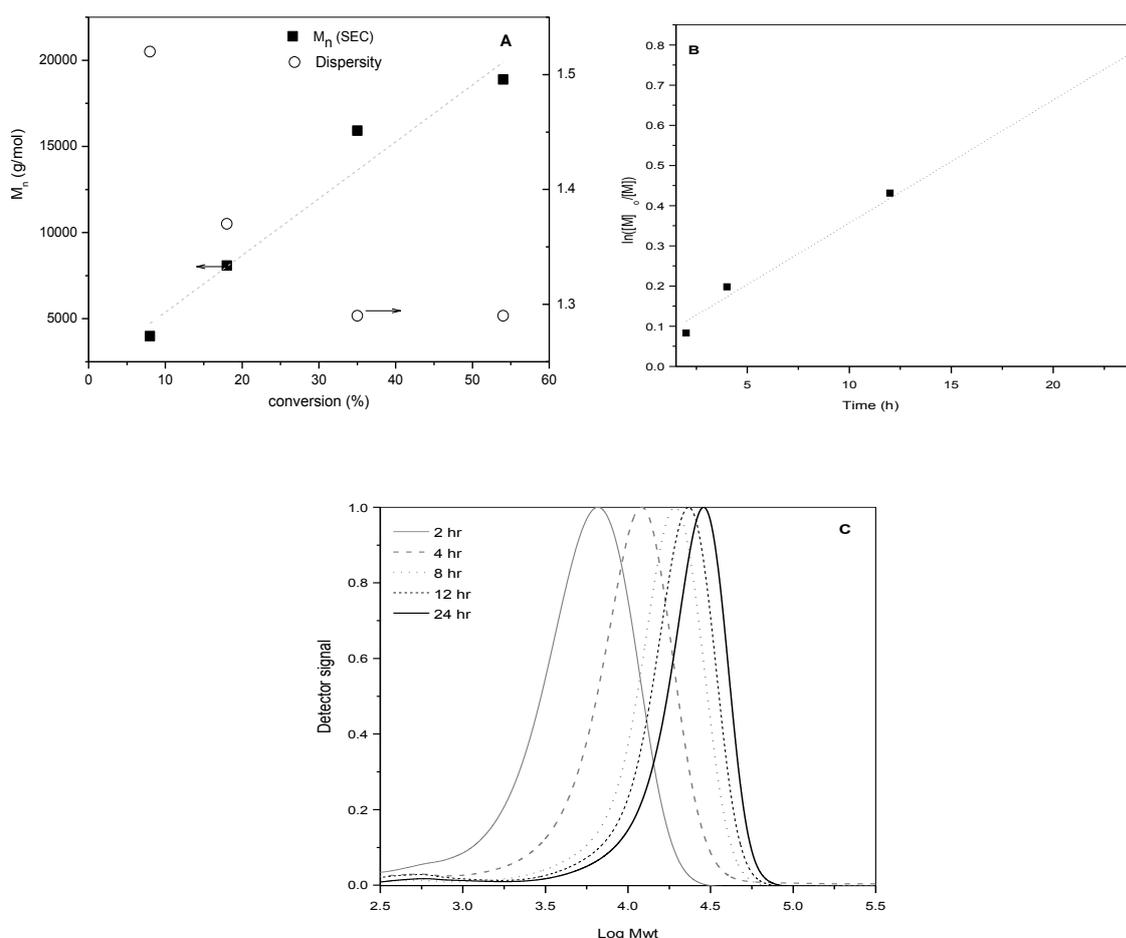

Figure 4.3 (A) Plots of evolution of molar mass (▪) and dispersity (○) vs. monomer conversion and (B) kinetic plot of free polystyrene as a function of time (C) Normalised molar mass distributions free PS

In order to investigate the "livingness" of the polymerisation in the presence of free CTA, samples were withdrawn from run 3 at set time intervals. There was a linear increase in molar mass with conversion together with a decrease in dispersity from 1.5 to 1.3 (Figure 4.3A) and the first order kinetic plot was linear (Figure 4.3B). The SEC molar mass distributions

(Figure 4.3C) were monomodal although there was some evidence of tailing in the low molar mass region. Fan *et al.*[15] suggested that the tailing was a result of termination reactions occurring at the beginning of the experiment as a result of the reaction between free PS and Lewis acid sites on the clay surface.[16]

Molar mass and end group analysis of free and grafted PS by ^{1}H NMR

Free PS

The assumption often made on the simultaneous growth of polymer from a solid surface and in solution via RDRP is that the polymer chains grow at the same rate. This was clearly not the case here. The grafted PS had lower molar masses and broader molar mass dispersities compared to the free PS. In addition, there was a significantly higher amount of dead polymer chains observed in the SEC traces of the grafted PS. This was similar to results obtained by Tsujii *et al.*[17] on SI-RDRP of styrene from silica particles.

In order to obtain clarity on the polymerisation mechanism at the surface and in solution, ^{1}H NMR and MALDI-TOF MS were used to investigate the end group structures of free and grafted PS. This is a new analytical approach to PCN characterisation.
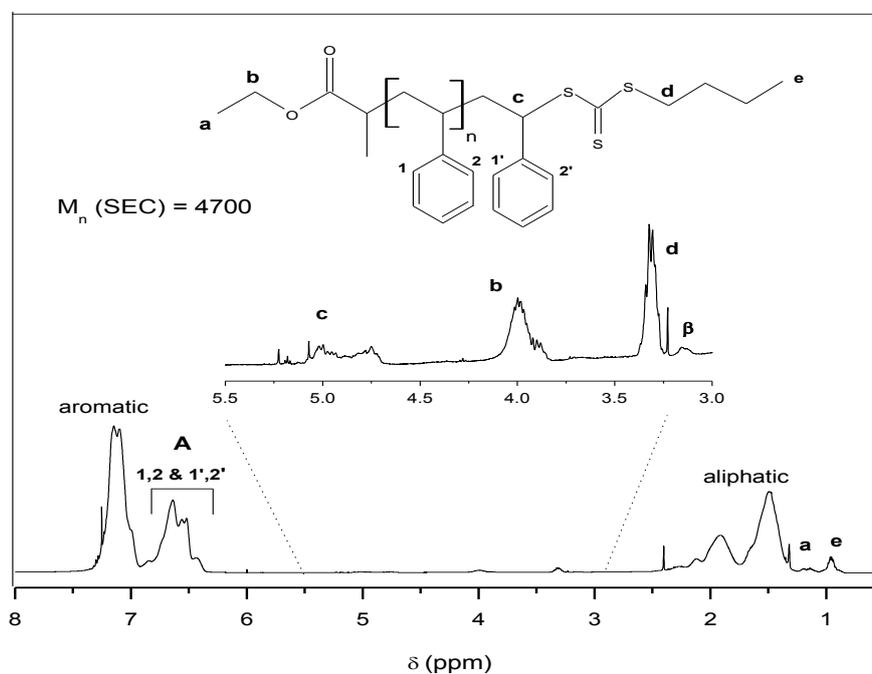

Figure 4.4 ^{1}H NMR spectrum of free polystyrene after 24 h and ideal structure of free RAFT agent derived PS

Figure 4.4 shows the typical ^{1}H NMR spectrum of free PS. The signals attributed to the polymer backbone and end group protons were assigned as shown in the figure. For the chain ends, the assignments were based on the chemical shifts of the free CTA, **RAFT2**.

The free PS samples from run 3 were also analysed by ^{1}H NMR spectroscopy, in order to investigate the end group structure evolution over time. What is evident from the spectra in Figure 4.5 is the presence of the resonance signals characteristic of the dormant polymer chains in all the samples. The signal at 3.7 ppm appearing from 4 h is attributed to the methyl protons of the quaternary ammonium group of the cationic CTA. The presence of cationic CTA derived chains could result from reversible detachment of the surface-tethered chains or the inability of successive dispersion-centrifugation steps to effectively separate highly grafted clay particles from free polymer. The latter is more probable and was confirmed by FT-IR, see Appendix 2. The signal observed at 3.5 ppm was attributed to residual methanol. The resonance signal at 3.1 ppm, observed at higher monomer conversions could not be assigned.
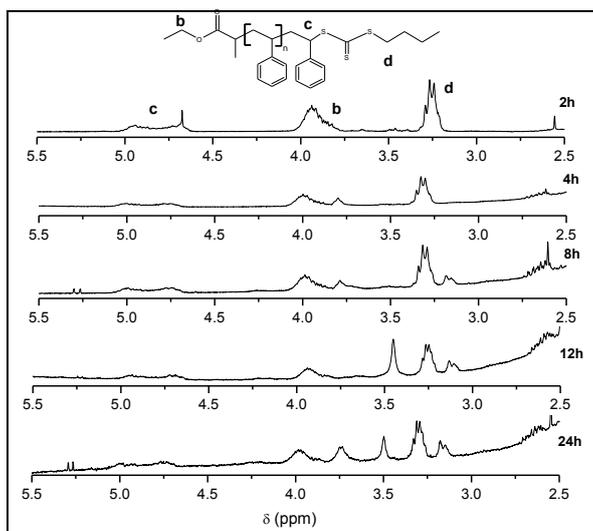

Figure 4.5 Selected region of ^{1}H NMR spectrum free PS and ideal structure of free RAFT agent derived PS

The percentage functionality of the free PS chains was determined from SEC and ^{1}H NMR data, by comparing the M_n values obtained from the two techniques, using equation 4.1[18]

$$\text{Functionality } (f) \quad = \frac{M_n}{M_{eq}} \times 100 \qquad\qquad (4.1)$$

where M_n is the number average molar mass as determined by SEC, and M_{eq} is the equivalent molar mass i.e. M_n per functional group as determined from ^1H NMR data, using equation 4.2.

$$M_{eq} = \frac{\int A / 2}{\int c} \times M_{st} \qquad\qquad (4.2)$$

where $\int A/2$ and $\int c$ are the area intensities of signal A divided by 2 and signal c, respectively. Only the signals for the two protons adjacent to the quaternary aromatic carbon were considered[19] for the calculation, as the signals for the other protons were overlapping with the $CHCl_3$ signal at 7.26 ppm. Another method for determining functionality is by comparing the area intensity of the protons at the terminating and initiating ends of the polymer (see equation 3.3). This approach could not be used here, as the resonance signals of interest were overlapping with other signals.

The M_n (NMR) values were higher than the M_n (SEC) in all the samples–a possible indication of a loss in thiocarbonyl thio functionality. It is worth mentioning that molar mass determination by using ^1H NMR can be determined with fair accuracy up to 25 000 g/mol.[20] However, this limit is dependent upon the sample and the sensitivity of the NMR instrument used.

Table 4.2 Comparison of molar mass data of free and grafted PS from SEC and NMR

Sample	Time [a]	Free PS		F [d]	Grafted PS	
		M_n (SEC) [b]	M_n (NMR) [c]		M_n (SEC)	M_n (NMR)
Run 1	24	4700	6100	77	5000	11 500
Run 2	24	8900	11 300	78	8300	–
Run 3	2	3990	5330	75	–	2760
	4	8080	10 380	78	–	7530
	8	12 680	15 530	82	–	–
	12	15 910	19 460	82	–	10 660
	24	18 880	24 660	77	12000	17 060

[a] Polymerisation time in hours, [b] *Number-average* molar mass as determined by SEC, [c] *Number-average* molar mass determined from NMR data, [d] F is the % functionality determined using equation 4.1

The functionality of the free PS at 24 h was relatively high for all three samples (see Table 4.2). When the functionality was followed over time (run 3), it was apparent that the functionality remained fairly constant throughout the polymerisation between 75 and 82%.

The relatively high functionality was consistent with the low molar mass tailing observed in the chromatograms, and is attributed to the termination of propagating radicals.

Grafted PS

The grafting of PS from the surface of Laponite clay was confirmed by FT-IR, see Appendix 3. The PS grafted to the clay surface was analysed directly by ^{1}H NMR spectroscopy. The grafted clay samples were dispersed in deuterated $CHCl_3$ and the ungrafted clay allowed to settle before shimming the magnet and acquiring the spectrum. One of the advantages of the direct analysis of PS grafted to clay by NMR is that NMR is non-destructive. Therefore, the recovered grafted clay sample can still be used for other analyses.
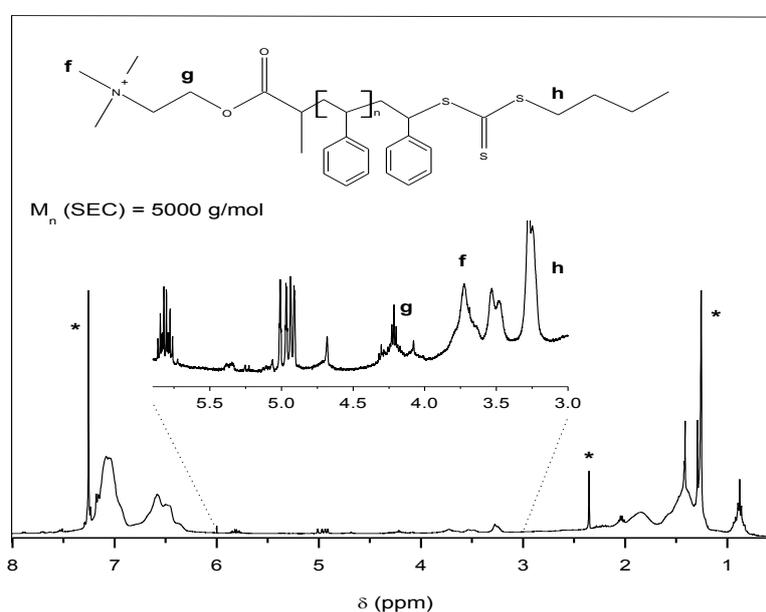

Figure 4.6 ^{1}H NMR spectrum of grafted polystyrene after 24 h and ideal structure of grafted PS

Similarly to free PS, the resonance signals attributable to the CH_2 and CH groups of the PS backbone were observed at 1.0–2.5 ppm and those of the aromatic protons at 6–7.5 ppm. The absence of the resonance signal attributable to the methylene protons of the free CTA at 4.0 ppm was an indication that the sample did not contain any **RAFT2** derived chains. The resonance signals characteristic of the cationic CTA which were observed at 4.2 ($CH_2C\textbf{H}_2O$), labelled **g** and 3.8 ppm ($N(C\textbf{H}_3)_3$), labelled **f** confirmed that the sample consisted predominantly of cationic CTA derived PS. The signal labelled **h** at 3.2 ppm was attributed to the methylene protons adjacent to the thiocarbonyl thio moiety.

Chapter 4: SI-RAFT polymerisation of styrene from Laponite clay surfaces

The M_n (NMR) of grafted PS was estimated by comparing the area intensity of the aromatic protons signal between 6 and 7 ppm to the signal at 3.75 ppm, labelled f. The area intensity of the CH_2–S– proton signal was higher than that for the $(CH_3)_3$ protons. This was not consistent with our expectations, showing the probability that the signal at 3.2 ppm was overlapping with other signals.

The M_n (NMR) values for grafted PS were lower than the values for free PS, see Figure 4.7. This was consistent with the values obtained from SEC data. The general shape of both curves showed the same behaviour, which was a further indication of the simultaneous growth of grafted and free PS.
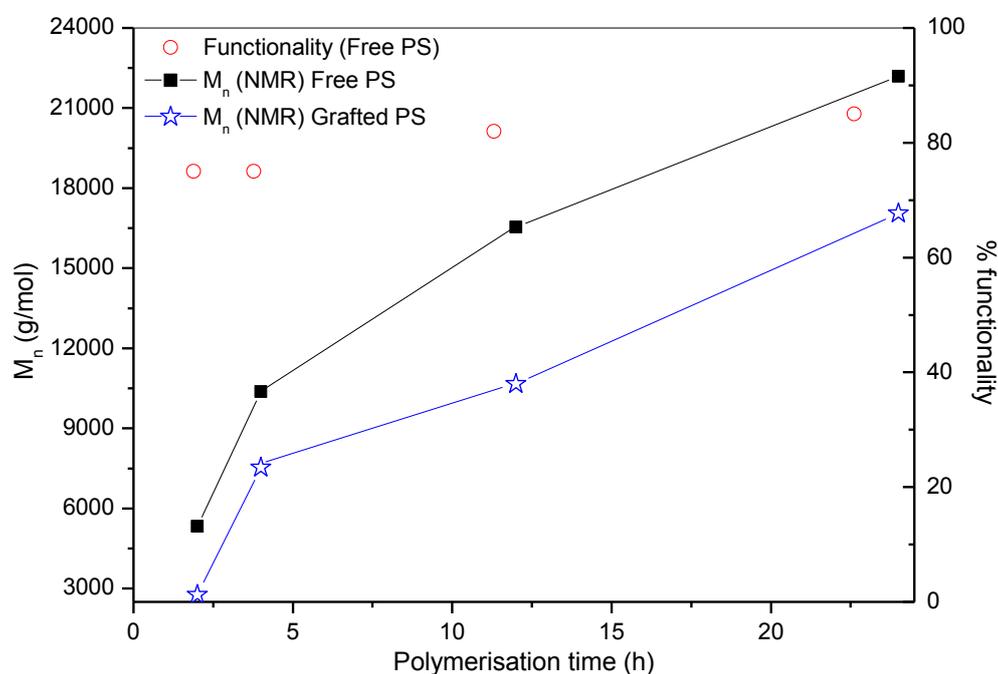

Figure 4.7 Comparison of M_{eq} of free and grafted PS

Figure 4.8 shows an expansion of a selected part of the ^{1}H NMR spectrum of grafted PS. The resonance signals between 4.6 and 6.0 ppm (labelled 1–5) are attributed to protons attached to a double bond (which typically appears between 4.5 and 6.5 ppm). Observing signals in this region was an indication of a more complex polymerisation mechanism occurring at the clay surface than in solution.

Protons of double bonds are typically non-equivalent and often give rise to complex splitting patterns. The concentration of these groups was determined relative to the aromatic protons, between 6 and 7 ppm.
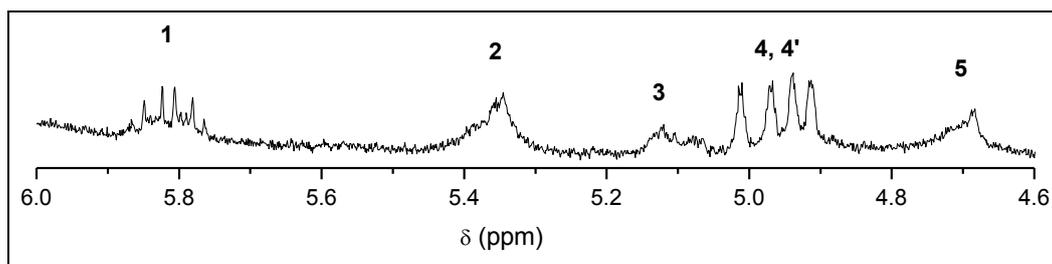
Figure 4.8 Magnification of a selected region of ^{1}H NMR spectrum of grafted PS

The signals at 4.9 and 5.8 ppm (labelled **1** and **4,4′** respectively) had the highest concentration. The splitting pattern observed was typical of an allylic compound or monosubstituted vinyl end group, $CH_2=CH–CH_2–$.
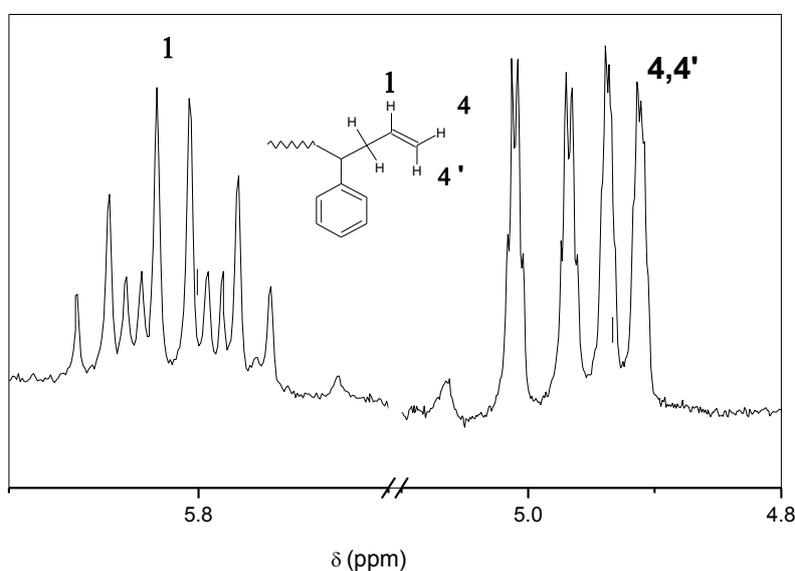

Figure 4.9 Magnification of the ^{1}H NMR spectrum of grafted PS showing a selected region

The two terminal vinyl hydrogen atoms (labelled **4,4′**) gave rise to a doublet of doublets owing to their individual coupling with the adjacent hydrogen atom, labelled 1. The *cis* coupling constant, $J_{4,1}$ was characteristically smaller than the *trans* coupling constant, $J_{4′,1}$ i.e. 10.1 and 17.5 Hz respectively. The hydrogen atom labelled 1 showed the most complicated splitting pattern, owing to its distinct coupling with protons 4 and 4′, which were further split by the adjacent methylene protons. The integrals of signals 1 and 4,4′ was 2:1 which is consistent with an allylic group. The multiplicity was still distinguishable meaning that the molecule was of low molar mass.

The proposed mechanism for the formation of the allylic group follows a free radical pathway. Polystyryl radicals are known to undergo β-C–C bond scission under high energy level conditions, generating primary and secondary radical centres. Based on theoretical calculations by Gies *et al.*[21] the bond energies for the benzylic hydrogen and phenyl group are similar. Therefore following the formation of a primary radical (see Scheme 4.2), loss of a β-Ph• results in the formation of an allylic group.
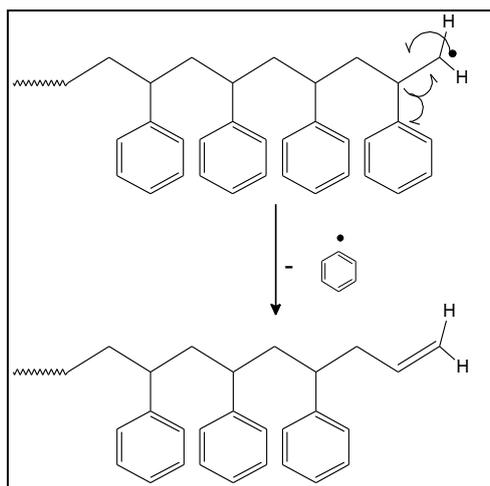

Scheme 4.2 Mechanism for the formation of the monosubstituted vinyl end group

In SI-RAFT polymerisation, the surface-confined propagating radical may undergo the RAFT process with a neighbouring grafted polymer or free polymer in solution.[17] The latter will occur only if there is free polymer within its vicinity. In the absence of neighbouring dormant PS chains for degenerative chain transfer, the surface-confined radical may undergo termination via recombination with a neighbouring grafted radical. This is the main termination pathway for polystyryl radicals.

The resonance signals observed at 4.7 and 5.1 ppm (labelled 3 and 5) are characteristic of a 1,1-disubstituted alkene end group.[22,23] Assuming that termination was to occur via disproportionation, a resonance signal characteristic of the 1,2-disubstituted alkene end group would have been observed at 6.0 ppm.[23]

The pathway that leads to the formation of PS with a 1,1-disubstituted alkene end group is outlined in Scheme 4.3. Chain transfer to polymer occurs via an inter- or intramolecular pathway. In the former case, a propagating radical abstracts a hydrogen atom from another polymer molecule, whilst in the latter case the abstraction occurs within the same molecule

(back-biting). The result from both pathways is an intermediate radical that undergoes β-scission to give the 1,1-substituted alkene, I_A^2 and primary radical, I_B. The ratio of the integrals of these two signals was 1:1.
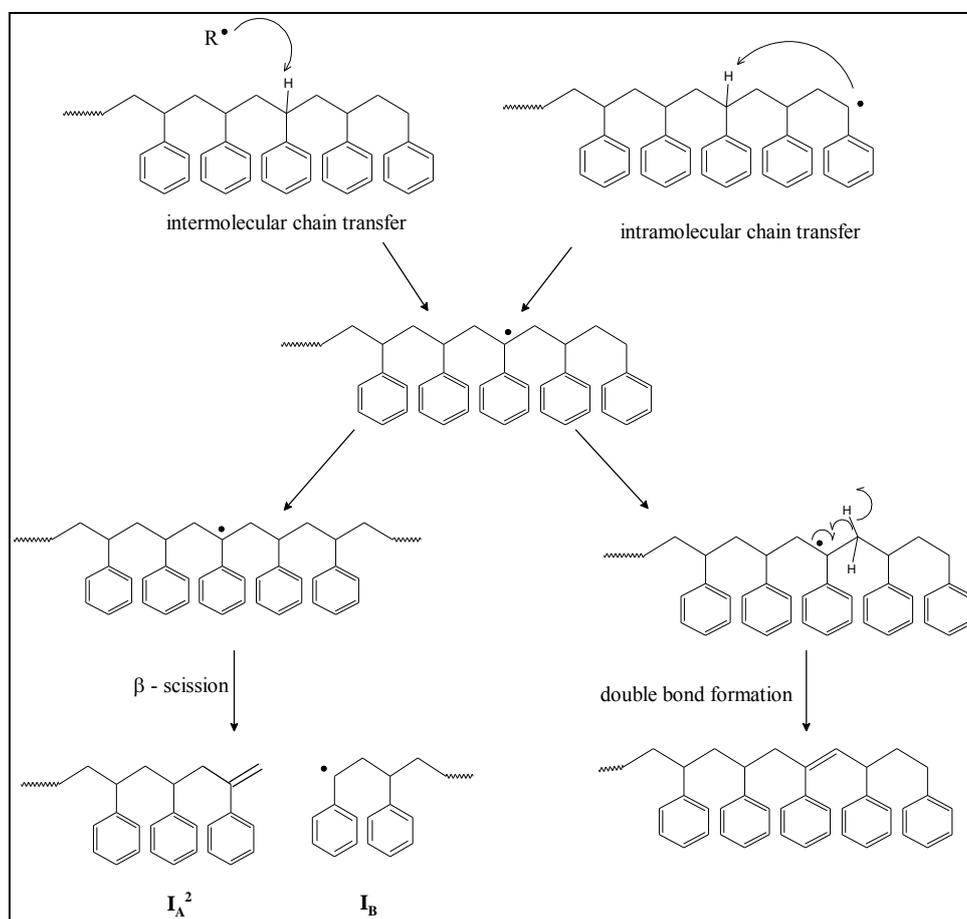
Scheme 4.3 Pathway for formation of 1,1-disubstituted alkene end group and mid chain double bond.

Another possible fate of the intermediate radical involves the loss of a β-H• resulting in the formation of a mid-chain double bond.[24] The resonance signal at 5.3 ppm possibly emanates from such a structure. The assumption was based on the following observations: resonance signals of hydrogen atoms on a double bond are often found in pairs. Since no complimentary resonance signals were present, it was apparent that the signal emanated from one hydrogen atom on a double bond.

The grafted clay samples from run 3 were also analysed in a similar way by ^{1}H NMR, and it was apparent that chain transfer-to-polymer reactions were occurring at the clay surface throughout the polymerisation.

Analysis of grafted PS by MALDI-MS

The free and grafted PS samples were analysed by MALDI-TOF MS to provide complimentary information on the end group structures. MALDI-MS analysis of grafted PS was carried out on grafted clay (after washing off physisorbed polymer) and cleaved polymer. The direct analysis of PS from clay was possible as the polymer was attached to the clay via electrostatic interactions between the R-group and the negative charges on the clay surface. This approach to the analysis of PCNs is novel and significant as it evades the extra ion exchange step.
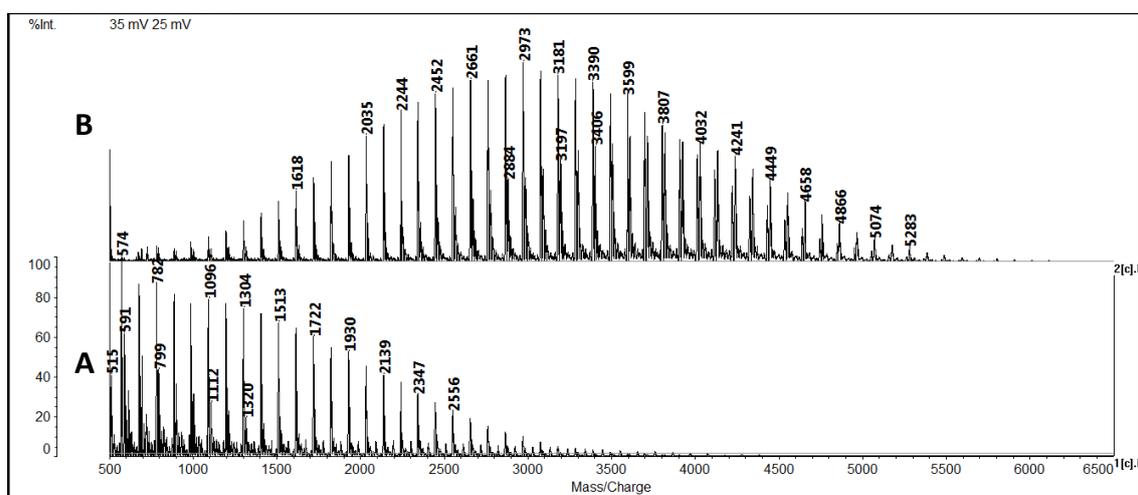

Figure 4.10 MALDI TOF MS spectra for PS analysed directly from clay (A) and analysed after detaching by ion exchange (B), M_n (SEC) = 5700 g/mol, M_p = 4430

Figure 4.10 shows the stacked MALDI-MS spectra of grafted PS analysed directly from clay (A) and after detaching via ion exchange (B). All spectra were acquired in the linear mode. What is obvious in the two spectra is that the molar mass range of spectrum B is wider than spectrum A. Molar mass discrimination effects are well-known in the analysis of polymers with broad molar mass distributions.[25-27] The result is a misrepresentation of the molar mass, which is evident in spectrum A. The purification step (precipitation and filtration) for the cleaved PS usually results in some degree of low molar mass product loss. This reduces the molar mass dispersity and widens the observed molar mass range, as shown in spectrum B.

Each spectrum shows a cluster of peaks, with each cluster being separated by 104 Da which is the molar mass of one styrene unit. Figure 4.11 is a magnification of the spectra showing a

selected region of m/z 2030–2340 (n=18 or 19). The different peaks present within each cluster represent polymer chains with different end groups.
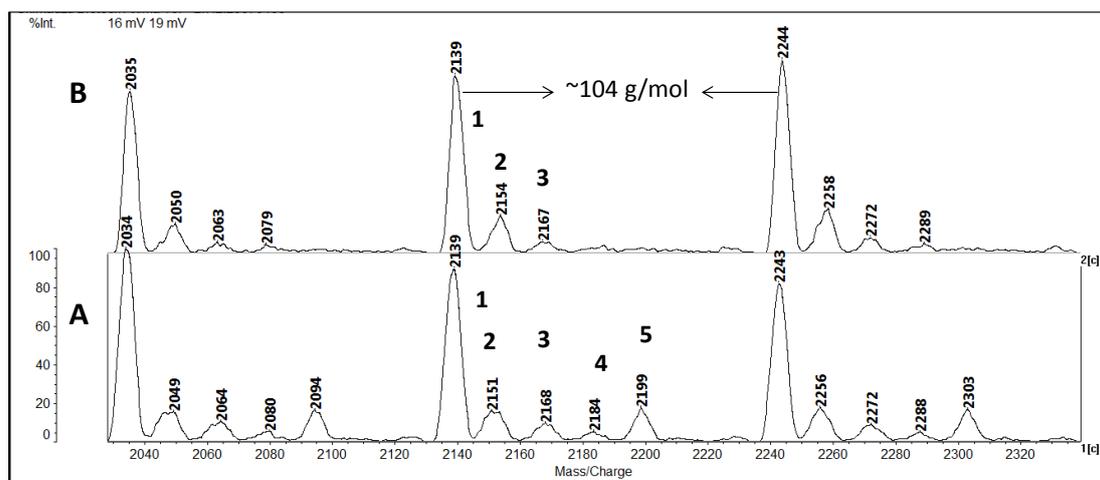

Figure 4.11 Selected parts of MALDI-MS spectra of (A) detached PS and (B) Lap-g-PS

Possible structural assignments for the different observed peaks are given in Table 4.3. It is worth mentioning that mass resolution is very low in the linear mode. As a result, it is difficult to distinguish structures differing by 1 or 2 Da. The polymer chains observed in the spectra were assigned to PS cationised by H^+ ions, $[M+H]^+$ or PS bearing the cationic R-group from the CTA, $[M]^+$.

The major distribution at m/z 2139 (labelled 1) corresponds to two possible structures. The first structure possesses the 1,2-disubstituted alkene end group. This structure was not observed in NMR; hence it was most likely formed during MALDI-MS analysis.[28] Labile end groups from RDRP are known to fragment fairly easily during MALDI-MS analysis; it is therefore not a surprise that these species form the major distribution in the spectra.

As mentioned previously, polystyryl radicals can undergo either intra- or intermolecular chain transfer reactions (see Scheme 4.3). The result is an H-terminated PS chain and an intermediate radical. H-terminated PS chains are a second possible contribution to the distribution. H-terminated PS chains are not easy to detect in ^1H NMR owing to the overlap of the resonance signal of the terminal H atom with other signals from the PS backbone. As a result, chain transfer to polymer is confirmed through the presence of species emanating from the fragmentation of the intermediate radical formed, i.e. 1,1-disubstituted alkene end group, (I_A^2) at m/z 2151.

Table 4.3 Structures corresponding to various peaks in Figures 4.11 and 4.14

Peak	m/z (expt)[a]	m/z (theo)[b]	Structure	n[c]
1	2139	2136		18
		2138		18
2	2151/2154	2150		18
3	2167/2168	–	–	–
4	2184	2182		18
		2183		19
5	2199	2198		18
6	4725	4724		43
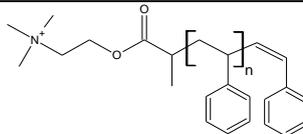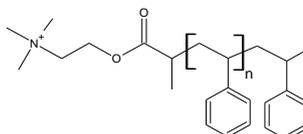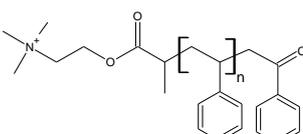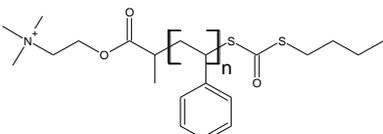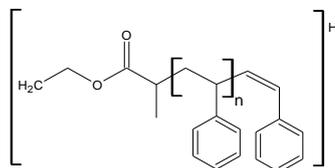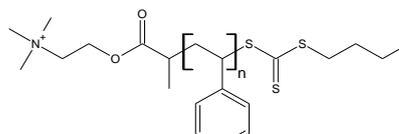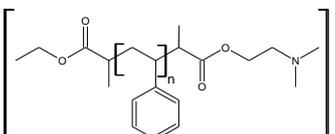
[a] Experimental molar mass, [b] Calculated molar mass, [c] Degree of polymerisation

From the RAFT mechanism,[29] the dormant polymer chains are those in which the RAFT agent is incorporated, i.e. (R) group at the initiating (α) end and the thiocarbonyl thio moiety bearing the stabilising (Z) group at the terminating (ω) end. The dormant PS chains from the RAFT process were observed at m/z 2199, peak labelled 5. It is evident from Figure 4.11 that peaks 4 and 5 were only present in the sample where PS was analysed directly from the clay. It appears as though the clay cushions the PS chains from fragmentation by absorbing some of the energy from the laser. This finding was unexpected and interesting.

Peaks 4 and 5 differ by ~16 Da, two possible structures had a calculated molar mass corresponding to the m/z of the peak. The first possible structure results from the oxidation of the trithiocarbonate moiety to a dithioester. This is known to occur during sample preparation[30] or the MALDI-MS experiment.[31] The possible mechanism for the formation of the second possible structure will be discussed later.

To confirm the structural assignments, tandem MS (MS/MS) experiments were carried out. Measurements performed through the coupling of MALDI-TOF MS with collision-induced dissociation (MALDI-TOF-CID) provide additional structural information e.g. sequence distribution[32] and chain end functionality.[33] In addition, MALDI-TOF-CID measurements have been used to study the behaviour of oligomer ions under high energy level conditions[21,34-36] and to distinguish between isobaric structures.

MALDI-TOF-CID measurements involve the isolation of a specific oligomer ion (parent/precursor ion) and its subsequent fragmentation to structurally diagnostic fragments through collision with a noble gas. In this study, **RAFT1** derived dormant species were selected as the precursor ion. The representative precursor ions (marked with circles in Figure 4.12) had molar masses of 740 (n=4), 844 (n=5) and 948 Da (n=6). Similar fragmentation patterns were observed with all three ions. The corresponding CID spectrum for the peak at m/z 844 is displayed in Figure 4.13. MALDI-TOF-CID was used in this study to distinguish species emanating from the fragmentation of the dormant PS chains, and those from other fragmentation processes occurring during the reaction.
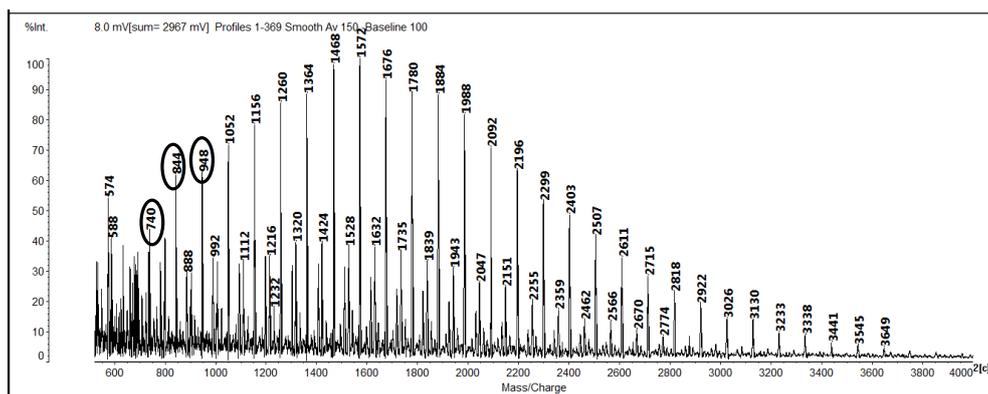
Figure 4.12 MALDI-MS spectrum of grafted PS analysed directly from clay in the reflectron mode
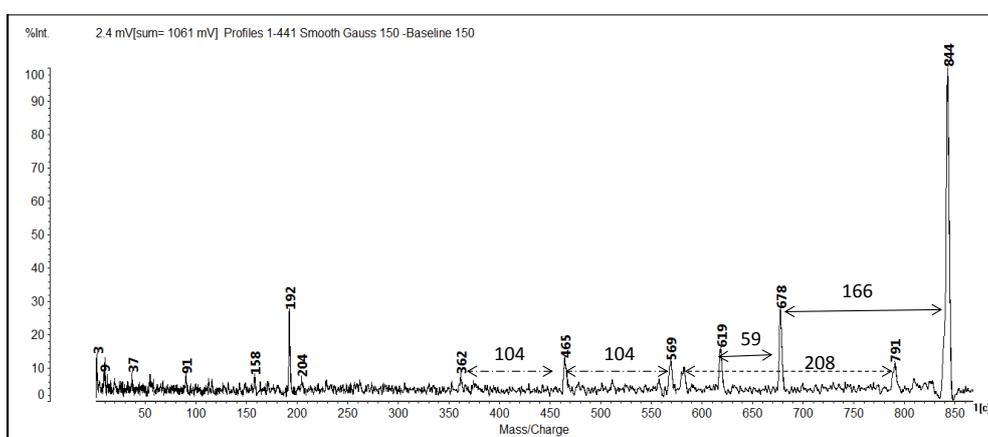
Figure 4.13 MALDI-TOF-CID spectrum of peak at m/z 844

Peaks at m/z 91 and 192 are characteristic fragments of PS; the former is the tropylium ion (C_7H_7) whilst the latter is the radical species with the following structure, CH(Ph)=CHCH(Ph).[21] The dormant PS chains have the following typical bonds C–H, C–C, C–O, C–N and C–S with the following approximate bond dissociation energies: 413, 347, 358, 305 and 259 kJ/mol, respectively. During fragmentation, the weaker bonds break first; breakage of the C–S bond yields unsaturated PS species at m/z 678, see Scheme 4.4. Subsequent cleavage of the C–N bond of the R-group gives structure 4 at m/z 619.
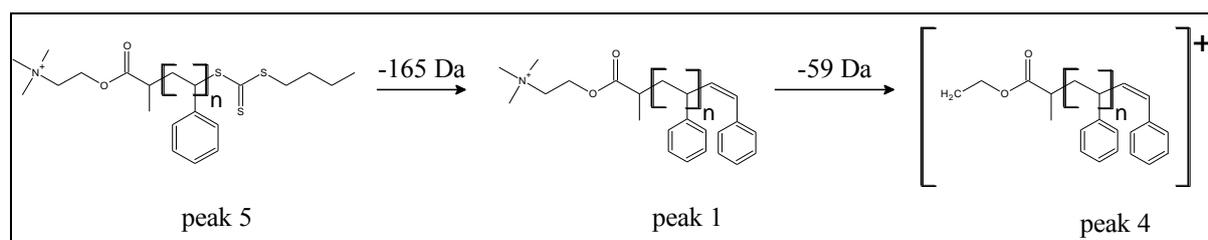
Scheme 4.4 Pathway for dissociation of dormant PS

The origin of the other fragments could not be identified.

Analysis of free PS by MALDI-MS

The MALDI-MS spectrum of free PS is illustrated in Figures 4.14 and 4.15. The spectrum was acquired without the addition of a cationising salt. Although ^{1}H NMR showed that **RAFT2** derived species were most abundant, MALDI-MS showed the cationic CTA derived species as having the major distribution. This was attributed mainly to the different ionisation efficiencies of the two PS structures. A new structure with a calculated molar mass corresponding to the m/z of peak 6 i.e. 4725 was observed. The structure possibly emanates from termination via recombination of tert-A RAFT-derived PS chains with **RAFT2**-derived chains.

Silver was added as the cationising salt in an attempt to improve the ionisation of **RAFT2**-derived chains, but this attempt only led to severe fragmentation of the polymer chains.
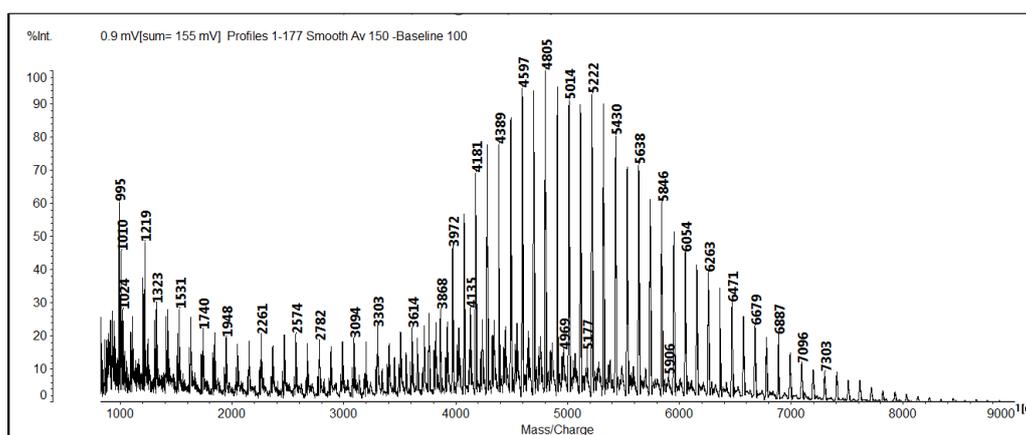

Figure 4.13 MALDI-TOF MS spectrum of Free PS, M_n (SEC) = 8580, *Đ*=1.27
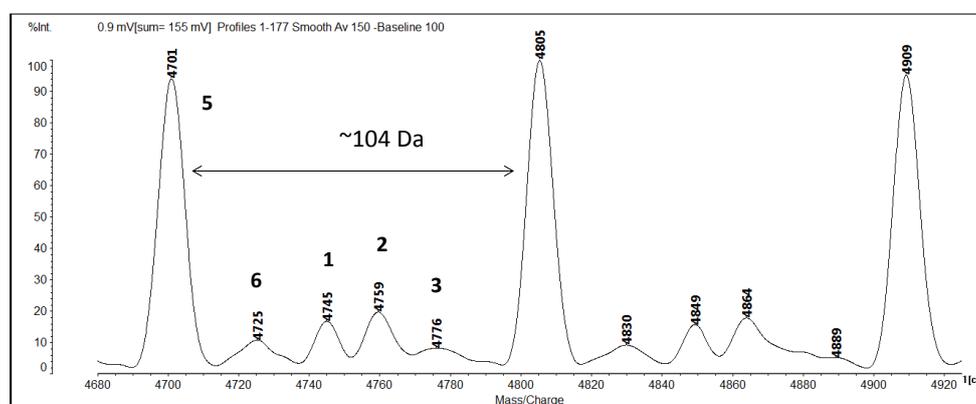

Figure 4.14 Selected portion of MALDI-MS spectrum of free PS

Grafting Parameters

The efficiency of a SI-polymerisation is often measured by the grafting density and free polymer content. The PCN (crude product) and the grafted clay particles were analysed by TGA. The observed weight losses were converted to the polymer content using equations 3.4, 3.5 and 3.8.

Table 4.4 Thermal analysis data for PCN and grafted clay particles

Run	Weight loss of crude product (%) [a]	Free polymer (mol/100g) [b]	Weight loss of grafted clay (%) [c]	Grafted amount (mol/100 g) [d]	δ_g (μmol/m^2) [e]	Tether-ed PS per nm^2 [f]
1	79	0.074	27.4	0.0048	0.130	0.08
2	86	0.066	30.0	0.0035	0.094	0.06
3	87	0.033	39.7	0.0043	0.117	0.07

[a],[c] Weight loss observed for PCN and grafted clay between 150 and 600 °C, [b],[d] PS content determined using Equation 3.4, [e] Grafting density determined from TGA using Equation 3.5, [f] Estimated using Equation 3.8.

The maximum grafting density that can be achieved in SI-polymerisation from clay is dependent upon the potential initiating sites, which are in turn dependent upon the CEC. In the case of the Laponite clay used in this study, this value lies between 1.35 and 1.49 μmol/m^2 i.e. approximately 0.8–0.9 sites per nm^2. The RAFT agent grafting density (from TGA data) for the CTA-modified clay used in the preparation of samples 1–3 was 1.05 μmol/m^2 (approx. 0.6 molecules per nm^2).

The grafting densities obtained in this study were relatively low compared to the starting surface-bound CTA molecules. However, the values were consistent with a moderately dense brush system (~0.05 chains/nm^2).[37] A number of factors can contribute to this (1) inaccessibility of the surface-bound CTA molecules by monomer due to steric hindrance, (2) inability of dispersion/centrifugation to sufficiently separate highly grafted clay particles from free polymer and (3) the inclusion of ungrafted clay with the grafted clay which leads to a misrepresentation of the grafted polymer to clay ratio. The ratio of the grafted to free polymer was very low, which is consistent with what has been reported by Tsujii *et al.*[17] for the RAFT mediated grafting of silica particles.

Thermal analysis

Thermogravimetric analysis

Thermal stability was investigated in terms of T_{10}, T_{20} and T_{50} i.e. the temperatures at which 10, 20 and 50% of the material degrades. The peak maximum for the 1st derivative curve (DTG_{max}) corresponding to the temperature where the rate of weight loss was highest; and the residual mass (%) i.e. the amount of inorganic residue remaining at 600 ^{o}C were also determined. Figure 4.15 shows TGA and DTG plots of pure PS, RAFT agent modified clay and sample 3 (nanocomposite and grafted clay). The DTG curves were normalised in order to have more comparable results.
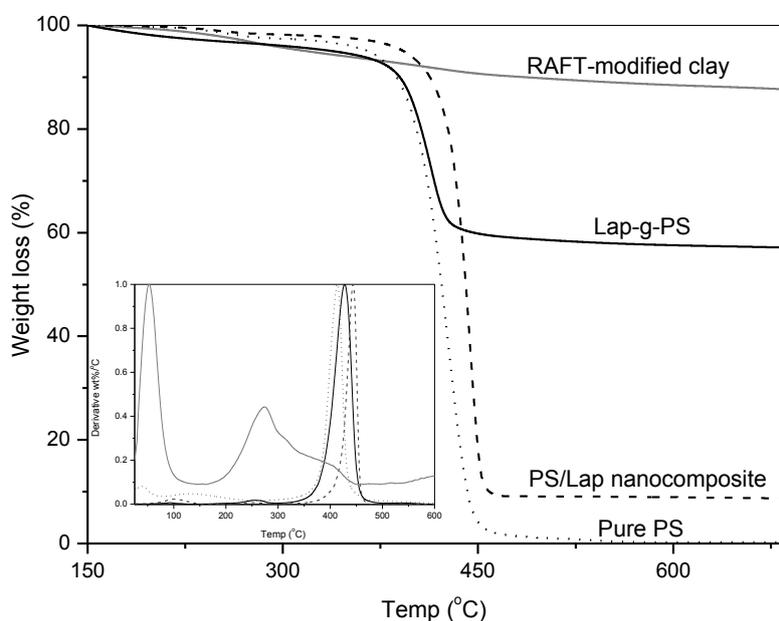
Figure 4.15 TGA and DTG curves of RAFT-modified clay, polymer-grafted clay, PCN and pure PS

As mentioned in Section 3.3.3, the thermal degradation of Laponite clay occurs in three steps. The first step which occurs at temperatures lower than 150 ^{o}C corresponds to the loss of adsorbed moisture. The weight loss between 150 and 500 ^{o}C for the CTA modified clay corresponds to the thermal degradation of the RAFT agent and the removal of interlayer water from the clay.

The thermal degradation of RAFT synthesised PS occurs in two main steps. The first step which occurs between 200 and 300 ^{o}C is due to the elimination of the thiocarbonyl thio moiety.[38,39] The main degradation step occurring between 350 and 550 ^{o}C was attributed to

the decomposition of the polymer backbone. For PS, thermal degradation occurs through β-scission of a chain end radical to form styrene monomer; and chain transfer reactions to form styrene dimers and trimers. The formation of small amounts of α-methyl styrene as a by-product has also been reported.[37] The thermal degradation mechanism for PS-clay has been reported to occur in a different way to that of neat PS. Chen *et al.*[37] reported that the main degradation step of PS-clay results in the formation of a substantial amount of α-methyl styrene, in addition to styrene monomer, dimers and trimers. The differences in thermal degradation behaviour were attributed largely to the brush structure of the surface-tethered chains.

Table 4.5 tabulates the TGA data for samples 1–3. The incorporation of clay within the polymer matrix resulted in an increase in thermal stability of up to 20 ^{o}C. A number of factors are known to influence this increase in thermal stability, and these include the barrier effect of the clay layers due to ablative reassembling of the silicate layers on the polymer surface.

Table 4.5 Thermal data for PS/clay nanocomposite

Sample	T_{10} [a]	T_{20} [b]	T_{50} [c]	DTG_{max} [d]	Mass loss [e]	Residual [f]
	(^{o}C)	(^{o}C)	(^{o}C)	(^{o}C)	(%)	(%)
Pure polystyrene[†]	387	403	422	428	99	0.2
1	405	423	441	443	79	17
2	409	425	441	446	86	8
3	414	426	440	444	87	9

[a] Temperature at which there is 10% weight loss, [b] Temperature at which there is 20% weight loss, [c] Temperature at which there is 50% weight loss, [d] 1st derivative curve peak maximum, [e] Mass loss between 150 and 600 ^{o}C, [f] Inorganic content remaining at 600 ^{o}C, [†] PS synthesised using tertiary amine functionalised RAFT agent.

Table 4.6 Thermal data for grafted clay particles

Sample	T_{10}	T_{20}	DTG_{max}	Residual
	(^{o}C)	(^{o}C)	(^{o}C)	(%)
Lap-**3_2**	400	–	275	80.0
1_Lap-g-PS	387	409	411	66.0
2_Lap-g-PS	394	414	417	63.4
3_Lap-g-PS	390	406	414	54.0

When considering the polymer-grafted clay particles, i.e. without the free polymer, a different trend was observed. The T_{10} and T_{20} for the grafted clay (Lap-g-PS) were lower than that for the nanocomposite (i.e. grafted clay + free polymer). This can be attributed to the higher clay content of the former compared to the latter. Another contributing factor is the high ratio of unpolymerised RAFT agent to grafted polymer. The small RAFT agent molecules present could trigger an early decomposition of the samples.

4.4   Conclusions

The SI-RAFT polymerisation of styrene from Laponite clay was successfully carried out in this study. Polymerisation control of free polymer (characterised by narrow molar mass distributions and predictable molar masses) was attained by performing the SI-polymerisations in the presence of free CTA. Molar mass data acquired from analysing the grafted and free polymer indicated that the polymer chains were growing simultaneously, but not at the same rate.

A new analytical approach was undertaken to characterise the PCN in order to get an understanding of the polymerisations occurring at the surface and in solution. Polymer grafted to the clay surface were analysed directly from the clay by ^{1}H NMR and MALDI-MS. The latter is a novel approach to PCN analysis and we recently reported it. NMR data and MALDI MS data showed that surface-confined radicals undergo conventional chain transfer reactions in addition to degenerative transfer. This finding has not been reported and is significant as there is an on-going interest in understanding the mechanism of SI-RDRP polymerisation to clarify the structure-property relationships.

The grafting densities obtained were relatively low compared to the initial CTA sites. This was attributed to steric hindrance of the already attached CTA molecules and the inability of successive centrifugation-dispersion processes to effectively separate grafted clay from PS. Relatively low grafted-to-free polymer ratios were obtained, which is a trend often observed in SI-RAFT mediated polymerisation.

The incorporation of clay within the polymer matrix resulted in a significant improvement in the thermal stability of the materials. However, the polymer brushes had a reduced thermal stability, probably due to the presence of high concentrations of unpolymerised RAFT agent.

References

(1)   Salem, N.; Shipp, D. A. *Polymer* **2005**, *46*, 8573–8581.

(2)   Akat, H.; Tasdelen, M. A.; Prez, F. D.; Yagci, Y. *Eur. Polym. J.* **2008**, *44*, 1949–1954.

(3)   Samakande, A.; Juodaityte, J. J.; Sanderson, R. D.; Hartmann, P. C. *Macromol. Mater. Eng.* **2008**, *293*, 428–437.

(4)   Samakande, A.; Sanderson, R. D.; Hartmann, P. C. *Eur. Polym. J.* **2009**, *45* 649–657.

(5)   Weimer, M. W.; Chen, H.; Giannelis, E. P.; Sogah, D. Y. *J. Am. Chem. Soc.* **1999**, *121*, 1615–1616.

(6)   Wheeler, P. A.; Wang, J.; Mathias, L. J. *Chem. Mater.* **2006**, *18*, 3937–3945.

(7)   Konn, C.; Morel, F.; Beyou, E.; Chaumont, P.; Bourgeat-Lami, E. *Macromolecules* **2007**, *40*, 7464–7472.

(8)   Turgman-Cohen, S.; Genzer, J. *J. Am. Chem. Soc.* **2011**, *133*, 17567–17569.

(9)   Choi, Y. S.; Choi, M. H.; Wang, K. H.; Sang Ouk Kim; Kim, Y. K.; Chung, I. J. *Macromolecules* **2001**, *34*, 8978–8985.

(10)   Chirowodza, H.; Hartmann, P.; Pasch, H. *Macromol. Chem. Phys.* **2012**, *213*, 847–857.

(11)   Zagorevskii, D. V.; Aldersley, M. F.; Ferris, J. P. *J. Am. Soc. Mass. Spectrom.* **2006**, *17*, 1265–1270.

(12)   Di, J.; Sogah, D. Y. *Macromolecules* **2006**, *39*, 1020–1028.

(13)   Ohno, K.; Morinaga, T.; Koh, K.; Tsujii, Y.; Fukuda, T. *Macromolecules* **2005**, *38*, 2137.

(14)   Perrier, S.; Takolpuckdee, P. *J. Polym. Sci., Part A: Polym. Chem.* **2005**, *43*, 5347–5393.

(15)   Fan, X.; Xia, C.; Advincula, R. C. *Langmuir* **2005**, *21*, 2537–2544.

(16)   Bellucci, F.; Camino, G.; Frache, A.; Saffa, A. *Polym. Degrad. Stab.* **2007**, *92*, 425–436.

(17)   Tsujii, Y.; Ejaz, M.; Sato, K.; Goto, A.; Fukuda, T. *Macromolecules* **2001**, *34*, 8872–8878.

(18)   Pasch, H.; Trathnigg, B. *HPLC of Polymers*; Springer: Berlin, 1997.

(19)   Nottelet, B.; Lacroix-Desmazes, P.; Boutevin, B. *Polymer* **2007**, *48*, 50–57.

(20)   Izunobi, J. U.; Higginbotham, C. L. *J. Chem. Educ* **2011**, *88*, 1098–1104.

(21)   Gies, A. P.; Vergne, M. J.; Orndorff, R. L.; Hercules, D. M. *Macromolecules* **2007**, *40*, 7493–7504.

(22)   Chiefari, J.; Jeffery, J.; Mayadunne, R. T. A.; Graeme Moad; Rizzardo, E.; Thang, S. H. *Macromolecules* **1999**, *32*, 7700–7702.

(23)   Postma, A.; Davis, T. P.; Evans, R. A.; Li, G.; Moad, G.; O'Shea, M. S. *Macromolecules* **2006**, *39*, 5293–5306.

(24)   Namboodiri, V. S.; George, S. D.; Hardt, S. *WASET* **2010**, *63*, 520–523.

(25)   Byrd, H. C. M.; McEwen, C. N. *Anal. Chem.* **2000**, *72*, 4568–4576.

(26)   Thomson, B.; Suddaby, K.; Rudin, A.; Lajoie, G. *Eur. Polym. J.* **1996**, *32*, 239–256.

(27)   Nielen, M. W. F.; Malucha, S. *Rapid Commun. Mass Spectrom.* **1997**, *11*, 1194–1204.

(28)   Ladavière, C.; Lacroix-Desmazes, P.; Delolme, F. *Macromolecules* **2009**, *42*, 70–84.

(29)   Moad, G.; Rizzardo, E.; Thang, S. H. *Aust. J. Chem.* **2005**, *58*, 379–410.

(30)   Zagorevskii, D. V.; Nasrullah, M. J.; Raghunadh, V.; Benicewicz, B. C. *Rapid Commun. Mass Spectrom.* **2006**, *20*, 178–180.

(31)   Favier, A.; Ladavière, C.; Charreyre, M.-T.; Pichot, C. *Macromolecules* **2004**, *37*, 2026–2034.

(32)   Mass, V.; Schrepp, W.; von Vacano, B.; Pasch, H. *Macromol. Chem. Phys.* **2009**, *210*, 1957–1965.

(33)   Dietrich, M.; Glassner, M.; Gruendling, T.; Schmid, C.; Falkenhagen, J.; Barner-Kowollik, C. *Polym. Chem.* **2010**, *1*, 634–644.

(34)   Chaicharoen, K.; Polce, M. J.; Singh, A.; Pugh, C.; Wesdemiotis, C. *Anal. Bioanal.Chem.* **2008**, *392*, 595–607.

(35)   Polce, M. J.; Ocampo, M.; Quirk, R. P.; Wesdemiotis, C. *Anal. Chem.* **2008**, *80*, 347–354.

(36)   Polce, M. J.; Ocampo, M.; Quirk, R. P.; Leigh, A. M.; Wesdemiotis, C. *Anal. Chem.* **2007**, *80*, 355–362.

(37)   Chen, K.; Susner, M. A.; Vyazovkin, S. *Macromol. Rapid Commun.* **2005**, *26*, 690–695.

(38)   Moad, G.; Chong, B.; Rizzardo, E.; Skidmore, M.; Thang, S. H. *Aust. J. Chem.* **2006**, *59*, 755–762.

(39)   Postma, A.; Davis, T. P.; Moad, G.; O'Shea, M. S. *Macromolecules* **2005**, *38*, 5371–5374.

Chapter 5

SI-RAFT polymerisation of n-butyl acrylate from Laponite clay surfaces

The following chapter presents results on the SI-RAFT mediated polymerisation of n-butyl acrylate. The synthetic and analytical methods introduced in Chapter 4 were used in the preparation and characterisation of poly(n-BA)-clay nanocomposites. The aim was to get insight into the SI-polymerisation of n-butyl acrylate from Laponite clay surfaces.

5.1   Introduction

Nanocomposite materials prepared from block copolymers of n-butyl acrylate (n-BA) and styrene have found significant interest because of their potential applications as elastomeric and adhesive materials. The material as it is known comprises a soft (flexible) part (n-BA) and a hard (rigid) part (styrene). For the preparation of block copolymers via RDRP, it is of paramount importance that the polymerisation mechanisms of both homopolymers be known. This allows regulation of end groups, whose retainment enables chain extension to form block copolymers. The SI-RAFT-mediated polymerisation of styrene was systematically studied in Chapter 4. The synthetic and analytical approaches devised therein were extended to n-BA monomer.

The n-BA monomer polymerises different to styrene, regarding their polymerisation kinetics. The n-BA radicals propagate faster and as a result high conversions are often easily attained. Polymerisations of n-BA are often accompanied by secondary reactions namely chain transfer to polymer or solvent. Secondary reactions in alkyl acrylate polymerisations are responsible for the inconsistencies found when determining kinetic values such as reaction order, propagation and termination rate constants.[1]

A number of researchers have devoted a great deal of effort to studying the side products formed during n-BA polymerisation.[2-5] Although chain transfer reactions become more significant at high polymerisation temperatures i.e. >100°C, they still occur to a reasonable extent at lower temperatures. The presence of chain transfer reactions is often confirmed through the analysis of the macromolecular structure of the polymer formed. This makes it

compelling to carry out a systematic approach in analysing the macromolecular structure of polymer formed during the SI-RAFT polymerisation of n-BA.

Similar to the PS system presented in Chapter 4, the systematic approach for the characterisation of surface-tethered and free polymer resulting from the SI-polymerisation of n-BA has not been reported.

5.2   Experimental

5.2.1   Materials

n-Butyl acrylate (n-BA, Sigma-Aldrich) was purified by distillation under reduced pressure. AIBN was purified as described in Section 3.2.2. The surface of Laponite clay was modified as described in Section 3.3.2. Free RAFT agent, ethyl 2-(butylthiocarbonothioylthio)propanoate was synthesised as descibed in Section 3.1.2.

5.2.2   SI-RAFT polymerisation of n-butyl acrylate

RAFT modified Laponite clay (0.266 g), n-BA (5 mL, 35.0 mmol), CTA, **RAFT2** (0.039 g, 0.18 mmol) and AIBN (0.0059 g, 0.036 mmol) were added to a 100 mL Schlenk flask. The mixture was stirred overnight in order to homogeneously disperse the clay in the solution, so enabling monomer, free RAFT agent and initiator to enter the clay galleries. The mixture was degassed by three successive freeze-pump-thaw cycles and backfilled with argon, sealed and placed in an oil bath set at 70 ^{o}C. After 24 h the polymerisation was halted by placing the reaction vessel in ice. The polymer/grafted clay mixture was then diluted with toluene. The free polymer was separated from the grafted clay by successive dispersion-centrifugation processes in toluene. The supernatant was dried under vacuum at room temperature. Grafted P(n-BA) was recovered from the clay surface by using ion exchange as described in Section 4.2.2.

5.2.3   Analyses

SEC

SEC analysis using THF as the eluent was carried out as described in Section 3.2.2. The instrument setup for the DMAc system comprised the following: a Waters 717plus autosampler, Shimadzu LC-10AT Isocratic pump, Waters 410 refractive index detector and a Waters 2487 dual wavelength detector. The columns used were three 300 x 8 mm i.d. GRAM

columns with a particle size of 10 μm. Two of them had a pore size of 3000 Å and the third a pore size of 100 Å. Sample concentrations of 1.0–1.5 mg/mL were prepared and the column injection volume was 100 μL. The column oven was held at 40 $^{\circ}$C. DMAc with BHT and 0.03% LiCl was the eluent and a flow rate of 1 mL/min was used.

NMR

All NMR spectra were acquired on a Varian Unity INOVA 400 MHz instrument. The procedure for sample preparation was described in Section 4.2.

MALDI-TOF-MS

Instrumentation and sample preparation is described in Section 4.2.

TGA

TGA was carried out as described in Section 3.3.2.

5.3 Results and Discussion

The SI-RAFT-mediated polymerisation of n-BA was carried out in a similar way to styrene. The polymerisation mixture consisting of CTA-modified clay, n-BA, free CTA and AIBN were stirred overnight in order to get a homogeneous dispersion of the clay in the free CTA-AIBN-monomer solution.

Table 5.1 contains the results of the SI-RAFT polymerisation of n-BA. The molar mass values obtained for the samples were consistent with a scenario where the surface-confined and free CTA were taking part in the polymerisation. The final molar mass of the P(n-BA) could be controlled by varying CTA-to-monomer ratio, and polymerisation time. However, it should be noted that the conditions tabulated in Table 5.1 were not optimised.

There were some inconsistences when comparing the molar mass values of free and grafted P(n-BA). This was most probably attributable to termination and chain transfer reactions. The latter are known to occur during the polymerisation of n-BA,[1,5] and dominate when high polymerisation temperatures are used and high molar masses and monomer conversions i.e. > 60% are targeted. The molar mass dispersities of the free polymer were narrow i.e. <1.4, as expected for RAFT polymerisation. The molar mass dispersity values of the grafted P(n-BA)

were broad, a clear indication of a more complex polymerisation mechanism, occurring at the clay surface. The amount of recovered grafted polymer from runs 11 and 12 was too low to get any meaningful information from SEC analysis.

Table 5.1 Experimental conditions for SI-RAFT polymerisation of n-butyl acrylate and molar mass data from SEC

Run	[M]/[RAFT] (mol/mol)[a]	Temp (°C)	Time (h)	M_n(calc) (g/mol)[b]	Free P(n-BA)		Grafted P(n-BA)	
					M_n	Đ	M_n	Đ
8	96	70	24	12 300	3700	1.35	12 700	2.17
9	128	70	24	16 700	28 000	1.31	56 000	2.00
10	334	60	20	43 100	38 610	1.19	11 580	2.15
11	345	60	6	44 520	28 770	1.17	–	–
12	150	70	5	19 520	19 700	1.19	–	–

[a] Ratio of monomer to total CTA concentration
[b] Theoretical number average molar mass at 100% monomer conversion estimated using equation 3.2
– Concentration of recovered P(n-BA) too low to get meaningful information from SEC analysis

"Living" polymer chains synthesised via the RAFT process retain the thiocarbonyl thio moiety. The retainment of the UV absorbing C=S group provides a way for measuring and detecting "living" polymer chains during a SEC experiment. An overlay of the RI and UV response gives an indication of the fraction of polymer chains that are no longer "living".

Figure 5.1 shows an overlay of RI and UV (measured at 320 nm) detector responses. The delay between the RI and UV detector was compensated for prior to plotting the chromatograms. The low molar mass fraction (at high elution volumes) was similar to that observed for PS, and was attributed to dead polymer chains or unpolymerised RAFT agent.[6,7]

The overlaid chromatograms of the grafted P(n-BA) from run 8 are shown in Figure 5.1A. The UV trace shows that the polymer contained the trithiocarbonate chromophore, suggesting that the grafted polymer consisted of dead and dormant polymer chains. The same cannot be said for runs 9 and 10. The UV traces only showed the presence of a low molar mass fraction, an indication that the higher molar mass fraction consisted of dead polymer chains. The differences observed in run 8 compared to runs 9 and 10 were attributed to the higher monomer conversions and molar masses obtained in runs 9 and 10.
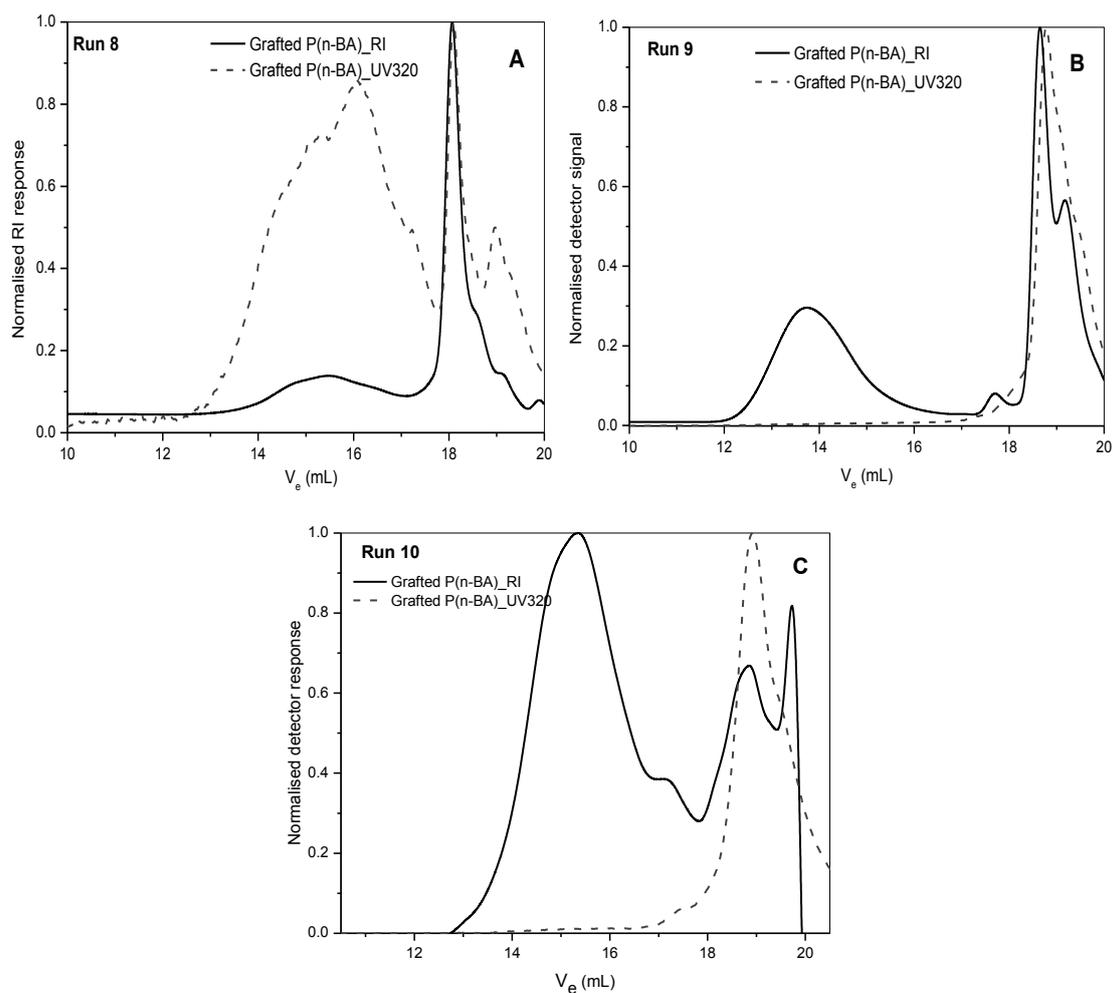
Figure 5.1 Overlays of UV and refractive index chromatograms of grafted P(n-BA) (A) run 8, (B) run 9 and (C) run 10

The SEC traces of the free P(n-BA) showed different molar mass distributions. The SEC molar mass distributions of runs 8, 10 and 11 were monomodal (see example in Figure 5.2B); but runs 9 and 12 showed bimodalility (see example in Figure 5.2A).

Bimodal or multimodal molar mass distributions are often observed in the RAFT-mediated polymerisation of acrylates. Multimodality has been attributed to two phenomena, (1) termination of the intermediate radical (see Scheme 4.3), resulting in the formation of 3- or 4- arm structures[8] and (2) copolymerisation of 1,1 disubstituted alkene macromonomer (mechanism for the formation of the macromonomer will be given shortly). The products would be structurally different. The 3- or 4-arm stars resulting from intermediate radical termination, would not be expected to have the C=S moiety of the RAFT agent whilst the product resulting from macromonomer copolymerisation would still have the C=S group at the terminating end.
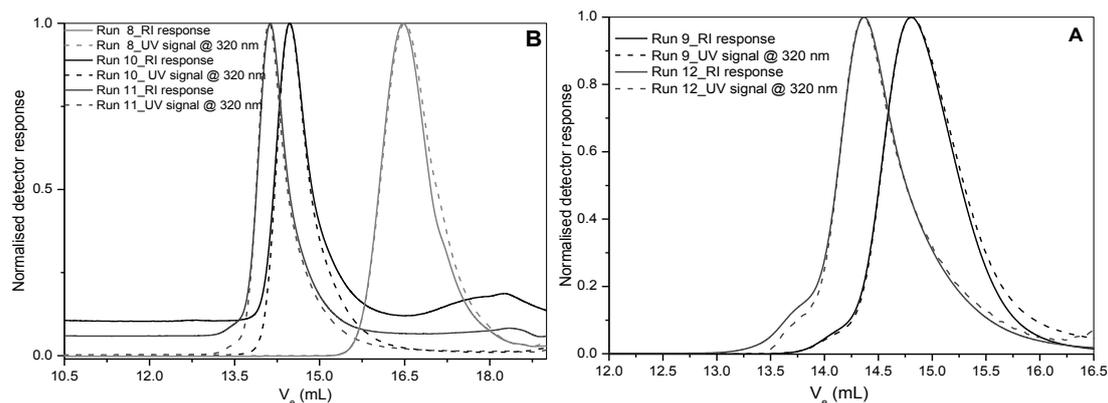
Figure 5.2 Overlay of UV and RI chromatograms of free P(n-BA) (A) runs 9 and 12 and (B) runs 8, 10 and 11

It is thus possible to distinguish the origin of the high molar mass shoulder, by overlaying the RI and UV chromatograms of the free polymer. The overlay of the RI and UV SEC traces of run 9 shows the presence of a high molar mass fraction which absorbs UV at 320 nm. This suggests that the high molar mass fraction most likely originates from the copolymerisation of the 1,1-disubstituted alkene macromonomer. The reason why the bimodality was observed in runs 9 and 12 and not 10 and 11 could be attributed to the slightly higher polymerisation temperatures used in the first two experiments, which could increase the propensity of chain transfer reactions to occur.[5]

Molar mass analysis of low molar mass free and grafted P(n-BA)

Free P(n-BA)

The low molar mass sample (run 8) was analysed further by ^{1}H NMR, ^{13}C NMR and MALDI-TOF MS in order to get insight into the surface-initiated RAFT polymerisation of n-BA. The expected molar mass at the attained monomer conversion of 20% was 3020 g/mol. The M_n values obtained from SEC, ^{1}H NMR and MALDI-TOF MS for free polymers were similar i.e. 3700, 4500 and 3600 g/mol respectively, see Table 5.2.

The slight differences in the molar mass values from NMR, SEC and MALDI-MS are explained as follows. The molar mass values reported for SEC are relative to PS standards. For MALDI-MS, the species with the highest ionisation efficiency were observed in the spectra and were thus considered for molar mass calculations. For NMR, the area intensities of the polymer backbone and the methine proton adjacent to the thiocarbonyl thio moiety were considered. In the case where most of the polymer chains are no longer "living", i.e.

without the thiocarbonyl thio moiety, this would lead to an overestimation of the M_n from NMR data.

Table 5.2 Analysis of free and grafted polymer

Free P(n-BA)					Grafted P(n-BA)					
$M_{n(calc)}$[a] $(\cdot 10^3)$ [g/mol]	$M_{n(SEC)}$ $(\cdot 10^3)$ [g/mol]	Đ[b]	$M_{n(NMR)}$ $(\cdot 10^3)$ [g/mol]	$M_{n(MALDI)}$ $(\cdot 10^3)$ [g/mol]	$M_{n(SEC)}$[c] $(\cdot 10^3)$ [g/mol]	Đ	$M_{n(SEC)}$[d] $(\cdot 10^3)$ [g/mol]	Đ	$M_{n(NMR)}$ $(\cdot 10^3)$ [g/mol]	$M_{n(MALDI)}$ $(\cdot 10^3)$ [g/mol]
3.02	3.70	1.35	4.50	3.60	12.70	2.17	2.70	1.73	3.03	2.52

[a] Theoretical molar mass estimated using equation 3.2, [b] Đ is the molar mass dispersity, [c] THF was used as the solvent for SEC analysis, [d] DMAC/LiCl was used as the solvent for SEC analysis

Grafted P(n-BA)

The molar mass values obtained for the grafted polymer from SEC data were higher than expected and the chromatogram showed a multimodal distribution, see Figure 5.3. However, the SEC data suggested that the grafted polymer consisted of dormant and dead polymer chains.
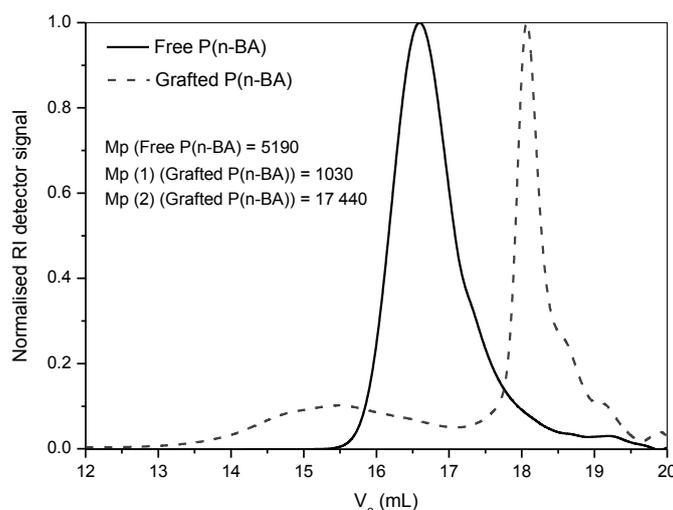
Figure 5.3 Normalised RI responses for free and grafted P(n-BA) from THF based SEC

When the same sample was analysed by SEC, using a different solvent system i.e. dimethyl acetamide doped with LiCl, the sample showed a M_n of 2700 g/mol relative to poly(methyl methacrylate) standards. This value was consistent with the M_n values obtained from ^{1}H NMR and MALDI-TOF MS data, i.e. 3030 and 2520 g/mol respectively. The discrepancy in the THF–SEC data and that acquired from other techniques was attributed to ionic interactions (repulsions) occurring between the positive charges of the detached polymer and the non-polar stationary phase of the column. These repulsions became less effective in the

DMAC/LiCl system as the lithium reduces the interactions of the polymer with the stationary phase. The non-ionic repulsions become less effective when higher molar mass samples are considered.[9]

End group analysis of grafted and free polymer by ^{1}H NMR

In order to obtain clarity on the mechanism of the polymerisation at the surface and in solution, ^{1}H NMR and MALDI-TOF MS were used to investigate the end group structures of the free and grafted polymers. Figure 5.4 shows the stacked NMR spectra of free and grafted P(n-BA).

The latter was acquired by analysing the grafted clay without detaching the polymer. The signals attributed to the polymer backbone and end groups were assigned as shown in the figure. For the chain ends, the assignments were based on the chemical shifts of the protons of the CTAs used.
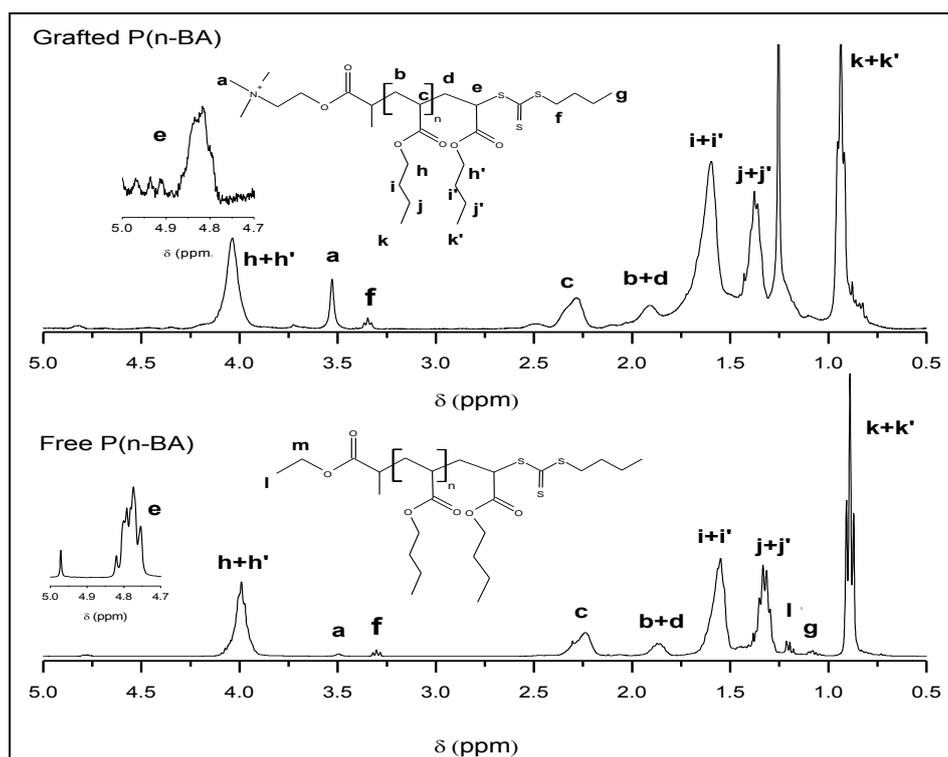

Figure 5.4 ^{1}H NMR spectra of grafted and free P(n-BA) in CDCl₃

For the grafted polymer, the ratio of the methine proton adjacent to the thiocarbonyl thio moiety labelled (e) to the methylene protons adjacent to the sulphur (f) and the methyl protons on the nitrogen (a) was approximately 1:2:9. Although this value could imply that most of the

polymer chains initiated by the RAFT agent were living, it should be taken into account that the signals could be overlapping with those of the unpolymerised RAFT agent.

The ^{1}H NMR spectrum of free P(n-BA) shows the presence of polymer chains initiated by cationic **RAFT1**. The presence of these polymer chains in the sample can be attributed either to the excess adsorbed **RAFT1** or modified clay particles in the free polymer. The peak at 1.25 ppm in the grafted clay NMR spectrum is an impurity.

MALDI-TOF MS analysis of P(n-BA) was carried out on PCN (crude product), grafted clay (after washing off the physisorbed polymer), free polymer and detached polymer. Direct analysis of the polymer from clay was possible as the polymer was attached to the clay via electrostatic interactions. No additional salt was added to enhance ionisation because the polymer chains present on the surface carried a positive charge. It was taken into consideration that P(n-BA) can be readily ionised by H^+ or Na^+ ions, but the results presented in Chapter 4 for PS clearly showed that the direct analysis of electrostatically bound polymer from clay is possible (PS is known to ionise more readily in the presence of Ag^+ or Cu^+ ions[10]). It is thus proposed in this study that in the MALDI process and during laser ablation the polymer detaches from the clay, desorbs, and transfers into the gas phase, and is then separated in the mass analyser prior to detection.

The molar mass values for grafted polymer obtained from NMR and MALDI were in agreement. The polymer chains observed in the spectra were assigned to P(n-BA) cationised by H^+ ions, $[M+H]^+$ or P(n-BA) bearing the reinitiating (R-group) from the cationic RAFT agent, $[M]^+$.

Figure 5.5 shows the stacked MALDI-MS spectra for the crude product, Lap-g-P(n-BA), free P(n-BA) and detached P(n-BA) (labelled A–D respectively). All spectra were acquired in the linear mode. The spectra show clusters of peaks with each cluster being separated by approximately 128 g/mol, which is the mass of a BA unit. The molar masses as determined by MALDI-MS are given in Figure 5.5. The most important feature to note is that the molar mass distributions observed by analysing the polymer directly from the clay (B) and after detaching (D) were similar– this was in agreement with our expectations. Figure 5.6 is a magnification of the spectra, showing a selected region of m/z 2365–2650 (n = 17 or 18). The different peaks that are present within each cluster show the different polymer end group structures present.
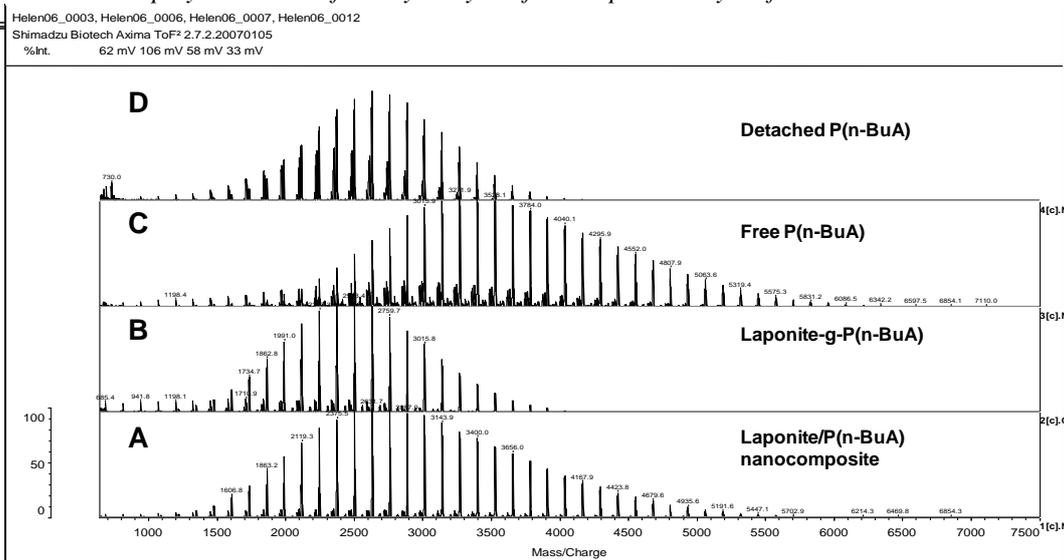
Figure 5.5 MALDI TOF MS spectrum of A-Laponite clay/poly(n-BA) nanocomposite [M_n = 3000 g/mol], B-Lap-g-P(n-BA) [M_n = 2520 g/mol], C-free P(n-BA) [M_n = 3600 g/mol] and D-detached P(n-BA) [M_n = 2680 g/mol]
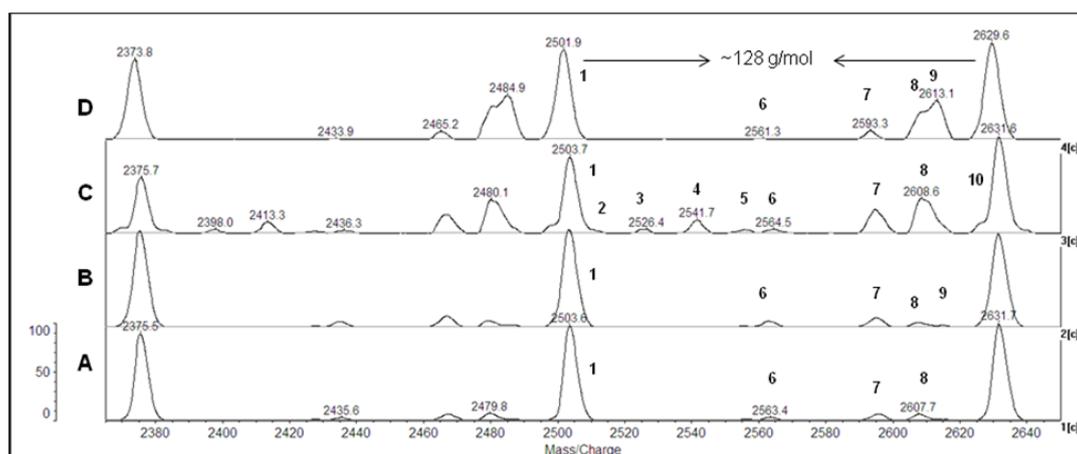

Figure 5.6 Selected parts of MALDI MS spectra of A- Laponite clay/poly(n-BA) nanocomposite, B-Lap-g-P(n-BA), C- free P(n-BA) and D- detached P(n-BA)

Although ^{1}H NMR showed that the free P(n-BA) sample comprised mostly polymer chains initiated by the free RAFT agent (~90%), MALDI-MS analysis showed the cationic RAFT agent-derived polymer chains as having the major distribution. This confirms that under these experimental conditions MALDI-MS cannot be used quantitatively as the charged polymer though less abundant was clearly detected more readily.

Chapter 5: SI-RAFT polymerisation of n-butyl acrylate from Laponite clay surfaces

Table 5.3 Structures corresponding to various peaks in Figure 5.5 and 5.6

Peak	m/z (expt) [a]	m/z (theo) [b]	Structure [c]	n
1	2503	2503		17
2	2511	2510		18
3	2524	2524		18
		2525		18
4	2540	2541		18
		2539		18
5	2554	2553		18
6	2563	2562		18
7	2595	2595		18
8	2607	2607		18
	2608	2609		18
9	2615	2616		18
10	2621	–	–	–
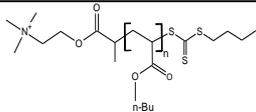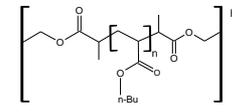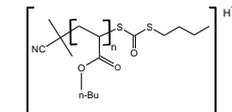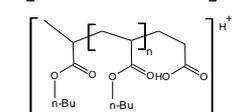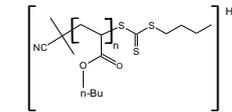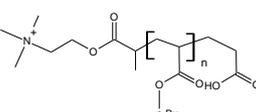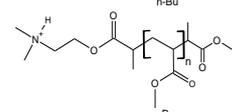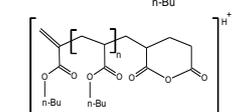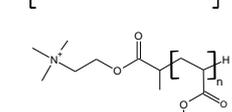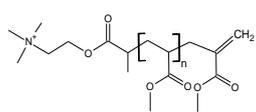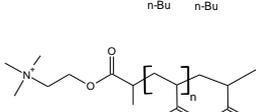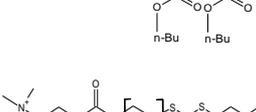
[a] Observed peak molar mass; [b] Calculated molar mass based on proposed structure; [c] n is the degree of polymerisation; –peaks not assigned

Possible structures for the different peaks were determined. They are tabulated in Table 5.3. The dormant polymer chains stemming from **RAFT1** were observed at m/z 2503 (labelled 1) It is apparent from Figure 5.6 that species 2, 3, 4, 5 and 10 were present only in the free polymer sample.

The conventional and controlled radical polymerisation of n-BA has been studied extensively.[1,5,11] It is known that the propagating P(n-BA) radicals can undergo either inter- or intra-molecular chain transfer reactions.[3] In the former case, a propagating radical abstracts a hydrogen atom from another polymer molecule while in the latter case the abstraction occurs within the same molecule (back-biting). Both reactions result in the formation of a species called a mid-chain radical (MCR). It is difficult to distinguish whether intra- or inter-molecular chain transfer reactions were at play here. However, many believe that at low monomer conversions, intra-molecular chain transfer predominates, whilst inter-molecular chain transfer predominates at higher monomer conversions.

The MCR has two possible fates: it can reinitiate polymerisation forming branched structures, or it can undergo fragmentation (β-C–C bond scission) to yield the products shown in Scheme 5.1 (structures I–IV).
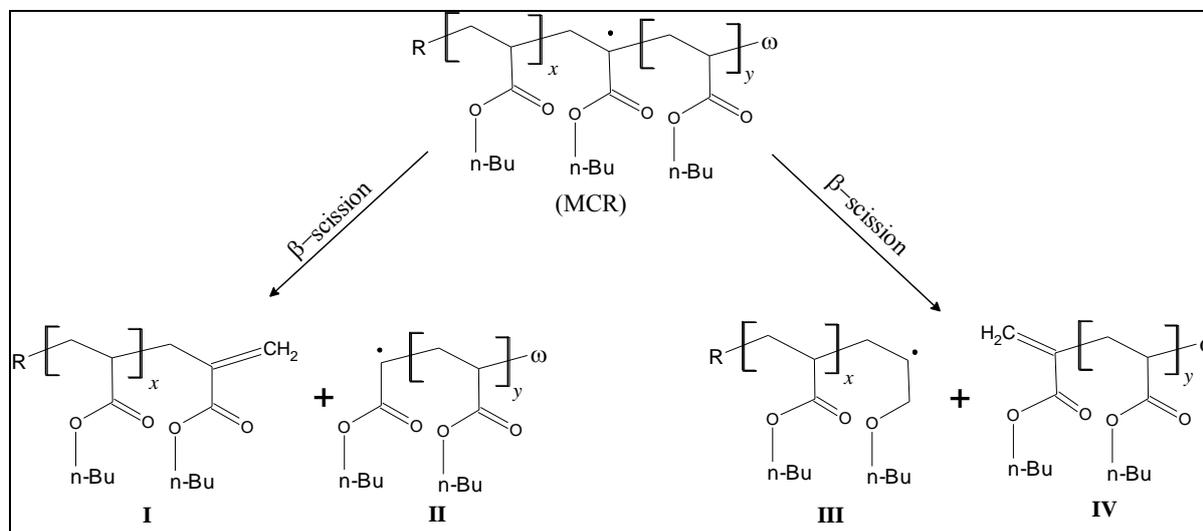
Scheme 5.1. The formation of β-scission products via the Midchain Radical species (ω = H, $C_5H_9S_3$ or another fragmentation species)

Branched polymer structures are more compact than linear polymer structures and have smaller hydrodynamic volumes. If branched structures were to form predominantly, this would lead to lower molar masses being observed by SEC.

However, this was not the case here. Three independent analytical techniques showed molar mass values that were in agreement with the calculated molar mass values. Nevertheless to completely rule out branching, ^{13}C and distortionless enhancement by polarisation transfer (DEPT) NMR were carried out. Results of the experiments did not show the presence of any branches.[5] The formation of I and IV was confirmed by structures corresponding to peak masses at m/z 2524, 2563 and 2607 (labelled 3, 6 and 8). Structures 6 and 8 have a cyclic anhydride and **RAFT1** reinitiating group as the other end groups respectively. The formation of the cyclic anhydride will be explained shortly.

In the linear mode, mass resolution was too low to allow the discrimination of structures that differed by 2 Da. After fragmentation, it is difficult to state whether the fragmented species are present in the unsaturated or saturated form; and thus both possibilities are presented in some of the peak assignments.

^{1}H and ^{13}C NMR did not show the presence of any 1,1-disubstituted alkene end groups, probably because they constitute a very small fraction of the sample. One could argue that structure I emanates from the fragmentation of a C–C bond during MALDI-MS analysis.[12] This is unlikely because dormant structures with the weaker C–S bond were found intact; meaning the formation of the fragmented species involves a different mechanism and most probably occurs during polymerisation. Peak masses matching those of structures derived from structure II were not observed. Structure III is similar to that of the propagating radical so it is difficult to distinguish polymer chains resulting from the two.

Intermolecular chain transfer not only leads to the formation of a MCR but also termination of propagating radicals, resulting in H-terminated polymer chains, as evidenced by the peak labelled 7, with m/z 2595. Besides chain transfer followed by fragmentation, there is also evidence of the oxidation of the trithiocarbonate to a dithiocarbonate, as evidenced by the peak at m/z 2615, which occurs during MALDI-MS analysis.[8,13] The accepted mechanism involves the oxidation of the trithiocarbonate to a sulfine, which then decomposes to elemental sulphur and a dithiocarbonate.

The free polymer showed some additional structures to those observed in the grafted polymer, some of which were attributed to the free RAFT agent that was added. The dormant polymer chains from **RAFT2** were not observed in the absence of additional cationising salt.

To confirm the structural assignments, i.e. whether the polymer was not being ionised by Na^+, Li^+ was added to the free polymer samples and there was no shift observed in the peak masses. However, a new peak was observed at m/z 2579, which corresponds to the calculated molar mass (2580 g/mol) of the dormant polymer chains derived from the free **RAFT2** and ionised by Li^+. The Na^+-attached species would have a calculated molar mass of 2595 g/mol, which makes them isobaric with structure 7. Upon addition of Li^+, these two structures were separated, and could be distinctly identified, see Figure 5.7.
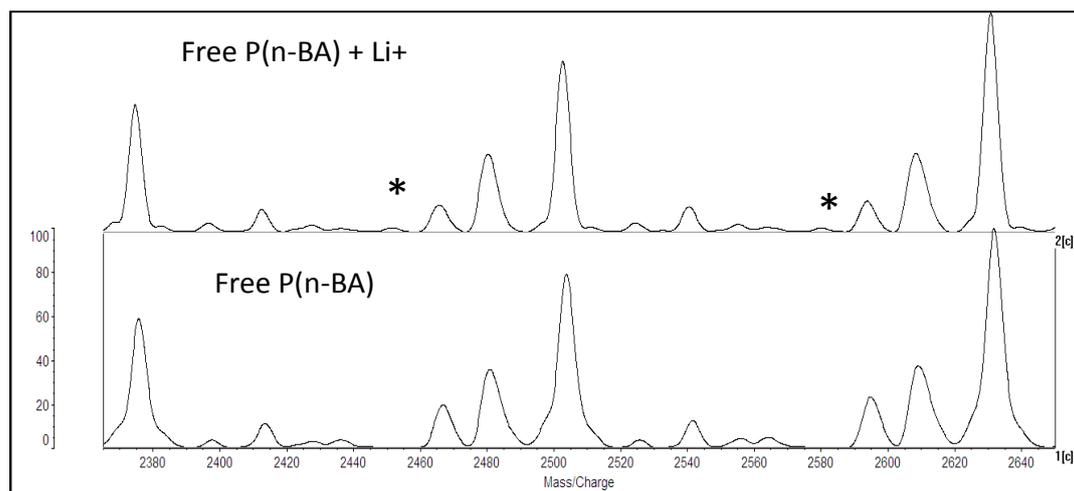
Figure 5.7 Selected parts of MALDI MS spectra of P(n-BA) with Li^+ added and without Li^+

Mechanistically, the RAFT process is superimposed onto a free radical polymerisation process meaning that termination reactions still do occur. Termination occurs via two main pathways: disproportionation and coupling/combination. The mass peaks at m/z 2511 and 2554 (labelled 2 and 5) show evidence of the latter. These structures were observed only in the free polymer.

Tandem mass spectrometry (MS/MS) measurements performed on linear P(n-BA) showed that the collision-induced dissociation (CID) of P(n-BA) involves primarily the fragmentation of the pendant ester groups.[12] The fragmentation occurs via two steps. In the first step, 1-butene is eliminated, resulting in a carboxylic acid group. This elimination can occur anywhere along the chain, resulting in the formation of more carboxylic acid groups. The acid can then attack an adjacent ester group, releasing 1-butanol and forming a cyclic anhydride, see Scheme 5.2.
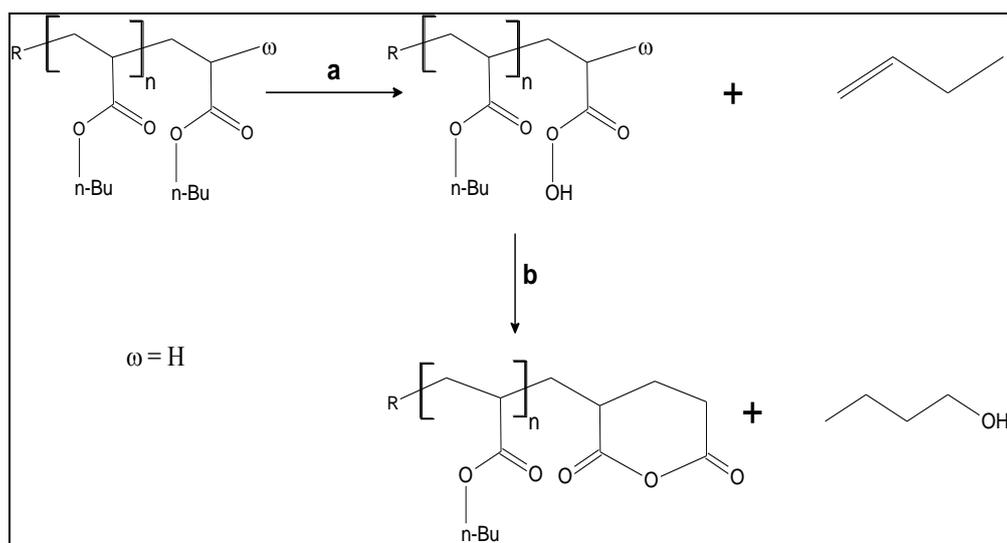
Scheme 5.2 Formation of (a) carboxylic end group via 1,5 rearrangement and (b) cyclic anhydride end group via an intramolecular displacement reaction

The peak mass at m/z 2524 (labelled 3) corresponds to the calculated mass of a fragmented species with a carboxylic acid group. The peak at m/z 2563 (labelled 6) matches with calculated molar mass of fragmentation species IV bearing the cyclic anhydride moiety. The peak at m/z 2540 (labelled 4) has two possible structures. The first is **RAFT1** initiated polymer chains with a carboxylic acid end group and the second is the initiator derived dormant polymer chains. It has been reported that initiator-derived species can be observed in MALDI when the ratio of the initiator to RAFT agent is high.[14,15] The initiator derived species are more probable here because a peak arising from the initiator derived dormant chains with an oxidised thiocarbonyl thio moiety was observed at m/z 2525; and also the species was only found in the free polymer sample.

Grafting parameters

In order to determine the efficiency of the SI-RAFT mediated polymerisation of n-BA from Laponite clay, the amount of free and grafted polymer was determined by using TGA. The crude product (PCN) and grafted clay particles (after washing off free polymer) were heated from 25 to 700°C, and the observed weight losses between 150 and 600°C, converted to the polymer content using equations 3.4, 3.5 and 3.8.

The values obtained for the high molar mass samples (run 9) were very low, tabulated in Table 5.4. This is most probably attributable to the loss of highly grafted material during the separation of grafted clay from free polymer during the dispersion-centrifugation process.

For the low molar mass sample (run 8), there were approximately 0.114 P(n-BA) chains per nm^2 (120 polymer chains per clay particle). This value was very low compared to the starting number of CTA molecules ~1.28 molecules/nm^2; however the values are consistent with a highly dense brush system.[16]

Similar to the PS system, a large amount of free polymer was formed. This is the normal observation in a SI-RAFT polymerisation system and emanates from the free thermal initiator added. The ratio of the free-to-grafted polymer chains are comparable to the values obtained by Tsujii *et al.*[17] when grafting PS from silica particles via RAFT mediated polymerisation.

Table 5.4 Analysis of polymer-grafted clay blend (crude product) and grafted clay particles by TGA

Run	Weight loss of crude product (%)[a)]	Free polymer (mol/100 g)[b)]	Weight loss grafted clay (%)[c]	Grafting amount (mol/100 g)[d]	δ_g (μmol/m^2)[e]	Tethered P(n-BA) per nm^2 [f)]
8	75	0.076	28.3	0.0070	0.190	0.114
9	76	0.011	25.1	0.00035	0.0095	0.006

[a),c)] determined by TGA in the range 150–600 °C, [b),d)] determined using equation 1, [e)] determined using equation 3.5 [f)] determined using equation 3.8.

Thermal analysis

Thermogravimetric analysis

The thermal stability of P(n-BA)/clay nanocomposites was investigated in terms of T_{10}, T_{20} and T_{50} i.e. the temperatures at which 10, 20 and 50% of the material degrades. The mechanism for the thermal degradation of P(n-BA) is different to that for PS. For P(n-BA), the RAFT end group is lost via homolytic cleavage of the C–S bond, and the formed secondary radical decomposes via a series of chain transfer reactions.[18]

Figure 5.8 shows TGA and DTG plots of pure P(n-BA), RAFT agent modified clay and sample 9 (nanocomposite and grafted clay). The DTG curves were normalised in order to have more comparable results. The grafted clay particles showed four distinct steps in their

thermal degradation. The first step which occurs below 150 ^{o}C was attributed to the loss of adsorbed moisture. The second step which occurs between 150 and 300 ^{o}C was attributed to the cleavage of the thiocarbonyl thio moiety. The main step occurring between 300 and 600 ^{o}C was attributed to the thermal degradation of the polymer backbone, whilst the step occurring at > 700 ^{o}C was attributed to dehydroxylation of the clay OH groups.
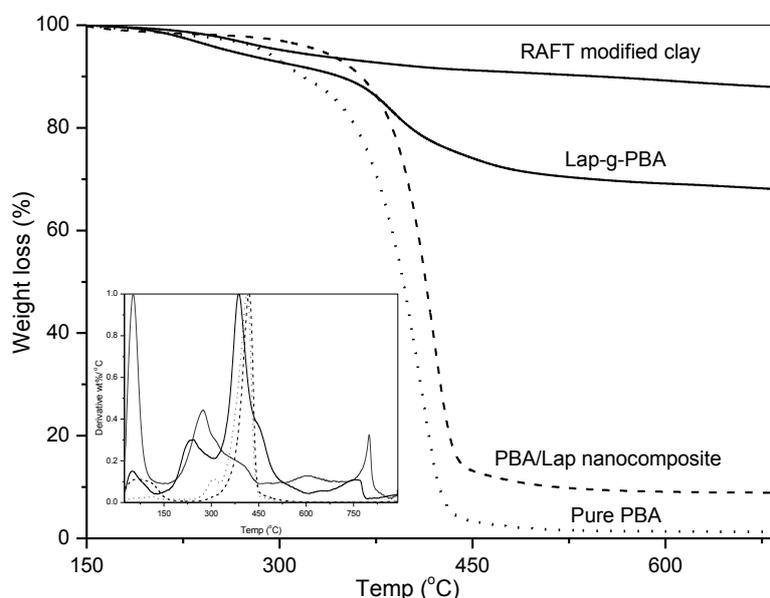
Figure 5.8 TG and DTG (insert) curves of RAFT-modified clay, Lap-g-PBA, PBA/clay nanocomposite and pure PBA

The results tabulated in Table 5.5 show that the incorporation of as little as 2 wt.-% of clay (determined from residual mass) resulted in a substantial improvement in the thermal stability of P(n-BA) under nitrogen. This was attributed to the barrier effect of the clay layers due to ablative reassembling of the silicate layers on the polymer surface.

Table 5.5 Thermal data for PBA/clay nanocomposite

Sample	T_{10}	T_{20}	T_{50}	DTG_{max}	Mass loss	Residual
	(^{o}C)	(^{o}C)	(^{o}C)	(^{o}C)	(%)	(%)
Pure PBA[†]	317	363	400	403	94	1
9	366	389	414	419	74	8
10	377	396	417	423	84	3
11	341	370	409	419	85	7
12	365	389	415	421	85	9

5.4   Conclusions

The SI-RAFT mediated polymerisation of n-BA from Laponite clay was successfully carried out. The molar mass of the final polymer was varied by changing the monomer to CTA (free and bound) ratio.

The inconsistencies observed when comparing the molar mass and molar mass dispersity values of free and grafted polymer were attributed to secondary chain transfer reactions, which are characteristic of n-BA polymerisations. From the SEC data presented for the high molar mass samples, it was evident that the surface-confined and free polymer chains were undergoing a slightly different polymerisation mechanism. The free polymer consisted mainly of dormant polymer chains, whilst the polymer chains at the surface were no longer living, because of termination via recombination or chain transfer reactions.

The low molar mass sample was systematically analysed using NMR and MALDI-TOF MS. The polymer species that were grafted from the clay surfaces were analysed directly by MALDI-TOF MS and NMR without the need to detach the polymer chains from the surface. A comparison was made between the chemical structures of the detached polymer and polymer analysed directly from clay and similar structures were observed. Although additional structures were observed in the free polymer, the **RAFT2**-derived dormant structures were observed only after addition of Li^+. ^1H and ^{13}C NMR were used to confirm the polymerisation mechanism occurring both in solution and at the surface of the clay. By comparison of the end group structures and molar masses, it was evident that in the presence of free RAFT agent the polymerisation occurring in solution was similar to that occurring at the surface, when low molar masses and conversions were targeted.

References

(1) Quan, C.; Soroush, M.; Gardy, M. C.; Hansen, J. E.; William J. Simonsick, J. *Macromolecules* **2005**, *38*, 7619–7628.

(2) Barner-Kowollik, C. *Macromol. Rapid Commun.* **2009**, *30*, 1961–1963.

(3) Koo, S.; Junkers, T.; Barner-Kowollik, C. *Macromolecules* **2009**, *42*, 62–69.

(4) Junkers, T.; Barner-Kowollik, C. *J. Polym. Sci., Part A: Polym. Chem.* **2008**, *46*, 7585– 7605

(5) Ahmad, N.; Heatley, F.; Lovell, P. *Macromolecules* **1998**, *31*, 2822–2827.

(6) Chirowodza, H.; Weber, W.; Hartmann, P.; Pasch, H. *Macromol. Symp.* **2012**, *313– 314*, 135–145.

(7) Pasetto, P.; Blas, H.; Audouin, F.; Boissière, C.; Sanchez, C.; Save, M.; Charleux, B. *Macromolecules* **2009**, *42*, 5983–5995.

(8) Venkatesh, R.; Staal, B. B. P.; Klumperman, B.; Monteiro, M. J. *Macromolecules* **2004**, *37*, 7906–7917.

(9) Elder, J. PhD, Durham, 2009.

(10) Pasch, H.; Schrepp, W. *MALDI-TOF Mass Spectrometry of Synthetic polymers*; Springer: Berlin, 2003.

(11) Farcet, C.; Belleney, J.; Charleux, B.; Pirri, R. *Macromolecules* **2002**, *35*, 4912–4918.

(12) Chaicharoen, K.; Polce, M. J.; Singh, A.; Pugh, C.; Wesdemiotis, C. *Anal. Bioanal.Chem.* **2008**, *392*, 595–607.

(13) Favier, A.; Ladavière, C.; Charreyre, M.-T.; Pichot, C. *Macromolecules* **2004**, *37*, 2026–2034.

(14) Ladavière, C.; Lacroix-Desmazes, P.; Delolme, F. *Macromolecules* **2009**, *42*, 70–84.

(15) Xu, J.; He, J.; Fan, D.; Wang, X.; Yang, Y. *Macromolecules* **2006**, *39*, 8616–8624.

(16) Chen, K.; Susner, M. A.; Vyazovkin, S. *Macromol. Rapid Commun.* **2005**, *26*, 690– 695.

(17) Tsujii, Y.; Ejaz, M.; Sato, K.; Goto, A.; Fukuda, T. *Macromolecules* **2001**, *34*, 8872– 8878.

(18) Postma, A.; Davis, T. P.; Moad, G.; O'Shea, M. S. *Macromolecules* **2005**, *38*, 5371– 5374.

Chapter 6

Asymmetrical Flow Field-Flow Fractionation (AF[4]) of Polymer-Clay Nanocomposites

This chapter presents preliminary results on the asymmetrical flow field-flow fractionation of polymer-clay nanocomposite materials. The theory underlying this technique is briefly discussed as well as the experimental conditions and considerations undertaken for the analysis of the polymer-clay samples are described.

6.1   Introduction

Polymer-clay nanocomposites are complex multicomponent materials. The polymer part of the material exhibits heterogeneity with respect to different properties such as molar mass, architecture and chemical composition, while the clay is disperse with respect to particle size. When PCNs are synthesised via surface-initiated polymerisation, some of the clay particles are grafted with polymer, and the variations in grafting density influence the particle size dispersity. All of the above mentioned properties, i.e. molar mass of free polymer and size distribution of grafted clay particles, have an influence on the bulk properties and hence the applications of the materials.

Known methods for investigating these properties involve first separating the polymer from the grafted clay by washing or extraction, followed by measuring the molar mass by SEC.[1,2] Grafted clay particle size is often estimated by dynamic light scattering (DLS), the challenges with this approach is that the presence of aggregates or other light scattering species in the sample e.g. dust particles can lead to an overestimation of the particle size. In addition, it is not easy to determine whether the inconsistencies in particle size emanate from the sample or from foreign particle contaminants. As such there is need to develop an analytical method that enables fractionation of these samples into the various components prior to their analysis.

Liquid chromatography (LC) has been an efficient method for separating and characterising complex polymer mixtures for decades. However its application to the analysis of high molecular weight polymers or nanoparticles is limited. The challenges with the column-based techniques have been circumvented by using open channels and an external field in so-called field-flow fractionation.

Flow field-flow fractionation (FlFFF) using an asymmetrical cross-flow (AF^4) has attracted significant attention in a number of fields, as it provides an efficient way of separating and characterising analyte species ranging from a few nanometres to tens of micrometres in diameter. AF^4 has not only been efficient in polymer characterisation, but also in the analysis of nanoparticles such as quantum dots,[3] environmental colloids,[4] proteins and protein-based viruses.[5] There is not much in the published literature on the use of AF^4 in the characterisation of polymer-clay nanocomposites. Schmidt *et al.*[6] have carried out migration studies of clay and polymer from polylactide-MMT nanocomposite materials into ethanol-water food simulants. Their experiments were conducted in aqueous media. The motivation and experimental approach presented in this study differ significantly from the work published by the above mentioned group.

The present work expands on the use of AF^4 to the characterisation of PCN material. The PCN material was dispersed in toluene and separated according to size. Three main distributions attributed to free polymer, grafted clay and ungrafted clay aggregates were observed and their assignments were confirmed by FT-IR.

6.2   Experimental

Instrumentation

The AF^4 experiments were carried out on a AF2000 FFF (Postnova Analytics, Germany) with a channel thickness of 350 μm, and a regenerated cellulose membrane with a molecular weight cut-off of 10000 Da. The main carrier flow (tip flow) and focusing flow were supplied by two HPLC pumps, PN1122 (Postnova Analytics, Germany). Toluene (Sigma-Aldrich) degassed via ultrasonication was used as the solvent at a constant detector flow rate of 0.5 mL/min. Two detectors were used for the analysis, a Postnova PN3140 refractive index detector and a DAWN DSP light scattering detector from Wyatt Technologies.

Sample Preparation

Samples for AF^4 analysis were prepared as follows: 2 mg/mL of PS-clay nanocomposite (crude product) in toluene were prepared via ultrasonication. Fresh samples were prepared daily for analysis.

Sample description

Samples 3 and 7 synthesised as described in Chapter 3 were used for method development.

Running the samples

A brief description of the AF^4 experiment from injection to sample detection is given below:

Field-flow fractionation involves the following steps: injection, focusing/relaxation, sample elution and sample detection. The sample is loaded and injected into the separation channel in the injection step. The generated cross-flow pulls the analyte molecules towards the accumulation wall in the focusing/relaxation step. Opposing diffusional forces cause the analyte molecules to move away from the wall and occupy regions of varying flow velocities, according to their different diffusion coefficients. Smaller molecules diffuse faster and occupy regions of higher velocity leading to them being eluted first in the elution step.
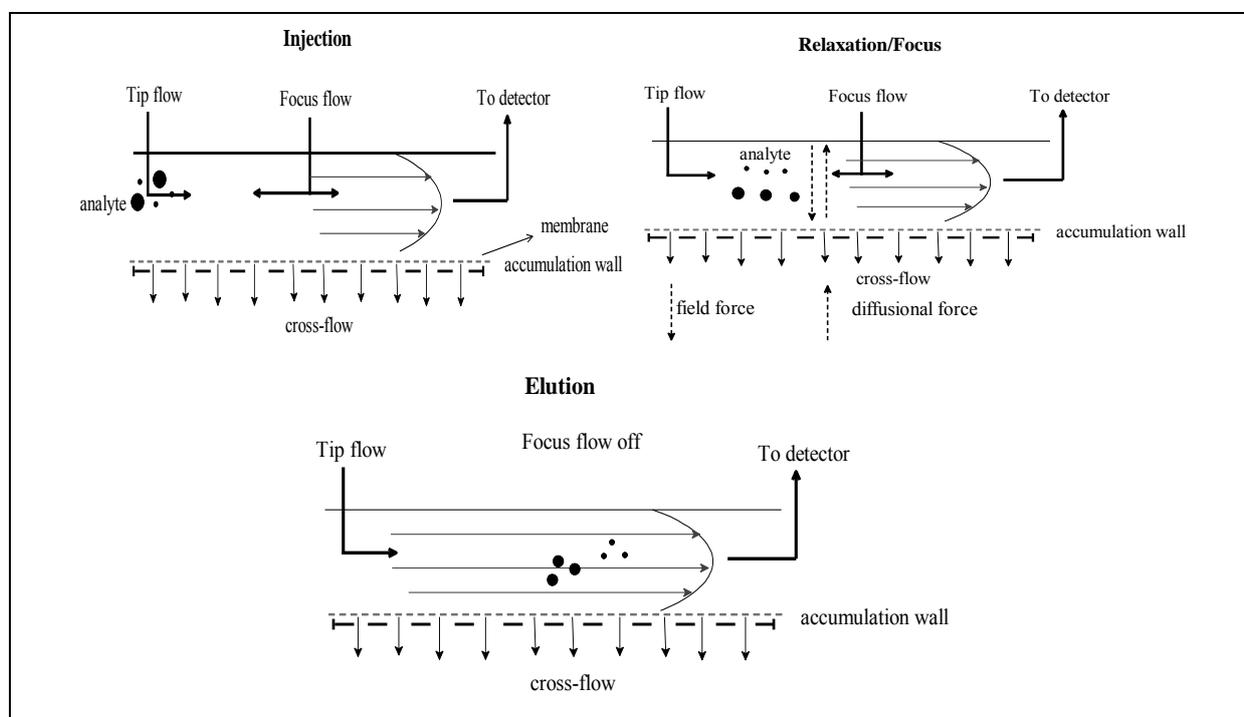

Figure 6.1 Three main steps involved in FFF

The operating conditions for the experiments conducted are given in Table 6.1.

Table 6.1 Operating parameters for the AF^4

AF^4 **program**

Sample 3

Injection step: Time: 10 min   Tip flow: 0.2 mL/min   Cross-flow: 0.4 mL/min
Elution step: Focus flow off

Time	Cross-flow (mL/min)	Type
0–15	0.40	Constant
15–30	0.35	Linear
30–40	0.30	Power
40–100	0.01	Constant

Sample 7

Injection step: Time: 10 min   Tip flow: 0.2 mL/min   Cross-flow: 0.3 mL/min
Elution step: Focus flow off

Time	Cross-flow (mL/min)	Type
0–15	0.30	Constant
15–30	0.25	Linear
30–40	0.20	Power
40–100	0.01	Constant

6.3   Results and Discussion

Testing of solvents

Due to the novelty of this work, a number of solvents were tested prior to analysis in order to find the best dispersant and carrier fluid for the samples. When selecting a solvent for particle analysis a number of considerations have to be made. The particles must form a stable dispersion in the solvent, and they must not swell or dissolve in it. The carrier fluid must also be compatible with the membrane and not swell it.

Three solvent systems were tested for their ability to homogeneously disperse the grafted clay (after washing off free polymer) and the PS-clay nanocomposite (crude product). Sample concentrations of 2 mg/mL were prepared and the samples ultrasonicated for 10 minutes. The results for the tests are given in Table 6.2.

Table 6.2 Testing of solvents for dispersing samples

Sample description	THF	Toluene	H_2O + Tween20 + sodium pyrophosphate
PS/clay blend	✓	✓	✗
Lap-g-PS	✓#	✓*	✓

✓ formed stable dispersion
✓# dispersed but settled after a few minutes
✓* dispersed better with dilute solutions i.e. concentrations < 2 mg/mL
✗ did not disperse at all

Of the three solvent systems, toluene gave the most promising results as a dispersant and carrier fluid. It is worth mentioning that although THF has been reported as a good dispersant for PS grafted clay,[7] it was difficult to re-disperse the dried grafted clay particles.

Analysis of PS-clay samples

All experiments were thus carried out using toluene. Overlays of the MALS and RI fractograms of samples 3 and 7 are shown in Figure 6.2.
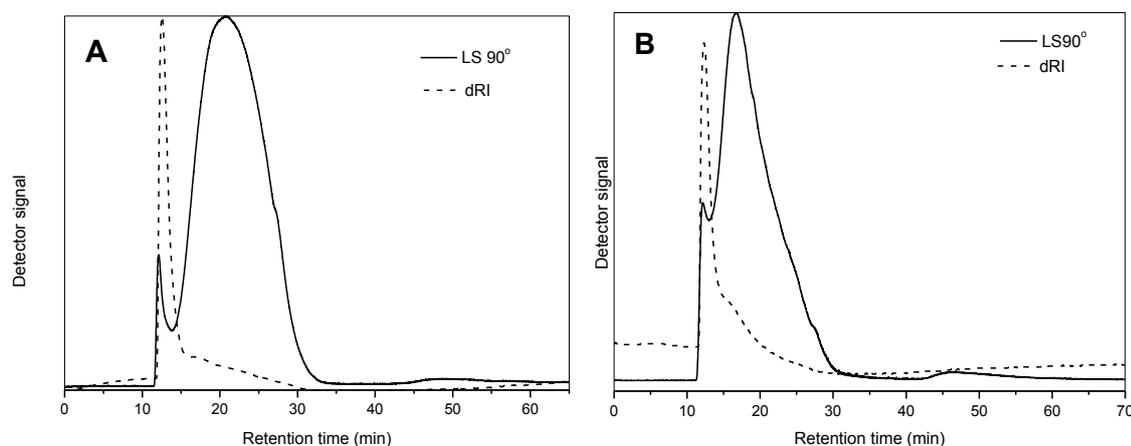

Figure 6.2 AF⁴-MALS and RI fractograms of polymer-clay nanocomposites (crude sample) (A) sample 3 and (B) sample 7.

The light scattering signals show the presence of three components in the samples. The conventional separation method of dispersion/centrifugation only separates the PCN into two components i.e. free polymer and the grafted/ungrafted clay blend. In the FFF fractograms, the second distribution (at 12.5–35.0 min) contained the major light scattering component, whilst the first distribution (at 10.0–12.5 min) contained the component with the highest concentration (from RI signal). The third distribution (at 40.0–60.0 min) contained a

component with large particles, but low concentration; hence it was not observed in the RI detector signal.

The first peak was fairly narrow implying a narrow size distribution. This was consistent with polymer synthesised via an RDRP process. The second peak showed a much broader size distribution. Though the concentration was lower than the first peak, the intense light scattering signal and broad size distribution indicated the presence of a heterogeneous component with a large particle size. The third component was observed at higher elution times implying the particles had a larger size than the first two components. The size distribution was similarly broad, an indication of a component very disperse with respect to particle size.

In order to identify the components, fractions were collected at the elution times indicated in Figure 6.3, for sample 3. The fractions were examined using FT-IR and UV spectroscopy. Online detection with UV could not be used for identifying PS, as the UV-cut-off for toluene is ~289 nm whereas the λ_{max} for PS is 254 nm.
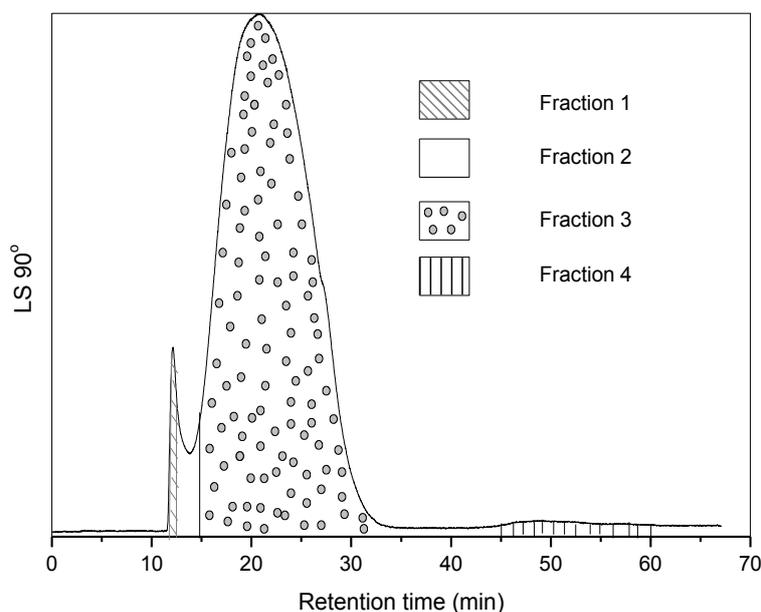

Figure 6.3 AF⁴ fractogram of sample 3 showing collected fractions

The FT-IR spectrum of Fraction 1 is shown in Figure 6.4. The peaks characteristic of PS stretching bands were observed at 3100, 2950, 1600 and 1490 cm⁻¹ (assignments will be given shortly) confirming that peak 1 was composed predominantly of free PS. This was confirmed by UV spectroscopy carried out in THF. The FT-IR and UV spectra of Fraction 2 were similar to that of Fraction 1.
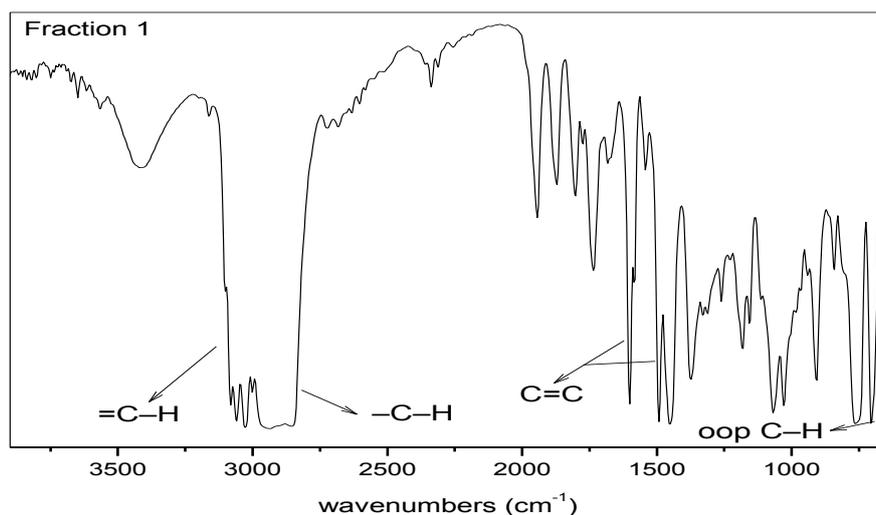
Figure 6.4 FT-IR spectrum of Fraction 1

The FT-IR spectrum of Fraction 3, which constitutes part of the second peak, is shown in Figure 6.5. The sample consisted of polymer-grafted clay as attested by the peaks characteristic of the clay silanol groups at 1000 cm⁻¹, and polystyrene at 3100, 2950, 1600 and 1491 cm⁻¹, ascribed to the aromatic and aliphatic C–H stretch bands, and the C=C stretching vibrations of the aromatic ring, respectively. The characteristic peaks (overtones) for a monosubstituted aromatic compound were also observed between 2000 and 1700 cm⁻¹.
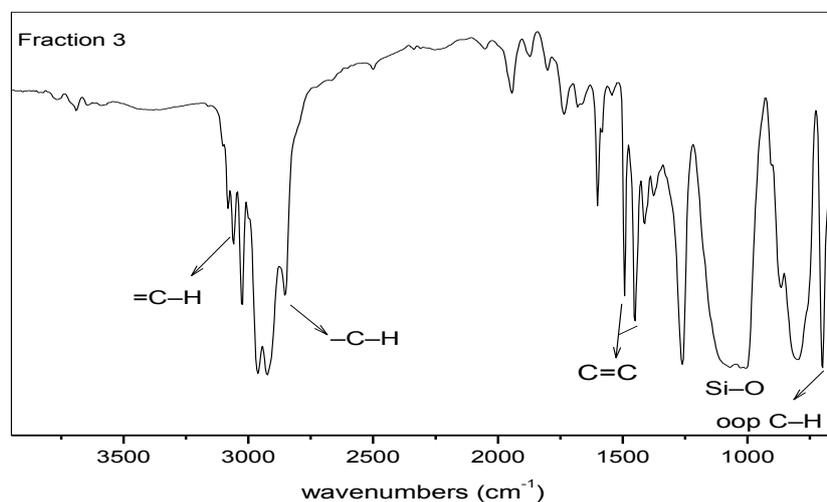
Figure 6.5 Typical FT-IR spectrum for Fraction 3 consisting of grafted clay particles

The UV spectra for Fraction 3 also confirmed the assignment. The spectra showed the presence of chromophores absorbing UV radiation at 254 and 320 nm, further confirming the presence of PS and the thiocarbonyl thio moiety of the RAFT agent.

Two different scenarios were presented following the FT-IR analysis of Fraction 4 from samples 3 and 7. The peak characteristic of the Si–O band was observed at 1090 cm^{-1}, an indication that the sample consisted of clay aggregates. Additional peaks characteristic of the cationic CTA were also observed at 1736 cm^{-1} (C=O), 1450 and 1375 cm^{-1} (CH$_3$) and at 1258 cm^{-1} (C–O). This was an indication that the clay aggregates consisted of CTA-modified clay.

For sample 3 (see Figure 6.6), peaks characteristic of PS were also observed. This indicated three possibilities (1) an intercalated morphology, where polymer chains were growing within stacked clay platelets, (2) grafted clay aggregation via inter-particle polymer chain termination and (3) reversible interaction of the grafted clay with the membrane causing later elution as compared to Fraction 3.
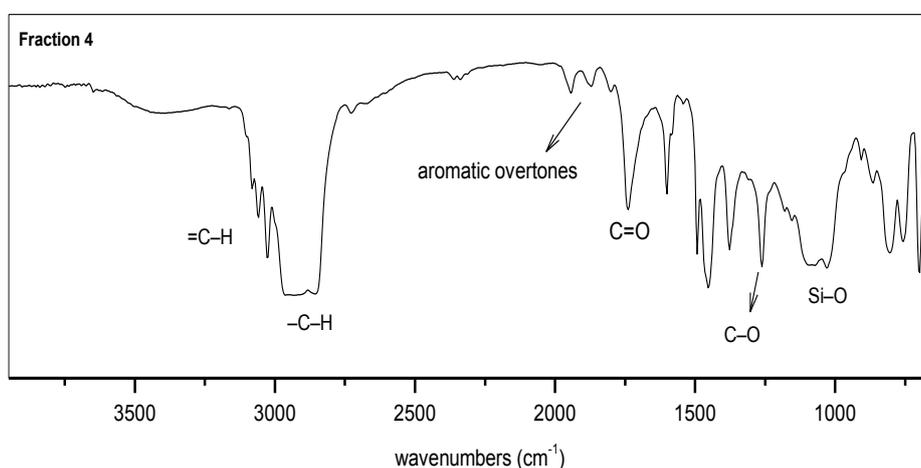

Figure 6.6 FT-IR spectrum for Fraction 4, in sample 3
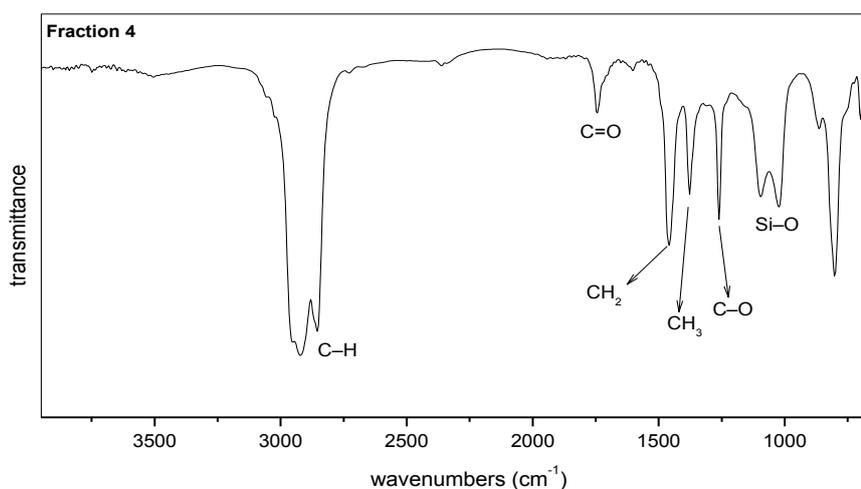
Figure 6.7 FT-IR spectrum of Fraction 4, in sample 7

For sample 7 (see Figure 6.7), no peaks attributed to PS were observed. An indication that the aggregates present were of ungrafted, CTA modified clay particles.

Although the FFF system was connected to a MALS detector, not much reliable information pertaining to molecular weight or particle size could be obtained. In order to determine the molecular weight using the ZIMM equation,[8,9] there is need to know the specific refractive index increment (dn/dc) values for the analyte in solution. This value varies with concentration, whose determination for a heterogeneous sample with dispersed particles is not quantitative. This reduces significantly the accuracy of the technique to determine the molecular weight of particles.

The main parameter reported for particles regarding their size following a MALS experiment is the radius of gyration (R_g) or root mean square radius (RMS). For spherical particles this can be estimated reliably using algorithms in the ASTRA software from the manufacturer of the detector. However for non-spherical particles such as clay platelets or aggregates, it is difficult to determine accurately the particle size of clay particles due to their high aspect ratio.[4] This is because particles in solution rotate due to rotational Brownian motion. As a result, different faces are presented to the light source consequently affecting the R_g determined. These challenges were met with the experiments conducted herein; hence the results obtained for R_g are not presented.

FT-IR could not be used to quantitatively determine the extent of grafting because of the practical challenges with mixing clay and polymer to prepare the calibration standards. Quantitation by comparison of peak intensity was also not practical due to the differences in dn/dc values for free PS and the grafted clay particles.

6.4   Conclusions

A method for separating the complex crude polymer-clay nanocomposite material into its various components was developed. The main fractions were obtained i.e. free PS, grafted clay and ungrafted clay, as expected from the method of synthesis. By the off-line coupling of the AF^4 technique to FT-IR additional information on the components of the system hence morphology of the nanocomposites was obtained. The clay aggregates eluting at high retention times had CTA and PS incorporated within them an indication of an intercalated morphology. In conclusion, it was found that the PCN generally had a mixed intercalated/exfoliated morphology.

References

(1)   Wheeler, P. A.; Wang, J.; Mathias, L. J. *Chem. Mater.* **2006**, *18*, 3937–3945.

(2)   Fan, X.; Xia, C.; Advincula, R. *Langmuir* **2003**, *19*, 4381–4389.

(3)   Fedotov, P. S.; Vanifatova, N. G.; Shkinev, V. M.; Spivakov, B. Y. *Anal. Bioanal. Chem.* **2011**, *400*, 1787–1804.

(4)   Kammer, F. v. d.; Baborowski, M.; Friese, K. *Anal. Chim. Acta.* **2005**, *552*, 166–174.

(5)   Pease, L. F.; Lipin, D. I.; Tsai, D.-H.; Zachariah, M. R.; Lua, L. H. L.; Tarlov, M. J.; Middelberg, A. P. J. *Biotechnol. Bioeng.* **2009**, *102*, 845–855.

(6)   Schmidt, B.; Petersen, J. H.; Koch, C. B.; Plackett, D.; Johansen, N. R.; Katiyar, V.; Larsen, E. H. *Food Addit. Contam.* **2009**, *26*, 1619–1627.

(7)   Konn, C.; Morel, F.; Beyou, E.; Chaumont, P.; Bourgeat-Lami, E. *Macromolecules* **2007**, *40*, 7464–7472.

(8)   Wyatt, P. J. *J. Colloid Interface Sci.* **1998**, *197*, 9–20.

(9)   Wyatt, P. J. *Anal. Chim. Acta* **1993**, *272*, 1–40.

Chapter 7

Summary, Conclusions and Future work

7.1   Summary

The synthesis of two novel cationic chain transfer agents (CTA) for the modification of Laponite clay surfaces was described in chapter 3. The procedure first involved the synthesis of a carboxy-functionalised CTA, which was then modified to a tertiary amine-functionalised CTA via a DCC/DMAP catalysed esterification. The efficiency of the synthesised CTA was investigated using styrene, and the chemical structures of the synthesised polymers investigated by MALDI-TOF MS and ^{1}H NMR. The results obtained showed that in the absence of clay, the synthesised CTA behaved "ideally" in controlling the polymerisation of styrene monomer. The surface of Laponite clay was then modified using the cationic CTA in order to make it organophilic and more compatible with the styrene monomer. The extent of CTA modification was varied by changing the concentration of RAFT agent modifier.

In chapter 4, the SI-RAFT mediated polymerisation of styrene was carried out. A new approach to the synthesis of PCN via RAFT-mediated polymerisation was introduced. A non-functionalised CTA was added to the polymerisation mixture in order create an overall concentration of CTA in the mixture, allowing the surface-confined and free polymer chains to grow simultaneously. A new systematic approach to the characterisation of the resultant PCN was developed. The molar masses of the free and grafted polymer chains were compared in order to get insight into the polymerisation rate of the free and grafted (surface-confined) polymer chains. The chain-end functionality of the free and grafted polymer chains were also compared in order to get insight into the differences/similarities of the polymerisation mechanism of the surface-confined and free polymer chains. The overall summary in this regard was that the free and grafted PS were growing simultaneously, but not at the same rate. This was attributed to conventional chain transfer reactions occurring between the surface-confined PS chains. There was a significant increase in the thermal stability of the PS following incorporation of clay.

The synthetic approach and analytical methods developed in chapter 4 for the synthesis of PCNs consisting of PS were extended to n-butyl acrylate monomer, as reported in chapter 5.

n-Butyl acrylate (n-BA) polymerises different to styrene, regarding their polymerisation kinetics. From the results obtained in this section, it was evident that the polymerisation of n-BA particularly when high molar masses are targeted was accompanied by significant conventional chain transfer reactions. Nonetheless there was a significant improvement in the thermal stability of the material.

In the final chapter preliminary results on the asymmetrical flow field-flow fractionation (AF^4) of PS-clay nanocomposite material was presented. AF^4 was used to fractionate the PCN into its various components namely free PS, grafted clay and ungrafted clay aggregates.

7.2   Conclusions

Polymer-clay hybrid materials consisting of polystyrene and poly(n-butyl acrylate) were prepared via SI-RAFT-mediated polymerisation. A new cationic CTA was designed and synthesised with the dual purpose of making the clay organophilic, and controlling the surface-initiated *in situ* polymerisation of monomer. The synthesised CTA was efficient in controlling the polymerisation of styrene in the absence of clay as attested by polymer with the characteristic properties of (1) well-defined end groups and (2) narrow molar mass distribution. The cationic CTA was successfully used to modify the clay surface.

Following the SI-RAFT mediated polymerisation experiments, the macromolecular structure of the free and grafted polymer chains was investigated. The two monomer systems investigated presented different scenarios. For the styrene system, it was apparent that the free and grafted polymer chains were growing simultaneously, but not at the same rate. Following end group analysis of the grafted and free polymer chains it was evident that the grafted polymer chains were undergoing a slightly different polymerisation mechanism to the free polymer. In addition to reversible deactivation chain transfer reactions, the grafted polymer chains were also undergoing conventional chain transfer reactions. This was attributed to the confinement of the surface-attached propagating radical.

The polymerisation of n-butyl acrylate showed a different polymerisation behaviour. When low molar masses and low monomer conversions were targeted, the free and grafted polymer chains grew simultaneously. End group analysis of the free and grafted polymer chains showed an equal probability of chain transfer reactions occurring at the surface and in solution. However, this was not the observed trend when high molar masses and monomer conversions were targeted. It was evident that chain transfer reactions were occurring both at

the surface of the clay and in solution. The chain transfer reactions occurred to a greater extent at the surface owing to the confinement of the surface-tethered propagating radicals.

The computer-based work of Genzer and coworkers indicated that the surface-grafted and free polymer chains grow at different rates owing to the confinement of the grafted chains. In the present work, it has been shown for the first time that this is attributed to conventional chain transfer reactions of the surface-tethered chains.

The overall conclusion from these results is that, despite adding free CTA to create an even distribution of CTA in the polymerisation mixture, there was still significant loss of functionality of the surface-confined polymer caused by conventional chain transfer reactions. This inadvertently creates challenges when attempting to synthesise clay nanoparticles decorated with block copolymers.

There was a significant improvement in the thermal stability of the polymer material after the addition of clay. However, the extent of thermal stability was independent of neither the molar mass of the polymer nor the grafting density.

A novel method for the separation of the PCN material into its various components according to size using asymmetrical flow field-flow fractionation was developed. Although the obtained data could not give any reliable information pertaining to the molar mass or particle size of the analyte constituents, off-line coupling with FT-IR confirmed the presence of free polymer, grafted clay and ungrafted clay aggregates. The presence of the ungrafted clay aggregates was a clear indication of mixed nanocomposite morphology.

7.3   Recommendations for future research

Suggested future work includes carrying out a detailed study to investigate the influence of grafting density on the kinetics of SI-RAFT-mediated polymerisation of different monomer systems from Laponite clay. In addition, an in-depth study on the influence of the grafting density on the simultaneous RAFT-mediated polymerisation of surface-tethered and free polymer chains should be carried out. The analytical methods devised in this study can be used to investigate surface-initiated NMP or ATRP, allowing for a comparison to be made to surface-initiated RAFT polymerisation, regarding the polymerisation kinetics and mechanism.

Synthesising PCNs consisting of block copolymers is a possible next step. Preliminary work already carried out in this direction has shown that the surface-tethered polymer chains do not chain extend. Investigating the full heterogeneity of these mixtures using thermal field-flow fraction and multidimensional chromatography will provide complimentary information to the results presented in this thesis.

Appendix 1

Figure A1.1 is the ESI-MS spectrum of the carboxy-functionalised chain transfer agent. The peak mass at m/z 238.9 was attributed to the carboxy-functionalised CTA ionised following the removal of an H^+. The peak at peak mass m/z 497.0 was attributed to two A structures cationised by a sodium ion, while the peak at peak mass 757.0 was attributed to three A structures cationised by 2 sodium ions.
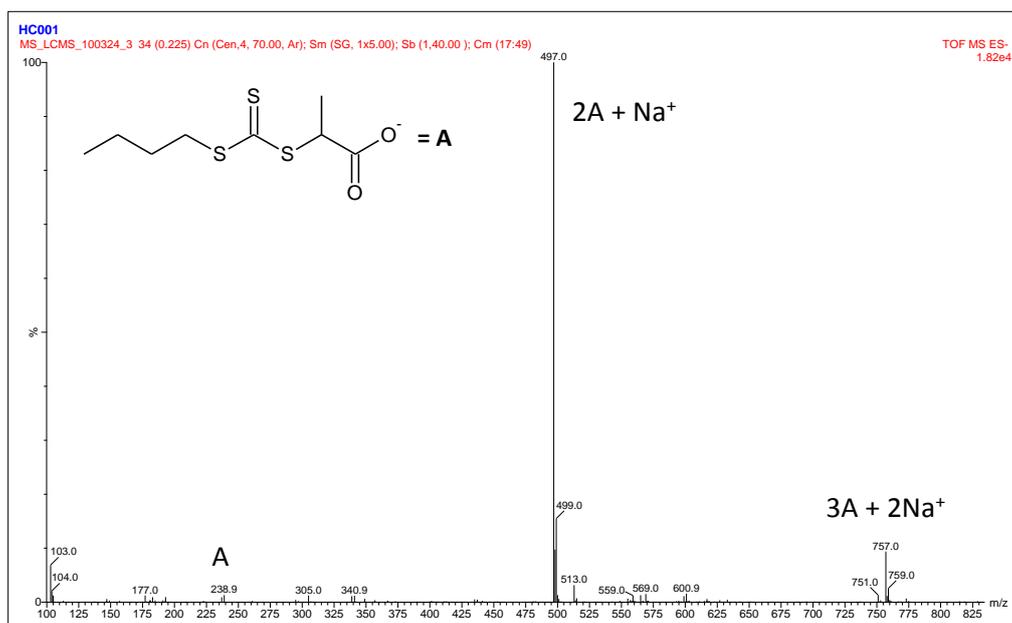

Figure A1.1 ESI-MS spectrum of carboxy-functionalised chain transfer agent

Figure A1.2 is the ESI-MS spectrum of the tertiary amine functionalised CTA synthesised in this study. The peak at mass 310.1 was attributed to the tertiary amine functionalised RAFT agent cationised by a proton.
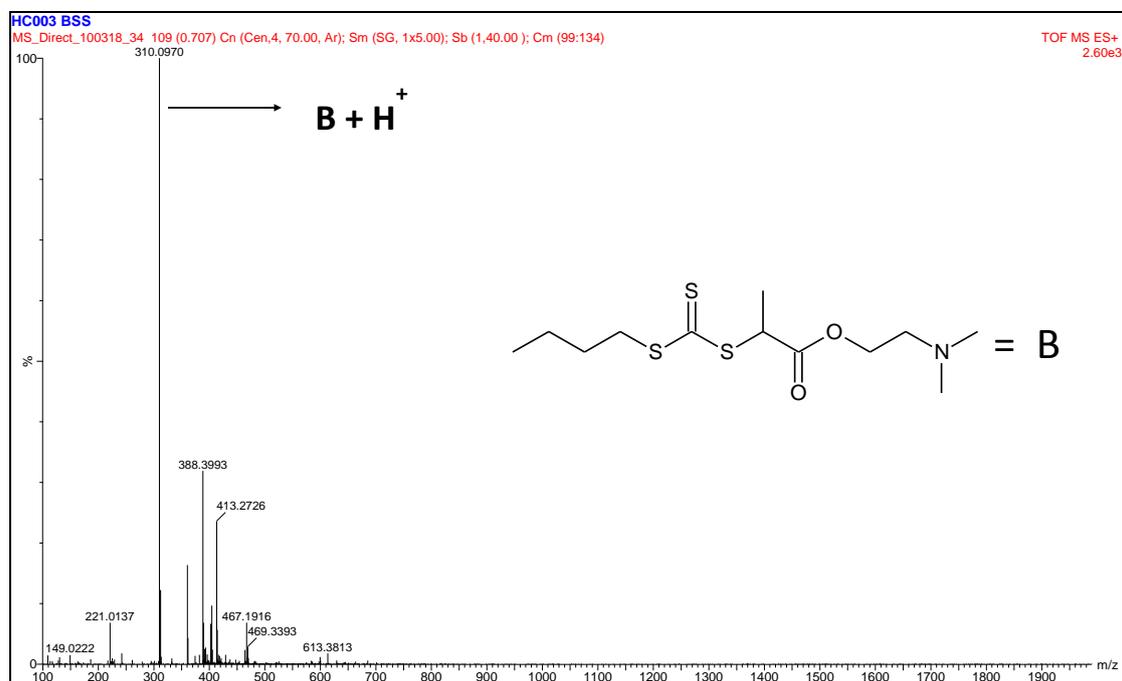

Figure A1.2 ESI-MS spectrum of the tert-amine-functionalised chain transfer agent

Figure A1.3 is the ESI-MS spectrum of the quaternary amine functionalised chain transfer agent. The peak at peak mass 324.1 was attributed to the cationic functionalised CTA.
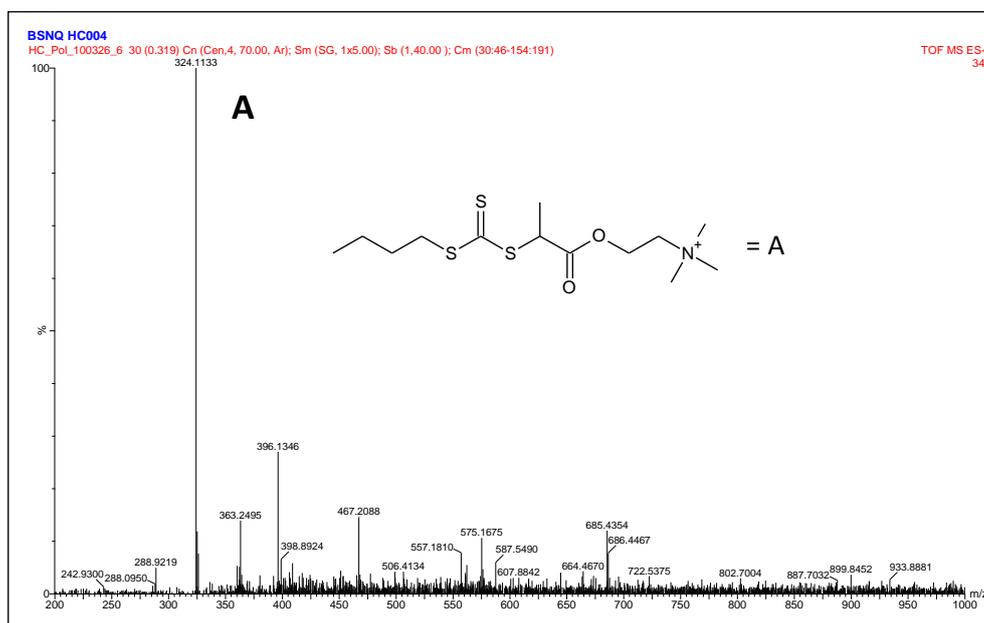

Figure A1.3 ESI-MS spectrum of the quaternary amine-functionalised chain transfer agent

Appendix 2

The FT-IR spectra for free PS and a PS standard (the latter for comparison) are shown in Figure A2, the peak at 1000 cm^{-1} indicated the presence of grafted Laponite clay in the free PS sample.
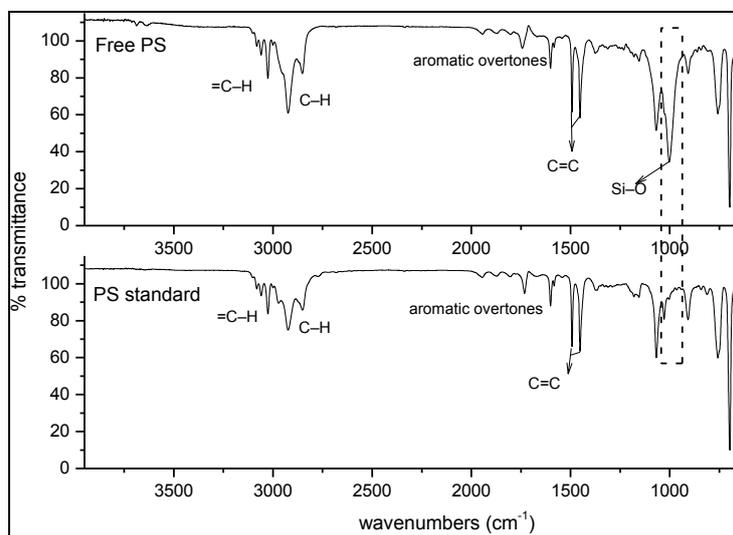
Figure A2 FT-IR spectra of free PS and a PS standard

Appendix 3

Figure A3 is the FT-IR spectrum of clay grafted with PS.
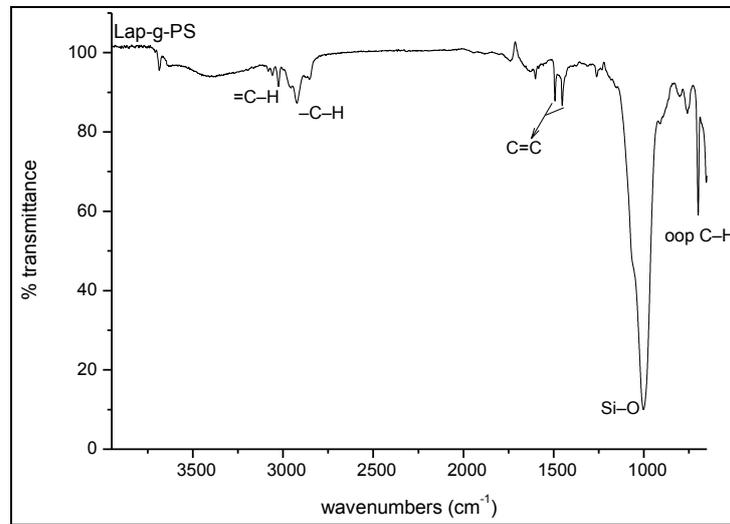
Figure A3 FT-IR spectrum of PS grafted Laponite clay